

DIMER FACE POLYNOMIALS IN KNOT THEORY AND CLUSTER ALGEBRAS

KAROLA MÉSZÁROS, GREGG MUSIKER, MELISSA SHERMAN-BENNETT, ALEXANDER VIDINAS

ABSTRACT. The set of perfect matchings of a connected bipartite plane graph G has the structure of a distributive lattice, as shown by Propp, where the partial order is induced by the *height* of a matching. In this article, our focus is the *dimer face polynomial* of G , which is the height generating function of all perfect matchings of G . We connect the dimer face polynomial on the one hand to knot theory, and on the other to cluster algebras. We show that certain dimer face polynomials are multivariate generalizations of Alexander polynomials of links, highlighting another combinatorial view of the Alexander polynomial. We also show that an arbitrary dimer face polynomial is an F -polynomial in the cluster algebra whose initial quiver is dual to the graph G . As a result, we recover a recent representation theoretic result of Bazier-Matte and Schiffler that connects F -polynomials and Alexander polynomials, albeit from a very different, dimer-based perspective. As another application of our results, we also show that all nonvanishing Plücker coordinates on open positroid varieties are cluster monomials.

CONTENTS

1. Introduction	1
2. Dimer lattices	3
3. Newton polytopes of dimer face polynomials	9
4. On dimers and links	11
5. Background on cluster algebras	18
6. Dimer face polynomials as F -polynomials	21
7. Further cluster algebra applications to links	36
8. Applications to cluster structures on positroid varieties	43
Acknowledgements	48
References	48

1. INTRODUCTION

Perfect matchings, also called *dimers*, are ubiquitous in mathematics. They appear in statistical mechanics [11, 32], the theory of cluster algebras [15, 27], the study of string theory [16, 23], and in knot theory [8, 9, 10], to name a few.

Propp [51] showed that the set of dimers of a connected plane graph G can be endowed with the structure of a distributive lattice, as long as every edge of G is in some perfect matching (see Theorem 2.5 below). One way to phrase this lattice structure, which is also due to Propp, is to give each matching M of G a height vector $\text{ht}(M) \in \mathbb{Z}^{\text{Face}(G)}$. The partial order on matchings is then given by coordinate-wise comparison of height vectors.

The main object of study throughout this paper is the height generating function of all perfect matchings

$$D_G = \sum_{M \text{ dimer}} \mathbf{y}^{\text{ht}(M)}$$

which we call the **dimer face polynomial**. The height function has been widely used and studied in literature on perfect matchings, for example in [17, 51]. For special graphs called *snake graphs*, the dimer face polynomial was studied in [43, 44, 45]. The dimer face polynomial also is implicit in work of [57] and [28] in the context of the Octahedron and Gale-Robinson recurrences, respectively. See also [16, Section 6] where such polynomials are studied for brane tilings in string theory, and are referred to as *colored partition*

functions. The dimer face polynomial is related to the edge generating function of perfect matchings, also sometimes called the *partition function*, by a change of variables followed by a rescaling (see Remark 3.5).

Our main results relate the dimer face polynomial on the one hand to knot theory, and on the other hand to cluster algebras. In the knot theory direction, building on results of Cohen, Dasbach, Russell and Teicher [8, 9, 10], we express the Alexander polynomials of links as specializations of dimer face polynomials:

Theorem A. *For a link diagram L and a segment i , let $G_{L,i}$ be the associated truncated face-crossing incidence graph. Then, the dimer face polynomial $D_{G_{L,i}}$ equals the Alexander polynomial $\Delta_L(t)$ after we specialize its variables to $-1, -t, -t^{-1}$ (as determined by L).*

Theorem A appears as Theorem 4.10 in the text. There are previous formulations of the Alexander polynomial in terms of dimers, using edges rather than faces [8, 9], which are closely related to Theorem A as we explain in Section 4.3. Indeed, there is a vast pool of combinatorial interpretations of the Alexander polynomial [13, 30, 42], and Theorem A adds another way of thinking about the Alexander polynomial by weighting the faces of planar bipartite graphs.

In the cluster algebra direction, we show the following result, which appears as Theorem 6.8.

Theorem B. *Let G be a connected plane graph and suppose every edge of G is in some perfect matching. Let Q_G denote the dual quiver of G . The dimer face polynomial of G is an F -polynomial in the cluster algebra $\mathcal{A}(Q_G)$.*

Further, we give an explicit mutation sequence giving this F -polynomial (which can be read off of G), determine the corresponding g -vector, and give a cluster expansion formula for the corresponding cluster variable x in terms of the dimers of G . Interestingly, the denominator vector of x is the all-1's vector.

Perfect matchings of plane graphs have appeared previously in cluster algebras and related fields. The F -polynomials in cluster algebras from surfaces can be obtained by specializing (attaching the same variable to multiple faces) dimer face polynomials of various *snake graphs* [44]. If the surface is a polygon, so the cluster algebra is type A , no specialization is necessary and the F -polynomials are dimer face polynomials. Theorem B recovers these dimer formulas for type A F -polynomials when G is chosen to be a snake graph (see Proposition 7.12). For special graphs coming from link diagrams, Theorem B has the following corollary, which appears in the text as Corollary 7.3.

Corollary. *The Alexander polynomial of any link L is a specialization of an F -polynomial in $\mathcal{A}(Q_L)$.*

This insight was first conjectured in the beautiful work of Bazier-Matte and Schiffler [1], which served as an inspiration for our work. It was also proved independently by Bazier-Matte and Schiffler in their recent preprint [2], which appeared during the final stages of the preparation of this manuscript.

We also give two applications of Theorem B. The first gives a deeper connection between the knot-theoretic and cluster algebraic results on the dimer face polynomial. Each link diagram for a link L gives rise to many dimer face polynomials, all of which specialize to the Alexander polynomial of L . In Theorem 7.2, we show that all of these dimer face polynomials are F -polynomials in a single cluster algebra, confirming part of a conjecture of [1]. A similar result independently appeared in [2].

There is a resemblance between the combinatorics of dimers on plane graphs and the study of almost-perfect matchings, see Definition 8.3, on planar bicolored graphs on a disk (plabic graphs). Almost-perfect matchings on plabic graphs have been used in the combinatorial study of total positivity as initiated by Postnikov [47], and in particular in the works [37, 40].

Using this connection, the second application of Theorem B involves *open positroid varieties* Π_G° . Open positroid varieties Π_G° are subvarieties of the Grassmannian, introduced in [33]. The coordinate ring $\mathbb{C}[\Pi_G^\circ]$ is generated as an algebra by Plücker coordinates. Additionally, $\mathbb{C}[\Pi_G^\circ]$ is a cluster algebra [25], and so is generated as an algebra by the cluster variables. We determine the relationship between these two generating sets in the result below, which appears as Theorem 8.9.

Theorem C. *All nonvanishing Plücker coordinates on Π_G° are cluster monomials.*

At first glance, this result has little to do with dimers. However, we prove Theorem C by relating the *almost perfect matching* formulas of Muller–Speyer for twisted Plücker coordinates $P_J \circ \tau$ [40] to the dimer formulation for F -polynomials in Theorem B.

We begin our paper with a focus on the combinatorics of graphs and lattices, followed by a presentation of topological and algebraic applications. In Section 2, we discuss the dimer lattice and the dimer face polynomial, as well as some of its properties. In Section 3 we study the Newton polytope of the dimer face polynomial D_G , show it is affinely isomorphic to the perfect matching polytope of G , and determine its face lattice. Section 4 covers background on Kauffmann's lattice and Alexander polynomial, followed by a proof of Theorem A. The remaining three sections focus on the dimer face polynomial and its relation to cluster algebras. In Section 5, we review the relevant theory of cluster algebras and then prove Theorem B in Section 6 after building up the theory even further. In Section 7, we restrict our attention to graphs coming from links, and show that many different F -polynomials specializing to the Alexander polynomial of L can be found in one cluster algebra. We also examine the case of 2-bridge links and their relation to snake graphs. In Section 8, we discuss open positroid varieties and prove Theorem C.

2. DIMER LATTICES

In this section, we introduce a distributive lattice of perfect matchings on plane bipartite graphs, following the work of Propp [51]. Using this lattice for a plane bipartite graph, we define the *dimer face polynomial* in terms of both *multivariate ranks* and *heights* of matchings. As we will discuss in Section 4, the dimer face polynomial generalizes the Alexander polynomial of a link, and as we will discuss in Section 6, it is an F -polynomial in a distinguished cluster algebra.

2.1. The dimer lattice of a plane graph. Recall that a plane graph is a planar graph with a choice of embedding in the plane \mathbb{R}^2 . We call the connected regions of the complement $\mathbb{R}^2 \setminus G$ the **faces** of G . We often identify the faces of plane graphs with the set of edges in their boundary. A **perfect matching** of a graph is a subset of the edges incident to each vertex exactly once. We often say “matching” or “dimer” instead of “perfect matching.”

Definition 2.1. A graph G has **property (*)** if it is a finite connected bipartite plane graph, with vertices properly colored black and white, and every edge is in some perfect matching. We view the vertex coloring as fixed, just as the embedding of G in the plane is fixed.

We denote the collection of all perfect matchings on a plane graph G by \mathcal{D}_G . Additionally, we use $\text{Face}(G)$ to denote the set of all non-infinite faces of G .

Definition 2.2. Let G be a bipartite plane graph. Choose a non-infinite face f of G whose boundary is a cycle. An edge e in the boundary of f is **black-white** in f if, going around f clockwise, we see first the black vertex of e and then the white vertex. The **white-black** edges of f are defined similarly.

Definition 2.3. Let G be a connected bipartite plane graph. Let M be a perfect matching and let $f \in \text{Face}(G)$ be a face whose boundary is a cycle. If M contains all of the black-white edges of f , then we may obtain a new matching M' by removing the black-white edges of f from M and replacing them with the white-black edges of f . We call this operation the **down-flip** at f . Similarly, if M contains all of the white-black edges of f , we may replace them with the black-white edges to obtain a new matching M' ; we call this operation the **up-flip** at f . In either of these situations, we say M, M' are related by a flip at f .

Remark 2.4. If G has property (*), then the boundary of any face is a cycle (otherwise, some edge would have the same face on both sides. We later show that this would lead to a contradiction, see Lemma 6.12). Thus, when G has property (*), flips are well-defined at any face $f \in \text{Face}(G)$.

Propp showed that the dimer sets of graphs with property (*) are very structured.

Theorem 2.5 ([51, Theorem 2]). *Let G be a graph with property (*). We define a binary relation on the set \mathcal{D}_G of dimers by declaring $M \leq M'$ if M is obtained from M' by applying a sequence of down-flips.*

*Then (\mathcal{D}_G, \leq) is a distributive lattice, which we call the **dimer lattice of G** .*

See Figure 2 for an illustration of Theorem 2.5.

Remark 2.6. One can place a distributive lattice structure on \mathcal{D}_G for an arbitrary bipartite plane graph as follows. If some edges of G are not in any perfect matching, delete them to obtain a new plane graph $G' = G_1 \sqcup \cdots \sqcup G_r$, possibly with multiple connected components. Each connected component G_i has property (*), so $(\mathcal{D}_{G_i}, \leq)$ is a lattice by Theorem 2.5. There is a natural bijection between \mathcal{D}_G and the product $\prod \mathcal{D}_{G_i}$, so one may endow \mathcal{D}_G with a lattice structure via this bijection. However, if any non-infinite

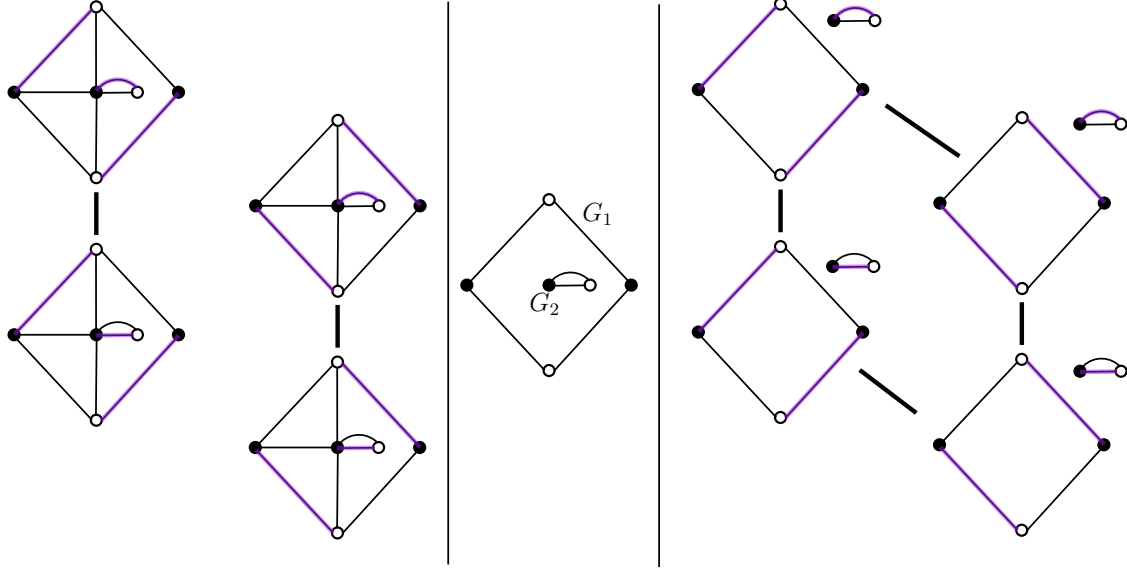


FIGURE 1. An illustration of Remark 2.6. Left: the poset (\mathcal{D}_G, \leq) for a graph G which does *not* have property $(*)$. Center: the graph $G' = G_1 \sqcup G_2$ obtained from G by deleting edges not in any matching. Right: The lattice $\mathcal{D}_{G_1} \times \mathcal{D}_{G_2}$. Note that there are two cover relations that are not present in (\mathcal{D}_G, \leq) , since the unique face of G_1 is not a face of G .

face of G_i is not a face of G , some covering relations in this lattice structure do not correspond to flips on faces of G . See an example of this in Figure 1.

2.2. The dimer face polynomial. In this section, building on [51, Section 2] and subsequent work (see [51, Section 5] for a detailed discussion), we associate a multivariate polynomial to a graph G with property $(*)$, using the dimer lattice. In particular, we associate to each dimer M a monomial *multivariate rank* $\text{mrk}(M)$, and the dimer face polynomial is the sum of these multivariate ranks. At the end of the section, we rephrase the dimer face polynomial using heights.

Definition 2.7. Let G be a graph with property $(*)$. Let C be a saturated chain $\hat{0} = M_0 \leq M_1 \leq \dots \leq M_\ell$ in the dimer lattice and suppose that M_{i-1}, M_i are related by a flip at face f_i . The **weight of the saturated chain** C is

$$\text{wt}(C) := y_{f_1} \cdots y_{f_\ell}.$$

Proposition 2.8. Let G be a graph with property $(*)$. Choose M a dimer on G and let C, C' be two saturated chains from $\hat{0}$ to M . Then $\text{wt}(C) = \text{wt}(C')$, or, in other words, the weight of a saturated chain depends only on the largest element in the chain.

We first prove a straightforward lemma.

Lemma 2.9. Let G be a graph with property $(*)$, and let M be a dimer on G . Suppose M' is obtained from M by a down-flip at face a and M'' is obtained from M by a down-flip at face b , where $a \neq b$. Then there exists a dimer M''' of G which is obtained from M' by a down-flip at face b and is obtained from M'' by a down-flip at face a .

Proof. By the assumption that we may do a down-flip at both a and b , the black-white edges of a and b are contained in M . This implies that a and b are disjoint. Indeed, suppose for contradiction that there is a vertex v in $a \cap b$. As M is a perfect matching, v is in a single edge e of M . Since we may perform a down-flip at both a and b , e must, in fact, be in both a and b . But then $e \in M$ is black-white in exactly one of a and b , a contradiction.

Since a and b are disjoint, flips at a and b commute. The desired matching M''' is the matching obtained from M' by a down-flip at b , which is the same as the matching obtained from M'' by a down-flip at a . \square

We now proceed to the proof of Proposition 2.8.

Proof of Proposition 2.8. We proceed by induction on the length of the saturated chain from $\hat{0}$ to M . The base case is $M = \hat{0}$, for which the statement is trivially true.

Suppose the length of any saturated chain from $\hat{0}$ to M is at least two. Let $C' = \hat{0} \triangleleft M_1 \triangleleft \dots \triangleleft M' \triangleleft M$ and $C'' = \hat{0} \triangleleft N_1 \triangleleft \dots \triangleleft M'' \triangleleft M$ be saturated chains from $\hat{0}$ to M . If $M' = M''$, then we have $\text{wt}(C) = \text{wt}(C')$ by the inductive hypothesis. If M' and M'' are distinct, say they are obtained from M by a down-flip at faces a, b respectively. By Lemma 2.9, there exists M''' covered by both M' and M'' such that $\text{wt}(M''' \triangleleft M') = y_b$ and $\text{wt}(M''' \triangleleft M'') = y_a$.

Now, fix any saturated chain $S = \hat{0} \triangleleft \dots \triangleleft M'''$ and let S', S'' be the chains obtained by adding M' and M'' to the end of this chain. We have

$$\text{wt}(C') = \text{wt}(\hat{0} \triangleleft M_1 \triangleleft \dots \triangleleft M') y_a = \text{wt}(S') \cdot y_a = \text{wt}(S) \cdot y_a y_b$$

where the second equality is by the inductive hypothesis and the third equality is by the choice of M''' . We have a similar string of inequalities for C'' :

$$\text{wt}(C'') = \text{wt}(\hat{0} \triangleleft N_1 \triangleleft \dots \triangleleft M'') y_b = \text{wt}(S'') \cdot y_b = \text{wt}(S) \cdot y_a y_b.$$

This shows $\text{wt}(C') = \text{wt}(C'')$ as desired. \square

Using Proposition 2.8, we now define the “multivariate rank” of a dimer and define the dimer face polynomial.

Definition 2.10. Let G be a graph with property $(*)$. For M a dimer on G and C any saturated chain from $\hat{0}$ to M , define the **multivariate rank** of M to be

$$\text{mrk}(M) = \text{wt}(C).$$

The **dimer face polynomial** of G is

$$D_G(\mathbf{y}) = \sum_{M \in \mathcal{D}_G} \text{mrk}(M).$$

In the remainder of this section, we give an alternate definition of the dimer face polynomial using heights. Height functions, as we use them, are first defined in Elkies, Larsen, Kuperberg, Propp [17, Section 2] as inspired by earlier work enumerating tilings including work of Conway-Lagarias [12] and Thurston [56]. The second author and Schiffler originated the use of height functions in the context of cluster algebras in [43, Section 5] in the special case of unpunctured surfaces and certain graphs known as snake graphs (see Definition 7.8 for more details). More broadly, the height of a matching was used by Propp to define the dimer lattice in Section 3 of [51], and so many of the properties of heights appear in [51]. For the reader's convenience, we provide self-contained proofs here.

We first need an elementary lemma, whose proof we omit.

Lemma 2.11. Let G be a graph with property $(*)$ and $M, M' \in \mathcal{D}_G$ two dimers. The symmetric difference $M \triangle M'$ is a disjoint union of cycles and isolated vertices.

To define heights, we first need to orient the cycles of $M \triangle \hat{0}$.

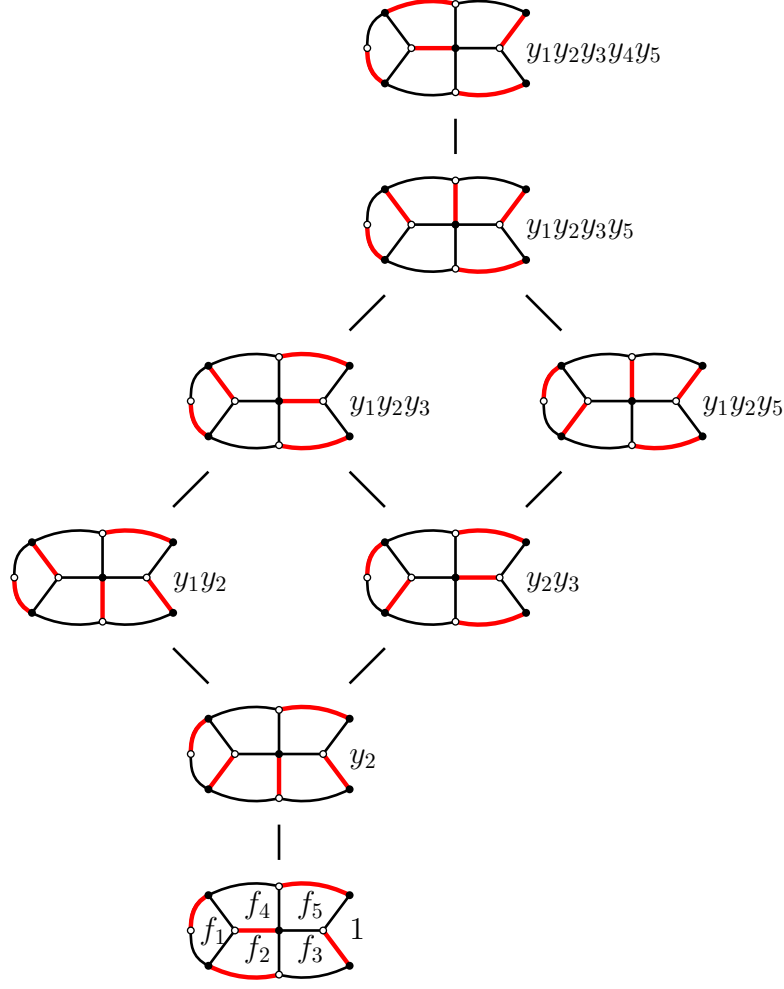
Definition 2.12. Let G be a graph with property $(*)$, and let $M \in \mathcal{D}_G$ be a dimer. Orient the edges of $M \triangle \hat{0}$ as follows: each edge of $M \setminus \hat{0}$ is oriented from black vertex to white and each edge in $\hat{0} \setminus M$ is oriented from white vertex to black. We denote the resulting collection of oriented cycles $\overrightarrow{M \triangle \hat{0}}$.

Note that any cycle in $\overrightarrow{M \triangle \hat{0}}$ is either “clockwise,” meaning all edges are oriented clockwise, or “counterclockwise.” See Figure 3 for an example.

Definition 2.13. Let G be a graph with property $(*)$, and let $M \in \mathcal{D}_G$ be a dimer. The **height** of M is the vector $\text{ht}(M) \in \mathbb{Z}^{\text{Face}(G)}$ where the coordinate indexed by $f \in \text{Face}(G)$ is

$$\text{ht}(M)_f = \#\{\text{clockwise cycles in } \overrightarrow{M \triangle \hat{0}} \text{ encircling } f\} - \#\{\text{counterclockwise cycles in } \overrightarrow{M \triangle \hat{0}} \text{ encircling } f\}.$$

¹By the Schoenflies theorem, the complement of any cycle C in $M \triangle \hat{0}$ has a bounded component and an unbounded component. The cycle C encircles f if f is in the bounded component.

FIGURE 2. The dimer lattice \mathcal{D}_G depicted with the multivariate rank of each dimer.

Equivalently, if p is any point in the face f ,

$$\text{ht}(M)_f = \sum_{C \in \overrightarrow{M\Delta\hat{0}}} -\text{wind}(C, p),$$

where $\text{wind}(C, p)$ is the winding number of C around p .

For convenience, we also allow $\text{ht}(M)$ to have a coordinate indexed by the infinite face. Following the definition above, this coordinate is 0 for all matchings.

Remark 2.14. The above notion of height is defined with respect to the minimal element $\hat{0}$ of the dimer lattice. However, we could have equally defined the height $\text{ht}_{\widetilde{M}}(M)_f$ with respect to a fixed matching \widetilde{M} in the dimer lattice [51]. Such a definition would satisfy $\text{ht}(M)_f = \text{ht}_{\widetilde{M}}(M)_f - \text{ht}_{\widetilde{M}}(\hat{0})_f$.

The height of a face can also be computed using walks on the dual graph G^* of G as in [51], which will be useful in proofs.

Proposition 2.15. *Let G be a graph with property $(*)$, let M be a dimer on G and let $f \in \text{Face}(G)$. Let $P = (p_1, \dots, p_n)$ be a walk in G^* from f to the infinite face. Starting at f and traveling along P , let $L_M(P)$ be the number of edges p_i which pass through an edge in $\overrightarrow{M\Delta\hat{0}}$ directed left-to-right, and let $R_M(P)$ be the number of edges p_i which pass through an edge in $\overrightarrow{M\Delta\hat{0}}$ directed right-to-left. We have*

$$\text{ht}(M)_f = L_M(P) - R_M(P).$$

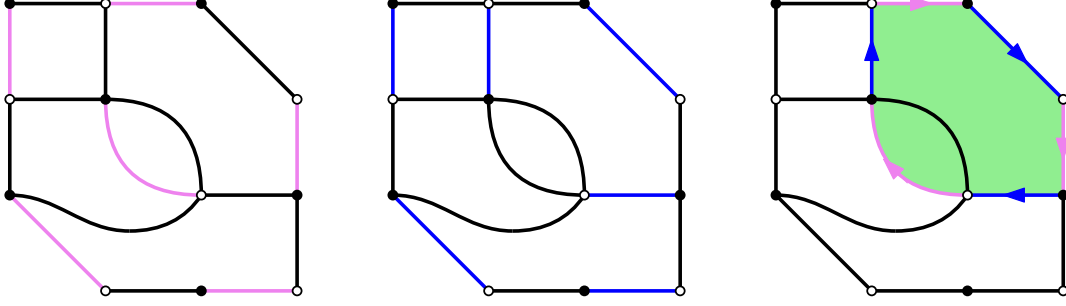


FIGURE 3. Left: the dimer $\hat{0}$ for the graph G depicted. Center: a dimer M . Right: the edges in $M \Delta \hat{0}$, which form a single clockwise cycle encircling the highlighted faces.

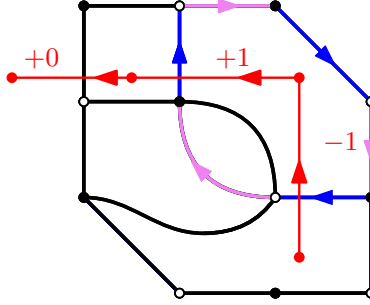


FIGURE 4. A walk from a height-0 face to the exterior, along with the contribution of each oriented edge, continuing the example in Figure 3.

Proof. We observe that the walk P must cross each cycle encircling f at least once. Moreover, if C encircles f , P must cross C an odd number of times to reach the infinite face. If C is oriented clockwise around f , each time P exits the region encircled by C , it crosses an edge directed left-to-right, and every time P re-enters, it crosses an edge directed right-to-left. As such, after performing all possible cancellations, C contributes $+1$ to the difference $L_M(P) - R_M(P)$. Similarly, if C is oriented counterclockwise around f , it contributes -1 to the difference (see Figure 4). On the other hand, if C does not encircle f , then P must cross C an even number of times, and the edges of C that P crosses have alternating orientations. \square

As we now show, the height of a matching is simply a reformulation of its multivariate rank (see also Figure 11 in [51, Section 3] for a description in terms of contour lines).

Theorem 2.16. *Let G be a graph with property $(*)$ and $M \in \mathcal{D}_G$ a dimer. Then*

$$\text{mrk}(M) = \mathbf{y}^{\text{ht}(M)}$$

and in particular, the coordinates of $\text{ht}(M)$ are nonnegative.

Moreover,

$$D_G(\mathbf{y}) = \sum_{M \in \mathcal{D}_G} \mathbf{y}^{\text{ht}(M)}.$$

To prove Theorem 2.16, we need a few preparatory statements.

Lemma 2.17. *If M' is obtained from M by an up-flip or a down-flip over f , then for any edge e bounding f , $e \in M' \Delta \hat{0}$ if and only if $e \notin M \Delta \hat{0}$.*

Proof. Let e be an edge bounding f . The edge e is in $M' \Delta \hat{0}$ if and only if $e \in M' \setminus \hat{0}$ or $e \in \hat{0} \setminus M'$. The former condition is equivalent to $e \notin M \cup \hat{0}$, and the latter is equivalent to $e \in \hat{0} \cap M$, since on the boundary of f , M and M' are complements. So $e \in M' \Delta \hat{0}$ if and only if $e \notin M \cup \hat{0}$ or $e \in \hat{0} \cap M$, which is equivalent to $e \notin M \Delta \hat{0}$. \square

Proposition 2.18. *Let G be a graph with property $(*)$ and let $M, M' \in \mathcal{D}_G$. Suppose that M is obtained from M' by a down-flip on face f . Then,*

$$\text{ht}(M) = \text{ht}(M') - \mathbf{e}_f.$$

Proof. We first compare $\text{ht}(M)_f$ and $\text{ht}(M')_f$. Let P be a walk in G^* from f to the infinite face and let p_1 be its first edge, which crosses edge e of f . Suppose $e \in M' \triangle \hat{0}$. Since M' contains exactly the black-white edges of f , if e is black-white then $e \in M'$. If e is white-black in f , then $e \in \hat{0}$. In either case, according to the definition of $M' \triangle \hat{0}$, e is oriented left-to-right with respect to p_1 . As such, $L_{M'}(P) = L_M(P) + 1$. If $e \notin M' \triangle \hat{0}$, then by Lemma 2.17, $e \in M \triangle \hat{0}$. A similar argument shows that e is oriented right-to-left with respect to p_1 , and so $R_{M'}(P) = R_M(P) - 1$. In either case, Proposition 2.15 implies $\text{ht}(M')_f = \text{ht}(M)_f + 1$.

Next, fix a face $f' \neq f$. We will show that $\text{ht}_{f'}(M) = \text{ht}_{f'}(M')$, which will complete the proof. Let P be a walk in G^* from f' to the infinite face. If P does not travel through the interior of f , then the equality is clear. Otherwise, some edge p of P passes into f through an edge e , then is followed by an edge q exiting f through some edge d . Note that each of e and d contribute to exactly one of $L_M(P)$, $R_M(P)$, $L_{M'}(P)$, and $R_{M'}(P)$. If $d \in M' \triangle \hat{0}$, the previous paragraph shows that d contributes 1 to $L_{M'}(P)$; otherwise, it contributes 1 to $R_M(P)$. Similar statements hold for e , switching M and M' . One can check that in all cases, the desired equality holds. \square

Proof of Theorem 2.16. The first sentence follows from Proposition 2.18 by induction on the rank of M . The base case is $\text{mrk}(\hat{0}) = 1 = \mathbf{y}^{\text{ht}(\hat{0})}$. The second sentence follows from the first, by the definition of D_G . \square

Finally, we deduce some corollaries from the formulation of D_G in terms of height.

Lemma 2.19. *Let G be a graph with property $(*)$. If $\mathbf{y}^{\text{ht}(M)} = \mathbf{y}^{\text{ht}(M')}$ for dimers $M, M' \in \mathcal{D}_G$, then $M = M'$.*

Proof. We claim that the height function $\text{ht}(M)$ uniquely determines the cycles in $M \triangle \hat{0}$, which in turn uniquely determines M . Let e be an edge of G , and let f and f' denote the faces on either side of e . Let p_0 denote the edge of G^* dual to e , and let $P' = (p_1, \dots, p_n)$ be a path from f' to the exterior face. Observe, $P = (p_0, \dots, p_n)$ is a path from f to the exterior. As such, $\text{ht}(M)_f$ and $\text{ht}(M)_{f'}$ differ if and only if e is in $M \triangle \hat{0}$. \square

Corollary 2.20. *The coefficients of $D_G(\mathbf{y})$ are all 0 and 1.*

Corollary 2.21. *Let G be a connected plane graph. Then G has property $(*)$ if and only if the boundary of the infinite face is a cycle and for every non-infinite face of f , there exists a matching M of G which admits an up-flip at f .*

Proof. Suppose G has property $(*)$ and choose a non-infinite face f of G . The face f has at least one black-white edge e which is not in the bottom matching $\hat{0}$ (otherwise, $\hat{0}$ would contain all black-white edges of f and we could perform a down-flip at f in $\hat{0}$, which is impossible). Since G has property $(*)$, there is a matching N which contains \overrightarrow{e} . We have $e \in N \triangle \hat{0}$. Let f' be the other face adjacent to e ; by Lemma 6.12, $f \neq f'$. Note that in $N \triangle \hat{0}$, e is directed black-to-white. Traveling from f to f' across e , e is oriented left-to-right. Using Proposition 2.15, we conclude that $\text{ht}(N)_{f'} = \text{ht}(N)_f - 1$. Since all components of $\text{ht}(N)$ are nonnegative, this implies $\text{ht}(N)_f \geq 1$. In other words, y_f divides $\mathbf{y}^{\text{ht}(N)}$. By Theorem 2.16 and the definition of $\text{mrk}(N)$, this implies that there is some matching $\hat{0} \leq M \leq N$ which admits an up-flip at f . Property $(*)$ also implies the condition on the boundary of the infinite face (see Remark 2.4).

Suppose that for every non-infinite face of f , there is a matching M which admits an up-flip at f . Suppose also that the boundary of the infinite face is a cycle. The first assumption implies that the boundary of every non-infinite face is a cycle, and so every edge in a non-infinite face f is either white-black or black-white in f . Since matching M of G admits an up-flip at f , there is a matching that contains every white-black edge of f . After applying this up-flip, we obtain a matching M' of G that contains every black-white edge of f . The assumption that the boundary of the infinite face is a cycle implies that every edge e is in a non-infinite face of G . In this face, e is either a white-black edge or a black-white edge, so the previous arguments imply that G is in fact bipartite and that every edge of G is in some matching, and thus G has property $(*)$. \square

3. NEWTON POLYTOPES OF DIMER FACE POLYNOMIALS

In this section, we investigate the combinatorics of the Newton polytope of the dimer face polynomial D_G . We show the Newton polytope is affinely isomorphic to the perfect matching polytope of G . From this, we determine the face lattice of the Newton polytope using results of [48] and show that all lattice points are vertices.

Definition 3.1. If p is a polynomial in a polynomial ring whose variables are indexed by some set I , the **support** of p is the integer point set in \mathbb{N}^I consisting of the exponent vectors of monomials with nonzero coefficient in p . The **Newton polytope** $\text{Newton}(p) \subseteq \mathbb{R}^I$ is the convex hull of the support of p .

In particular, if G is a graph with property $(*)$ and D_G its dimer face polynomial, then

$$\text{Newton}(D_G) = \text{ConvHull}(\text{ht}(M) : M \text{ is a perfect matching of } G) \subset \mathbb{R}^{\text{Face}(G)}.$$

Note that $\text{Newton}(D_G) \subset \mathbb{R}^{\text{Face}(G)}$ is a full dimensional polytope, as can be concluded based on its definition and Corollary 2.21.

Definition 3.2. The **perfect matching polytope** $PM(G)$ of a bipartite graph G is

$$PM(G) = \text{ConvHull}(\chi_M \mid M \text{ is a perfect matching of } G),$$

where $\chi_M \in \mathbb{R}^{E(G)}$ is the indicator vector of the perfect matching M .

Note that $PM(G)$ is a 0/1-polytope. As such, the integer points $PM(G) \cap \mathbb{Z}^{E(G)}$ of $PM(G)$ and the vertex set of $PM(G)$ are both exactly the set of the incidence vectors χ_M .

We will show that $\text{Newton}(D_G)$ and $PM(G)$ are affinely isomorphic.

Definition 3.3. Let $P \subset \mathbb{R}^d$ and $Q \subset \mathbb{R}^l$ be polytopes. Fix $A \in \mathbb{R}^{l \times d}$, $\mathbf{x} \in \mathbb{R}^d$ and $\mathbf{v} \in \mathbb{R}^l$. The affine map $\pi : \mathbb{R}^d \rightarrow \mathbb{R}^l$ defined by

$$\pi(\mathbf{x}) = A\mathbf{x} + \mathbf{v}$$

is an **affine isomorphism** between P and Q if $\pi|_P$ is a bijection whose image is Q .

Assume that G has property $(*)$. We define the affine transformation ψ between $\text{Newton}(D_G) \subset \mathbb{R}^{\text{Face}(G)}$ and $PM(G) \subset \mathbb{R}^{E(G)}$ as follows.

To each non-infinite face $f \in \text{Face}(G)$, we associate a vector $\mathbf{v}_f \in \mathbb{R}^{E(G)}$ as follows. For an edge $e \in E(G)$, we set

$$(\mathbf{v}_f)_e = \begin{cases} 1 & \text{if } e \text{ a black-white edge of } f \\ -1 & \text{if } e \text{ a white-black edge of } f \\ 0 & \text{if } e \text{ is not in the boundary of } f. \end{cases}$$

Let $A_G \in \mathbb{R}^{E(G)} \times \mathbb{R}^{\text{Face}(G)}$ be the matrix in whose column vectors are \mathbf{v}_f . Moreover, recall that $\chi_{\hat{0}} \in \{0, 1\}^{E(G)}$ is the indicator vector of the minimal element of \mathcal{D}_G .

Proposition 3.4. Suppose G has property $(*)$. Let $\psi : \mathbb{R}^{\text{Face}(G)} \rightarrow \mathbb{R}^{E(G)}$ be the affine map defined by $\psi(\mathbf{x}) = A_G \mathbf{x} + \chi_{\hat{0}}$. We have that

$$\psi(\text{Newton}(D_G)) = PM(G).$$

Proof. Recall that by Theorem 2.16, $\text{Newton}(D_G)$ is the convex hull of $\{\text{ht}(M)\}_{M \in \mathcal{D}_G}$. In particular, each vertex of $\text{Newton}(D_G)$ is a height vector of some matching.

We will show that ψ maps the height vector $\text{ht}(M)$ to the indicator vector χ_M and in particular is a bijection between $\{\text{ht}(M)\}_{M \in \mathcal{D}_G}$ and $\{\chi_M\}_{M \in \mathcal{M}_G}$. We then use this to show that $\psi(\text{Newton}(D_G)) = PM(G)$.

To show that ψ is a bijection between $\{\text{ht}(M)\}_{M \in \mathcal{D}_G}$ and $\{\chi_M\}_{M \in \mathcal{D}_G}$, we proceed by induction on rank in \mathcal{D}_G .

Base case: the unique rank 0 perfect matching in \mathcal{D}_G corresponds to the integer point $(0, \dots, 0) = \text{ht}(\hat{0}) \in \text{Newton}(D_G)$, whereas it corresponds to $\chi_{\hat{0}} \in PM(G)$. Note that

$$\psi((0, \dots, 0)) = \chi_{\hat{0}}$$

as desired.

Inductive hypothesis: Given a matching $M \in \mathcal{D}_G$ of rank k for some fixed $k \geq 0$, the height $\text{ht}(M)$ is mapped to χ_M under ψ . That is:

$$(1) \quad \psi(\text{ht}(M)) = A_G(\text{ht}(M)) + \chi_{\hat{0}} = \chi_M.$$

Inductive step: Consider a matching M' of rank $k+1$ in \mathcal{D}_G . Let M be a matching of rank k that M' covers and let f be the face of G at which we perform a down-flip to get from M' to M .

By Proposition 2.18,

$$(2) \quad \text{ht}(M') = \text{ht}(M) + \mathbf{e}_f$$

where $\mathbf{e}_f \in \mathbb{R}^{\text{Face}(G)}$ is the coordinate vector with 1 in the coordinate indexed by f and 0s elsewhere.

By definition,

$$(3) \quad \chi_{M'} = \chi_M + \mathbf{v}_f.$$

Then, putting equations (1), (2), (3) together, we obtain:

$$\begin{aligned} \psi(\text{ht}(M')) &= \psi(\text{ht}(M) + \mathbf{e}_f) \\ &= A_G(\text{ht}(M) + \mathbf{e}_f) + \chi_{\hat{0}} \\ &= (A_G(\text{ht}(M)) + \chi_{\hat{0}}) + A_G(\mathbf{e}_f) \\ &= \chi_M + \mathbf{v}_f = \chi_{M'} \end{aligned}$$

as desired.

Now, since $\{\chi_M\}_{M \in \mathcal{D}_G}$ is the set of vertices of $PM(G)$, ψ maps $\{\text{ht}(M)\}_{M \in \mathcal{D}_G}$ to $\{\chi_M\}_{M \in \mathcal{D}_G}$, and affine maps preserve convex combinations, the set of vertices of $\text{Newton}(D_G)$ is $\{\text{ht}(M)\}_{M \in \mathcal{D}_G}$. Thus ψ is a bijection between the vertices of $\text{Newton}(D_G)$ and $PM(G)$. This implies that $\psi(\text{Newton}(D_G)) = PM(G)$. \square

Remark 3.5. There is another polynomial associated to the dimers of a planar bipartite graph G , called the *partition function* Z_G . The partition function is in “edge variables” $\{z_e\}_{e \in E(G)}$ rather than “face variables” $\{y_f\}_{f \in \text{Face}(G)}$, and is defined as

$$Z_G := \sum_{M \in \mathcal{D}_G} \prod_{e \in M} z_e.$$

The polytope $PM(G)$ is the Newton polytope $\text{Newton}(Z_G)$. The above proposition shows that to go from the dimer face polynomial D_G to the partition function Z_G , one substitutes

$$(4) \quad y_f \mapsto \prod_{\substack{e \in f \\ \text{black-white}}} z_e \prod_{\substack{e \in f \\ \text{white-black}}} z_e^{-1},$$

and then multiplies by $\prod_{e \in \hat{0}} z_e$. Note that the alternating product of edge weights as in (4) is important in the dimer theory literature, cf. [31, Sec. 3.2].

Theorem 3.6. *The affine map*

$$\begin{aligned} \psi : \mathbb{R}^{\text{Face}(G)} &\rightarrow \mathbb{R}^{E(G)} \\ \mathbf{x} &\mapsto A_G \mathbf{x} + \chi_{\hat{0}} \end{aligned}$$

is an affine isomorphism of the polytopes $\text{Newton}(D_G)$ and $PM(G)$.

Proof. We already know from Proposition 3.4 that $\psi(\text{Newton}(D_G)) = PM(G)$. So by Definition 3.3, it suffices to show that A_G is injective. Since $|E(G)| > |\text{Face}(G)|$, we will prove this by showing that the columns of A_G , the vectors $\{\mathbf{v}_f\}_{f \in \text{Face}(G)}$, are linearly independent.

Let

$$\sum_{f \in \text{Face}(G)} c_f \mathbf{v}_f = \mathbf{0},$$

where $c_f \in \mathbb{R}$ for $f \in \text{Face}(G)$. We will show that $c_f = 0$ for all $f \in \text{Face}(G)$.

Note that any edge $e \in E(G)$ in the boundary of the infinite face, there is exactly one face $f \in \text{Face}(G)$ that contains e , and in particular, exactly one vector among $\{\mathbf{v}_f\}_{f \in \text{Face}(G)}$ with a nonzero coordinate in position e . We thus conclude that for all faces $f \in \text{Face}(G)$ neighboring the infinite face of G , we have $c_f = 0$. With similar reasoning, we can conclude that for all faces $f \in \text{Face}(G)$ that neighbor any of the

faces neighboring the infinite face of G , we have $c_f = 0$. Continuing this way, we obtain that $c_f = 0$ for all $f \in \text{Face}(G)$, as desired. \square

Recall that affine isomorphism of polytopes implies combinatorial isomorphism; that is, affinely isomorphic polytopes have isomorphic face lattices. We will use this to describe the face lattice of $\text{Newton}(D_G)$. We first need the following definition.

Definition 3.7. A subgraph H of G is *elementary* if it contains every vertex of G and every edge of H is used in some perfect matching. Equivalently, H is a union of several perfect matchings of G .

The next proposition follows directly from [48, Theorem 7.3], which establishes the face lattice of $PM(G)$ once conventions are translated appropriately.

Proposition 3.8. *Suppose G has property $(*)$. The face lattice of $\text{Newton}(D_G)$ is isomorphic to the lattice of all elementary subgraphs of G , ordered by inclusion.*

Proof. Since $\text{Newton}(D_G)$ and $PM(G)$ are affinely isomorphic, their face lattices are isomorphic. It follows from [48, Theorem 7.3] that the face lattice of $PM(G)$ is isomorphic to the lattice of elementary subgraphs of G , ordered by inclusion. In more detail, in [48], they deal with planar graphs embedded in a disk, perhaps with some vertices on the boundary. So to apply [48, Theorem 7.3], one should draw G in a disk to obtain the graph G' . The graph G' satisfies [48, Definition 2.2] (with $n = 0$), a perfect matching of G is an *almost-perfect matching* of G' , and $PM(G)$ is equal to the polytope $P(G')$ from [48, Definition 4.1]. \square

We can also determine the integer points of $\text{Newton}(D_G)$.

Corollary 3.9. *Suppose G has property $(*)$. Then every integer point of $\text{Newton}(D_G)$ is a vertex.*

Proof. By Theorem 3.6, the map ψ is an affine isomorphism from $\text{Newton}(D_G)$ to $PM(G)$. Observe that by definition, the map ψ sends integer points to integer points, so the integer points \mathbf{x} of $\text{Newton}(D_G)$ inject into the integer points of $PM(G)$. The polytope $PM(G)$ is a 0,1-polytope with all integer points being vertices. As ψ sends vertices bijectively to vertices, this implies that in the Newton polytope of D_G , every integer point is a vertex. \square

A special case of this corollary appeared in [2, Theorem 1.10], when $G = G_{L,i}$ is a truncated face-crossing incidence graph of a prime link diagram L with no curls (see Definition 4.5), and $D_G = F_{T(i)}$ (see Proposition 4.13).

4. ON DIMERS AND LINKS

In this section, we describe connections between knot theory and dimers. We first recall Kauffman's lattice of states and how it can be used to compute the Alexander polynomial of a link. We describe how to associate a bipartite plane graph G_L to each (oriented) link diagram L . We show that Kauffman's lattice of states is isomorphic to the dimer lattice of a related graph $G_{L,i}$ (see Lemma 4.9). The latter isomorphism is also stated in the work of Cohen and Teicher [10], and this section is in part inspired by their work. We conclude this section by a proof of Theorem A, which shows that the Alexander polynomial of L can be obtained by specializing the dimer face polynomial $D_{G_{L,i}}$.

4.1. Kauffman's clock lattice and Alexander polynomials. In this section, we review the *state summation* formula for the Alexander polynomial of an oriented link, given by Kauffman [30]. We assume some familiarity with knot theory; see e.g. [3] for details.

If L is an oriented link diagram, we write $\Delta_L(t) \in \mathbb{Z}[t, t^{-1}]$ for its Alexander polynomial. The Alexander polynomial is defined up to multiplication by a signed power of t . We use the notation $P \sim Q$ to indicate that $P, Q \in \mathbb{Z}[t, t^{-1}]$ are related by multiplication by $\pm t^k$ for some integer k .

Fix an oriented link diagram L and a distinguished **segment** i of L (that is, a curve between two crossings). The two planar regions adjacent to i are called **absent**; the remaining regions are **present**. Weight the present regions around each crossing as in Figure 5, left.

A **state** is a bijection between crossings in the diagram and the present regions so that each crossing is mapped to one of the four regions it meets. This bijection is represented diagrammatically by adding a **state marker** to the region each corner is mapped to; see Figure 6 for examples. We denote by $\mathcal{S}_{L,i}$ the set of states of the link diagram L with distinguished segment i . The **weight** of a state S , denoted $\langle L|S \rangle$, is the product of the weights corresponding to the marked regions at each crossing. See Figure 6 for examples.

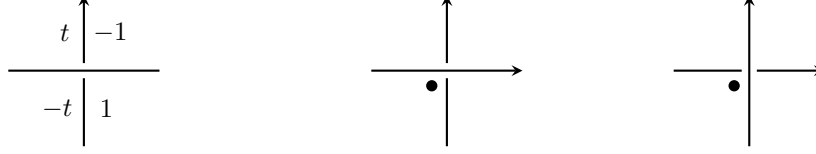


FIGURE 5. Left: the weighting of present regions around each crossing in the definition of the state sum. Note that the orientation of the horizontal strand does not matter. Center and right: black holes.

A state marker is called a **black hole** if it is in the configuration depicted in Figure 5, center or right. Let $b(S)$ be the number of black holes in a fixed state S .

Theorem 4.1 ([30] pg. 176). *Let L be an oriented link diagram and i a segment. Then,*

$$\Delta_L(t) \sim \sum_{S \in \mathcal{S}_{L,i}} (-1)^{b(S)} \langle L|S \rangle.$$

We now define the clock lattice.

Definition 4.2. A **clock move** on a state is the following transposition of state markers at two adjacent crossings (regardless of the orientation of strands and the crossing information).



Note that the state markers move *clockwise* in the clock move, hence the name.

Theorem 4.3 ([30, Theorem 2.5]). *Define $S \leq S'$ whenever S is obtained from S' by a sequence of clock moves. The set of states $\mathcal{S}_{L,i}$ equipped with the binary relation \leq is a lattice.*

We call the lattice of Theorem 4.3 the **clock lattice of the link diagram L** , and in an abuse of notation denote it by $\mathcal{S}_{L,i}$. Figure 6 depicts an example of $\mathcal{S}_{L,i}$.

4.2. Bipartite plane graphs for link diagrams. As in [9, 10], we associate a bipartite plane graph G_L to each link diagram² L . In other references the graph G_L is also referred to as the *overlaid Tait graph* of a link.

Definition 4.4. Let L be a link diagram. The **face-crossing incidence graph**, G_L , is a plane graph defined as follows. Place a black vertex b_c on each crossing c of L and a white vertex w_r in each of its planar regions r . There is an edge (b_c, w_r) in G_L if and only if crossing c touches region r . The faces of G_L are in bijection with the segments of L , and in particular, each segment is contained in a unique face. We use f_j to denote the face of G_L containing segment j .

Note that any link diagram L and graph G_L may be viewed on the sphere by compactifying \mathbb{R}^2 . For any fixed segment i of L , stereographically projecting through any point in a region adjacent to i yields a drawing of L in the plane for which i bounds the exterior region, and a drawing of G_L in which f_i is in the infinite face. See Figure 7.

The graph G_L has two more white vertices than black vertices. In order to make connections to dimer lattices, we will delete white vertices of G_L corresponding to the choice of a segment in the definition of Kauffman's state lattice, see Definition 4.5. Such a construction also appears under the name of *balanced overlaid Tait graph* in other references.

Definition 4.5. Let L be a link diagram, and fix a segment i of L . Changing the stereographic projection of L if necessary, we may assume that f_i is the infinite face of G_L . The **truncated face-crossing incidence graph** is the plane graph $G_{L,i}$ obtained by deleting the two white vertices of f_i .

We will impose some constraints on the link diagram L to ensure that the graph $G_{L,i}$ has property (*). The “prime-like” condition for links introduced in [10] turns out to be just what we need.

²In fact, G_L does not depend on the crossing information of the link diagram.

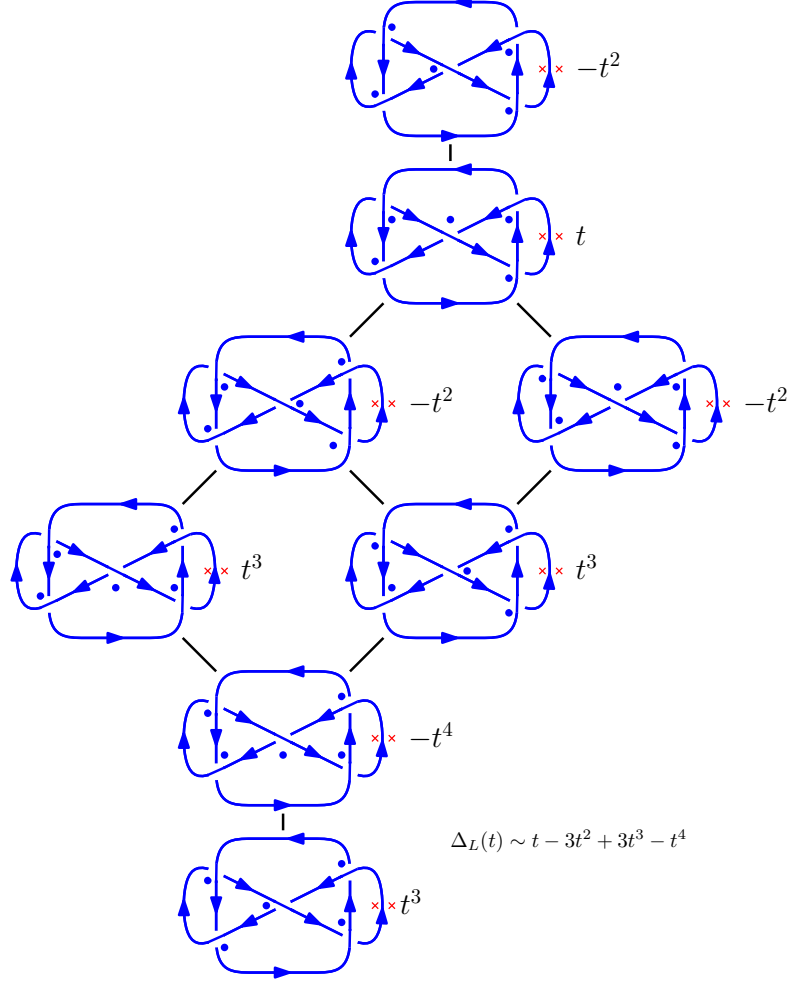


FIGURE 6. The clock lattice for the Whitehead link, where the distinguished segment is the one adjacent to the red crosses. To the right of each state is its weight.

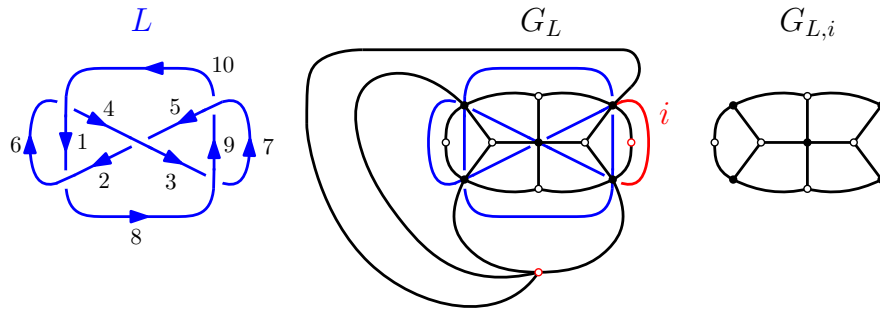


FIGURE 7. Left: In blue, a link diagram for the Whitehead link. Center: The face-crossing incidence graph G_L , with f_7 as the infinite face. Right: The truncated face-crossing incidence graph $G_{L,i}$ for $i = 7$.

Definition 4.6. A link diagram L is

- **connected** if it has a single connected component;

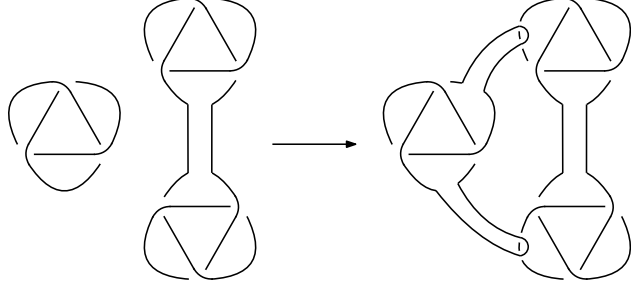


FIGURE 8. To the left, a non-prime-like and disconnected link diagram, and to the right, an isotopic prime-like and connected diagram.

- **prime-like** if there does not exist a simple closed curve γ which intersects L in exactly 2 points such that L has crossings both inside and outside of γ , or equivalently, if L is not the connect sum of two link diagrams that both have crossings (see Figure 12, left).

A crossing c of L is **nugatory** if there exists a simple closed curve γ which intersects L only at c .

The following theorem gives a sufficient condition for $G_{L,i}$ to have property (*). It is proved in [10, Theorems 4.6 and 4.7] for prime-like knot diagrams with no nugatory crossings. A careful reading shows that the proof there also holds if “knot diagram” is replaced with “connected link diagram.” We state the version for link diagrams below.

Theorem 4.7 (cf. [10, Theorems 4.6 and 4.7]). *Let L be a connected prime-like link diagram without nugatory crossings. Then for any segment i , the plane graph $G_{L,i}$ satisfies property (*).*

Assumption 4.8. We assume throughout the remainder of the paper that L is a connected prime-like link diagram with no nugatory crossings. Every link has a connected prime-like diagram without nugatory crossings. Indeed, given any diagram for the link, one can always uncross any nugatory crossings. Then one can repeatedly apply the reverse direction of the second Reidemeister move to make the diagram connected and prime-like (see Figure 8).

Recall that, for L a link diagram and i a segment of L , a state S in Kauffman’s model can be viewed as a pairing of the present regions of L and the crossings of the diagram, where each crossing is paired with a region adjacent to it. Using this, we obtain the following lattice isomorphism between the state lattice of L with respect to i and the dimer lattice of $G_{L,i}$. This isomorphism is also stated in [10].

Lemma 4.9. *Let L be a link diagram and let i be a segment of L . Fix an embedding of L for which i is on the boundary of the exterior region. Let $S \in \mathcal{S}_{L,i}$, and define the dimer $D_S \in \mathcal{D}_{G_{L,i}}$ by $e = (b_c, w_r) \in D_S$ if the state marker near crossing c in S is in region r . The map*

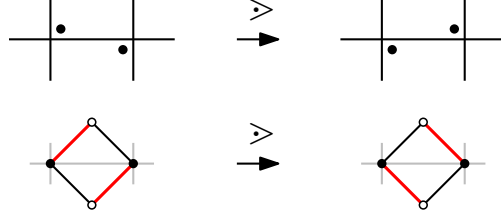
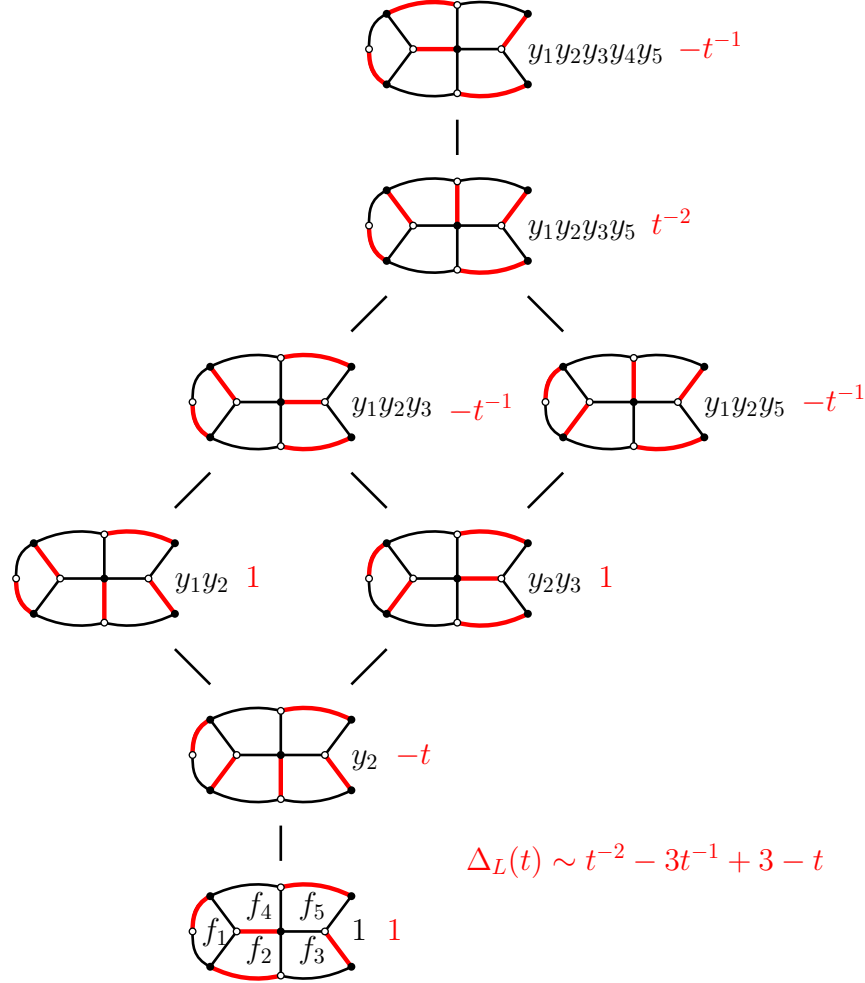
$$\begin{aligned} \mathcal{S}_{L,i} &\rightarrow \mathcal{D}_{L,i} \\ S &\mapsto D_S \end{aligned}$$

is a lattice isomorphism.

Proof. The map $S \mapsto D_S$ is a bijection between states in $\mathcal{S}_{L,i}$ and dimers in $\mathcal{D}_{G_{L,i}}$, and it remains to show that this map respects cover relations in both lattices. Clock moves relate to flips as shown in Figure 9. Because a clock move is never performed on the segment i , each clock move corresponds to a flip of an internal face of $G_{L,i}$. \square

Theorem 4.10. *Let L be a link diagram, and fix a segment i of L . Let $\Delta_L(t)$ denote the Alexander polynomial of L . Let $D_{G_{L,i}}(t)$ be obtained from $D_{G_{L,i}}(\mathbf{y})$ by specializing*

$$(5) \quad y_j \mapsto \begin{cases} -t & \text{if segment } j \text{ exits an undercrossing and enters an overcrossing,} \\ -t^{-1} & \text{if segment } j \text{ exits an overcrossing and enters an undercrossing, and} \\ -1 & \text{otherwise.} \end{cases}$$


 FIGURE 9. The relationship between clock moves on L and flips on G_L .

 FIGURE 10. The Alexander polynomial of the Whitehead link in Figure 7, computed as a weighted sum of dimers. The original monomials are in black and their specializations are in red. Notice that the result is the same as that in Figure 6 up to \sim .

Then we have

$$(6) \quad D_{G_{L,i}}(t) = \left((-1)^{b(\hat{0})} \langle L | \hat{0} \rangle^{-1} \right) \sum_{S \in \mathcal{S}_{L,i}} (-1)^{b(S)} \langle L | S \rangle$$

and in particular,

$$D_{G_{L,i}}(t) \sim \Delta_L(t).$$

Figure 10 depicts an example of this calculation. Motivated by Theorem 4.10, we sometimes call $D_{G_{L,i}}(\mathbf{y})$ a **multivariate Alexander polynomial** for L .

Proof. In both sides of (6), the term indexed by $\hat{0}$ is 1. So to show the equality in (6), it suffices to show that if S is a Kauffman state obtained from state S' by performing a clock move on segment j , then

$$\frac{(-1)^{b(S)} \langle L|S \rangle}{(-1)^{b(S')} \langle L|S' \rangle} = \begin{cases} -t & \text{if segment } j \text{ exits an undercrossing and enters an overcrossing,} \\ -t^{-1} & \text{if segment } j \text{ exits an overcrossing and enters an undercrossing, and} \\ -1 & \text{otherwise.} \end{cases}$$

In all cases, performing a clock move causes S to either lose or gain a black hole. Suppose first that segment j exits an overcrossing and enters an undercrossing. Then, the Kauffman weights incident to the crossings are the following. Below, α is ± 1 or $\pm t$.

$$\begin{array}{c} \begin{array}{|c|} \hline \alpha \quad -t \\ \hline \end{array} \\ \begin{array}{|c|} \hline -\alpha \quad 1 \\ \hline \end{array} \end{array} \rightarrow \begin{array}{c} \begin{array}{|c|} \hline \alpha \quad -t \\ \hline \end{array} \\ \begin{array}{|c|} \hline -\alpha \quad 1 \\ \hline \end{array} \end{array}$$

The clock move increases the degree of $\langle L|S' \rangle$ by one. Additionally, S' either loses or gains a black hole, meaning the clock move changes the sign of $(-1)^{b(S')} \langle L|S' \rangle$. And so, $(-1)^{b(S)} \langle L|S \rangle = (-t)(-1)^{b(S')} \langle L|S' \rangle$.

Suppose that segment j exits an undercrossing and enters an overcrossing. We have the following.

$$\begin{array}{c} \begin{array}{|c|} \hline t \quad -\alpha \\ \hline \end{array} \\ \begin{array}{|c|} \hline -1 \quad \alpha \\ \hline \end{array} \end{array} \rightarrow \begin{array}{c} \begin{array}{|c|} \hline t \quad -\alpha \\ \hline \end{array} \\ \begin{array}{|c|} \hline -1 \quad \alpha \\ \hline \end{array} \end{array}$$

So, the clock move decreases the degree of $\langle L|S' \rangle$ by one. As a result, $(-1)^{b(S)} \langle L|S \rangle = (-t^{-1})(-1)^{b(S')} \langle L|S' \rangle$. Finally, if i either exits an undercrossing or either exits and enters an overcrossing, performing a clock move leaves $\langle L|S' \rangle$ unchanged. Hence, $(-1)^{b(S)} \langle L|S \rangle = (-1)(-1)^{b(S')} \langle L|S' \rangle$. The two cases are depicted below.

$$\begin{array}{c} \begin{array}{|c|} \hline \alpha' \quad -\alpha \\ \hline \end{array} \\ \begin{array}{|c|} \hline -\alpha' \quad \alpha \\ \hline \end{array} \end{array} \rightarrow \begin{array}{c} \begin{array}{|c|} \hline \alpha' \quad -\alpha \\ \hline \end{array} \\ \begin{array}{|c|} \hline -\alpha' \quad \alpha \\ \hline \end{array} \end{array} \quad \left| \quad \begin{array}{c} \begin{array}{|c|} \hline t \quad -t \\ \hline \end{array} \\ \begin{array}{|c|} \hline -1 \quad 1 \\ \hline \end{array} \end{array} \rightarrow \begin{array}{c} \begin{array}{|c|} \hline t \quad -t \\ \hline \end{array} \\ \begin{array}{|c|} \hline -1 \quad 1 \\ \hline \end{array} \end{array}$$

Finally, the fact that $D_{G_{L,i}}(t) \sim \Delta_L(t)$ is immediate from (6) and Theorem 4.1, since $(-1)^{b(\hat{0})} \langle L|\hat{0} \rangle^{-1}$ is equal to $\pm t^k$ for some k . \square

4.3. Connections to partition function specializations. A formula for the Alexander polynomial of L as a weighted sum over dimers of $G_{L,i}$ was given in [9, Proposition 3.4]. The authors of that work used edges rather than faces, and so wrote the Alexander polynomial as a specialization of the partition function of $G_{L,i}$ (see Remark 3.5) rather than as a specialization of the dimer face polynomial. The proof of [9, Proposition 3.4] utilized Kasteleyn matrices, so is rather different from the proof of Theorem 4.10. Here, we briefly discuss the connection between their specialization of the partition function and our specialization of the dimer face polynomial in Theorem 4.10.

In Cohen's work, at each crossing, for each present region incident to the crossing, one assigns two weights: a *local weight* and a specific *Kastelyn weight* informed by Kauffman's state summation model.

Definition 4.11 (cf. [9, Algorithm 3.2, (D2) and (D3)]). Let L be a link diagram and let i be a segment of L . For $e = (b_c, w_r) \in E(G_{L,i})$, define $\alpha(e)$ to be the product of the local weight and Kastelyn weight region r receives near crossing c as in Figure 11.

The next proposition explains the relationship between the specialization $z_e \mapsto \alpha(e)$ and the specialization of (5). Essentially, they intertwine with the change of variables from the dimer face polynomial to the partition function.

Proposition 4.12. *Let L be a link diagram, \bar{L} the diagram obtained from L by switching overcrossings and undercrossings, and let i be a segment of L . Throughout, we use $\alpha(e)$ to denote the weight of e an edge of $G_{\bar{L},i}$, that is, using the crossing information of \bar{L} . Let M be a matching of $G_{L,i} = G_{\bar{L},i}$, S the*



FIGURE 11. Left: the local weighting of present regions around each crossing in [9]. As before, the orientation of the horizontal strand does not matter. Right: the Kasteleyn weighting from [9]. Note the under- and overcrossing information does not change the weighting.

corresponding state (cf. Lemma 4.9), and let \mathbf{z}_M denote the corresponding term of the partition function $Z_{G_{\bar{L},i}}$. Let $p := (-1)^{b(\hat{0})} \langle L | \hat{0} \rangle$. Then $\mathbf{z}_{\hat{0}}|_{z_e \mapsto \alpha(e)} = \sigma \cdot p$ where $\sigma \in \{\pm 1\}$. Further, we have

$$\begin{array}{ccc} \mathbf{y}^{\text{ht}(M)} & \xrightarrow{(4) \text{ and multiply by } \mathbf{z}_{\hat{0}}} & \mathbf{z}_M \\ (5) \downarrow & & \downarrow z_e \mapsto \alpha(e) \\ (-1)^{b(S)} \langle L | S \rangle \cdot p^{-1} & \xrightarrow{\text{multiply by } \sigma \cdot p} & \sigma \cdot (-1)^{b(S)} \langle L | S \rangle \end{array}$$

where in the specialization (5) we use the crossing information from L .

Proof. Comparing Figure 11 applied to \bar{L} with Figure 5 applied to L , we see that if we exchange overcrossings and undercrossings, the present regions around each crossing are weighted in the same way, up to sign. In Figure 11, these weightings give the specialization $z_e \mapsto \alpha(e)$. In Figure 5, these weightings are used to compute $(-1)^{b(S)} \langle L | S \rangle$. Using the bijection between matchings of $G_{\bar{L},i} = G_{L,i}$ and states of L (cf. Lemma 4.9), we have that $\mathbf{z}_{\hat{0}}|_{z_e \mapsto \alpha(e)} = \sigma \cdot p$ where $\sigma \in \{\pm 1\}$.

We now turn to the commutative diagram. The top arrow is Remark 3.5, the left vertical arrow is Theorem 4.10, and the bottom arrow is clear. The right arrow may be deduced from [9, Algorithm 3.2, (D4) and Algorithm 3.6].

Alternately, one can check using case analysis that under the specialization $z_e \mapsto \alpha(e)$, we have

$$\prod_{\substack{e \in f \\ \text{black-white}}} \alpha(e) \prod_{\substack{e \in f \\ \text{white-black}}} \alpha(e)^{-1} = \begin{cases} -t & \text{if segment } j \text{ exits an overcrossing and enters an undercrossing in } \bar{L} \\ -t^{-1} & \text{if segment } j \text{ exits an undercrossing and enters an overcrossing in } \bar{L}, \text{ and} \\ -1 & \text{otherwise.} \end{cases}$$

This means that the change of variables in (4) followed by the specialization $z_e \mapsto \alpha(e)$ has exactly the same effect on y_f as (5). So the top arrow followed by the right arrow has the effect of performing (5) on $\mathbf{y}^{\text{ht}(M)}$ and then multiplying by the specialization of $\mathbf{z}_{\hat{0}}$, which is $\sigma \cdot p$. This is the same as the effect of the left arrow followed by the bottom arrow. \square

4.4. Multivariate Alexander polynomials and submodule polynomials. In the work [1], for a curl-free diagram L of a prime link and any fixed segment i of L , the authors define a polynomial $F_{T(i)}(\mathbf{y})$ which specializes to the Alexander polynomial via the same specialization as in Theorem 4.10. In this section, we explain the relationship between $F_{T(i)}$ and the dimer face polynomial $D_{G_{L,i}}$.

We briefly review the setup of [1]. Fix L a curl-free diagram of a prime link. The authors define a quiver³ Q_L whose vertices are the segments, and a potential W on Q_L . For each choice of segment i , they define a module $T(i)$ over the Jacobean algebra associated to (Q_L, W) . The module $T(i)$ consists of a vector space for each segment of L (equivalently each face of $G_{L,i}$, since segment i is assigned the zero-dimensional vector space), as well as maps between these vector spaces. The polynomial $F_{T(i)}$ is the *submodule polynomial*⁴ of

³which is $Q_{G_L}^{\text{ext}}$ (see Definition 7.1) up to reversing all arrows and adding two-cycles

⁴In [1], $F_{T(i)}$ is called the “ F -polynomial” of $T(i)$, because submodule polynomials are often F -polynomials in a related cluster algebra. In the recent work [2], Bazier-Matte and Schiffrer show that $F_{T(i)}$ is indeed an F -polynomial of a cluster algebra; this can also be deduced from Theorem 6.8 of this work.

$T(i)$ and by [1, Corollary 6.8 (b)] is equal to

$$F_{T(i)} = \sum_{M \subset T(i)} \mathbf{y}^{\dim M}.$$

The sum is over submodules M of $T(i)$ and $\mathbf{y}^{\dim M} \in \mathbb{Z}^{\text{Face}(G_{L,i})}$ records the dimension of the vector space of M sitting in each face of $G_{L,i}$.

By [1, Theorem 1.2], the submodule lattice of $T(i)$ is isomorphic to Kauffman's clock lattice $\mathcal{S}_{L,i}$, and thus by Lemma 4.9, to the dimer lattice $\mathcal{D}_{G_{L,i}}$. This suggests that $F_{T(i)}$ is closely related to the dimer face polynomial $D_{G_{L,i}}$, as the next proposition verifies.

Proposition 4.13. *Let L be a curl-free diagram of a prime link, and let i be a segment of L . The polynomial $F_{T(i)}$ is equal to $D_{G_{L,i}}$.*

Proof. We prove equality term by term, going up the Kauffman lattice. The submodule of $T(i)$ corresponding to the clocked state $\hat{0}$ is the zero module, so the corresponding term of $F_{T(i)}$ is 1. This is the same as the term of $D_{G_{L,i}}$ corresponding to the clocked state.

Let $S, S' \in \mathcal{S}_{L,i}$ be states in the Kauffman lattice and suppose S is obtained from S' by a clock move at segment a , so $S < S'$. Let N, N' the corresponding submodules of $T(i)$, and M, M' the corresponding matchings of $G_{L,i}$. Then by [1, Lemma 6.4], the module N' is obtained from N by increasing the dimension at segment a by 1 (and changing the maps). That is, if segment a is in face f_a of $G_{L,i}$, then $\mathbf{y}^{\dim N'} = y_{f_a} \mathbf{y}^{\dim N}$. By Lemma 4.9, we also have $\text{mrk}(M') = y_{f_a} \text{mrk}(M)$. So if $\mathbf{y}^{\dim N} = \text{mrk}(M)$, we also have $\mathbf{y}^{\dim N'} = \text{mrk}(M')$. \square

4.5. On multivariate Alexander polynomials of composite links. In this section, we show factorization for (certain) multivariate Alexander polynomials of connect sums of link diagrams. This can be viewed as a generalization of the well-known fact that the Alexander polynomial of a composite link factors.

To form the connect sum of two link diagrams L_1 and L_2 , one breaks segments i_1 of L_1 and i_2 of L_2 bounding the exterior region and adjoins them in a way which is consistent with orientation and does not introduce any additional crossings (see Figure 12).

Proposition 4.14. *Let L_1 and L_2 be link diagrams. Label the segments of L_1 by $1, \dots, m$, and label the segments of L_2 by $m+1, \dots, n$. Fix segments i_1 of L_1 and i_2 of L_2 bounding the exterior region. Choose one of the segments of $L_1 \# L_2$ formed by joining i_1 and i_2 , and denote it $i_\#$. Then,*

$$G_{L_1 \# L_2, i_\#} = G_{L_1, i_1} \sqcup G_{L_2, i_2}$$

and

$$D_{G_{L_1 \# L_2, i_\#}}(y_1, \dots, y_n) = D_{G_{L_1, i_1}}(y_1, \dots, y_m) \cdot D_{G_{L_2, i_2}}(y_{m+1}, \dots, y_n).$$

Proof. Let R_1 and R_2 denote the non-exterior regions of L_1 and L_2 bounded by i_1 and i_2 , respectively. Let R denote the region of $L_1 \# L_2$ formed by joining i_1 and i_2 .

The connect sum $L_1 \# L_2$ has the crossing-region adjacency relations of L_1 and L_2 , except that any crossing incident to R_1 in L_1 is incident to R in $L_1 \# L_2$. Similarly, any crossing incident to R_2 in L_2 is incident to R in $L_1 \# L_2$. This shows the statement about $G_{L_1 \# L_2, i_\#}$.

The statement about the dimer face polynomials follows in a straightforward way from the statement about the graphs. \square

5. BACKGROUND ON CLUSTER ALGEBRAS

In this section, we review skew-symmetric cluster algebras of geometric type, as well as their F -polynomials, g -vectors, and d -vectors. See e.g. [22] for additional details.

Definition 5.1 (Quiver and quiver mutation). A **quiver** is a directed graph Q with no loops or directed 2-cycles. Edges of Q are called **arrows**. Each vertex of Q is declared either **mutable** or **frozen**. The **mutable part** of Q is the induced subquiver of Q on the mutable vertices. If k is a mutable vertex of Q , **mutating Q at k** produces a new quiver $\mu_k(Q)$, which is obtained from Q by

- (1) adding an arrow $i \rightarrow j$ for every path $i \rightarrow k \rightarrow j$;
- (2) reversing all arrows incident to k ;

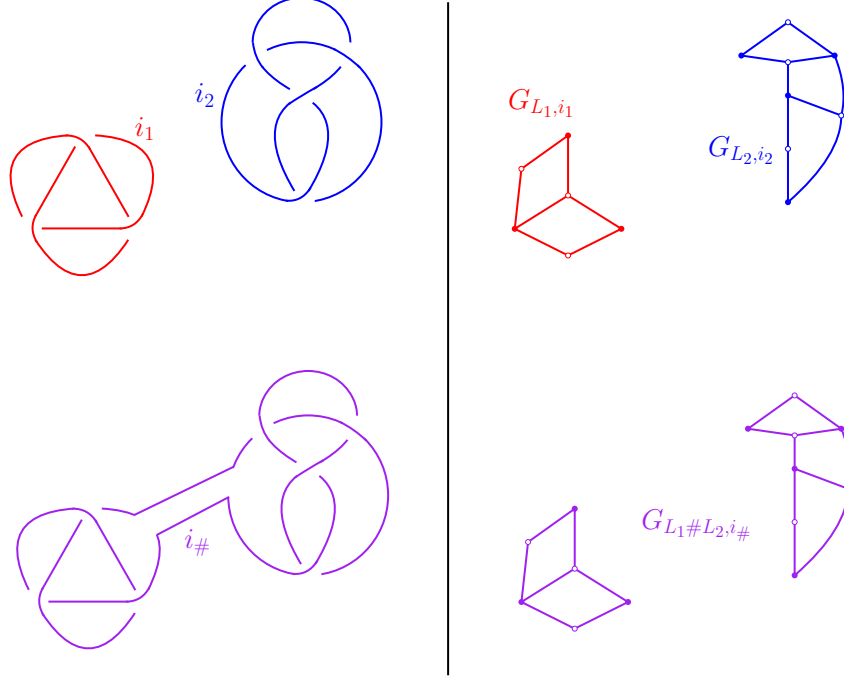


FIGURE 12. Left, top: link diagram L_1 in red and link diagram L_2 in blue. Left, bottom: the connect sum $L_1 \# L_2$ along segments i_1 and i_2 . Right: the corresponding truncated face-crossing incidence graphs.

(3) deleting all 2-cycles, one by one.

Definition 5.2 (Seeds). Let \mathcal{F} be a field of rational functions in n algebraically independent variables over \mathbb{C} . A **seed** of rank $r \leq n$ in \mathcal{F} is a pair $\Sigma = (\mathbf{x}, Q)$ where $\mathbf{x} = (x_1, \dots, x_r, \dots, x_n)$ is a free generating set for \mathcal{F} and Q is a quiver on $[n]$ where vertex i is mutable if $i \leq r$ and is frozen otherwise. The tuple \mathbf{x} is a **cluster**, the elements x_i are **cluster variables**, and the cluster variable x_i is **mutable** if $i \leq r$ and **frozen** otherwise.

Definition 5.3 (Seed mutation). Let $\Sigma = (\mathbf{x}, Q)$ be a seed in \mathcal{F} and let k be a mutable vertex of Q . **Mutating Σ at k** produces a new seed $\mu_k(\Sigma) = (\mathbf{x}', \mu_k(Q))$. The cluster \mathbf{x}' is defined by $\mathbf{x}' = \mathbf{x} \setminus \{x_k\} \cup \{x'_k\}$ where

$$x_k x'_k = \prod_{i \rightarrow k} x_i + \prod_{k \rightarrow i} x_i.$$

Seed mutation is an involution. That is, $\mu_k(\mu_k(\Sigma)) = \Sigma$.

Definition 5.4 (Cluster algebra). Given a seed Σ in field \mathcal{F} , let \mathcal{C} denote the set of cluster variables obtained by performing arbitrary sequences of mutations to Σ . The cluster algebra $\mathcal{A}(\Sigma)$ is the \mathbb{C} -subalgebra of \mathcal{F} generated by the elements of \mathcal{C} , together with the inverses of the frozen variables⁵.

Notice that $\mathcal{A}(\Sigma)$ is completely determined by any seed which can be obtained from Σ by mutation.

The following theorem summarizes a number of central results in the theory of cluster algebras. The *Laurent phenomenon*, or the Laurent polynomial expression for each cluster variable in terms of an initial cluster, is due to [21]. The sharper *positive Laurent phenomenon*, which asserts the coefficients of this Laurent polynomial are positive, is due to [34] for our definition of cluster algebras. The nonnegativity of the denominator vector and its relation to compatibility are due to [5].

⁵Other common conventions include taking $\mathcal{A}(\Sigma)$ to be the \mathbb{Z} -subalgebra with this generating set, or to omit the inverses of frozen variables from the generating set.

Theorem 5.5. Let $\Sigma = ((x_1, \dots, x_n), Q)$ be a seed and let z be a cluster variable of the cluster algebra $\mathcal{A}(\Sigma)$ which is not in Σ . Then z has a positive Laurent expression in terms of the initial cluster variables x_1, \dots, x_n . More precisely,

- (1) there is a polynomial $P_z^\Sigma(x_1, \dots, x_n) \in \mathbb{Z}_{\geq 0}[x_1, \dots, x_n]$ which is not divisible by any x_i and a vector $\mathbf{d}_z^\Sigma = (d_j) \in (\mathbb{Z}_{\geq 0})^n$ such that

$$z = \frac{P_z^\Sigma(x_1, \dots, x_n)}{x_1^{d_1} \cdots x_n^{d_n}}.$$

- (2) We have $d_j = 0$ if and only if z and the initial cluster variable x_j are **compatible**, meaning that they appear together in some seed.

Remark 5.6. The vector \mathbf{d}_z^Σ of Theorem 5.5 is called the *denominator vector* of the cluster variable z . It is conjectured that different cluster variables have different denominator vectors, see [22, Conjecture 7.6].

We now turn to F -polynomials and g -vectors, which are another way to encode cluster variables. First, we define a special choice for the frozen parts of a quiver and seed. This special choice turns out to encode the cluster variables for arbitrary frozen variables.

Definition 5.7 (Principal coefficients). Let Q be a quiver with mutable vertices $[r]$. The **framed quiver** Q^{pr} is the quiver obtained from Q by deleting all frozen vertices, adding r additional frozen vertices $1^\bullet, \dots, r^\bullet$ and one arrow $i^\bullet \rightarrow i$ for each $i \in [r]$. For a seed $\Sigma = ((x_1, \dots, x_n), Q)$, the *framing* of Σ is the seed $\Sigma^{\text{pr}} = ((x_1, \dots, x_r, y_1, \dots, y_r), Q^{\text{pr}})$. We say that Σ^{pr} has **principal coefficients**.

Because the mutable parts of Q and Q^{pr} are the same, [7, Theorem 4.8] implies that there is a one-to-one correspondence between mutable variables of $\mathcal{A}(\Sigma)$ and $\mathcal{A}(\Sigma^{\text{pr}})$. Concretely, if the seed $\mu_{j_q} \circ \cdots \circ \mu_{j_1}(\Sigma)$ has cluster $(z_1, \dots, z_r, x_{r+1}, \dots, x_n)$ and the seed $\mu_{j_q} \circ \cdots \circ \mu_{j_1}(\Sigma^{\text{pr}})$ has cluster $(z'_1, \dots, z'_r, y_1, \dots, y_r)$, then z_i corresponds to z'_i .

Definition 5.8 (F -polynomials). Let Σ be a seed. Let z be a mutable cluster variable in $\mathcal{A}(\Sigma)$, and let z' be the corresponding cluster variable in $\mathcal{A}(\Sigma^{\text{pr}})$. We define the **F -polynomial** of z with respect to Σ as

$$F_z^\Sigma(y_1, \dots, y_r) := P_{z'}^{\Sigma^{\text{pr}}}(1, \dots, 1, y_1, \dots, y_r)$$

where $P_{z'}^{\Sigma^{\text{pr}}}$ is as in Theorem 5.5. If Q is the quiver of Σ , we may also write F_z^Q for F_z^Σ .

Notice that the F -polynomial F_z^Σ is computed using $\mathcal{A}(\Sigma^{\text{pr}})$, so it may seem strange to associate the F -polynomial to a cluster variable of $\mathcal{A}(\Sigma)$. As we will now review, from the F -polynomial F_z^Σ and the seed Σ , one can in fact recover the cluster variable z of $\mathcal{A}(\Sigma)$.

We will need the following notion which is based on [22, Prop. 3.9] but first appeared in this form in [24]. (See also [47, Section 11] and [37, Remark 7.2] which define the same quantity, called a *face weight* and *shear weight* respectively, in the special case that the x_i 's label faces of a plabic graph.)

Definition 5.9. Let $\Sigma = (\mathbf{x}, Q)$ be a seed. For j a mutable vertex, the **exchange ratio** is

$$\hat{y}_j := \frac{\prod_{i \rightarrow j} x_i}{\prod_{j \rightarrow i} x_i}.$$

The next theorem involves the g -vector of a cluster variable, which can be viewed as the degree of the corresponding variable in $\mathcal{A}(\Sigma^{\text{pr}})$ with respect to a particular \mathbb{Z}^r -grading [22, Section 6]. There is also a recursive definition for g -vectors (see e.g. [39]). We will not need the explicit definition, so do not recall it here.

Theorem 5.10 ([22, Corollary 6.3]). Let Σ be a seed with cluster (x_1, \dots, x_n) and let z be a mutable cluster variable of $\mathcal{A}(\Sigma)$. Then there is a vector $\mathbf{g}_z^\Sigma = (g_j) \in \mathbb{Z}^r$, called the **g -vector** of z such that

$$z = x_1^{g_1} \cdots x_r^{g_r} \cdot F_z^\Sigma(\hat{y}_1, \dots, \hat{y}_r).$$

We note that again, the g -vector \mathbf{g}_z^Σ depends only on the cluster variable z' in $\mathcal{A}(\Sigma^{\text{pr}})$ corresponding to z . We will sometimes use the notation \mathbf{g}_z^Q instead of \mathbf{g}_z^Σ . We also note that, due to the algebraic independence of the initial cluster variables, once we write $x_1^{g_1} \cdots x_r^{g_r} \cdot F_z^\Sigma(\hat{y}_1, \dots, \hat{y}_r)$ in lowest terms over a common denominator, we obtain $P_z^\Sigma(x_1, \dots, x_n)/(x_1^{d_1} \cdots x_n^{d_n})$.

We next describe how F -polynomials and g -vectors behave under the addition of mutable vertices to the quiver Q .

Proposition 5.11. *Let Q be a quiver with mutable vertices $[r]$ and Q' be a quiver with mutable vertices $[r']$ with $r \leq r'$ such that the induced subgraph of Q' on $[r]$ is the mutable part of Q . Fix a sequence of mutations $\mu_{\mathbf{p}}$ of Q . Consider the mutable cluster variable $w := w_i$ in $\mu_{\mathbf{p}}(\mathbf{x}, Q)$ and the mutable cluster variable $w' := w'_i$ in $\mu_{\mathbf{p}}(\mathbf{x}', Q')$. Denote their respective g -vectors by $\mathbf{g}_w^Q := (g_i) \in \mathbb{Z}^r$ and $\mathbf{g}_{w'}^{Q'} := (g'_i) \in \mathbb{Z}^{r'}$. Then*

$$F_w^Q(y_1, \dots, y_r) = F_{w'}^{Q'}(y_1, \dots, y_{r'}) \quad \text{and} \quad g_j = g'_j \text{ for } j \in [r].$$

Proof. We may assume that both Q and Q' are framed quivers, since the F -polynomials and g -vectors are determined by the framings of Q and Q' .

We will use induction on the length of the mutation sequence. The base case is when the length of the mutation sequence is 0; in this case, all F -polynomials in both seeds are 1, and the g -vector of the initial cluster variable x_i is the standard basis vector \mathbf{e}_i .

Now suppose the length of the mutation sequence is at least 1. It is straightforward to check, again by induction, that the induced subgraph of $\mu_{\mathbf{p}}(Q')$ on $[r]$ is exactly $\mu_{\mathbf{p}}(Q)$. Moreover, in $\mu_{\mathbf{p}}(Q')$, there are no arrows from the frozen vertices $(r+1)^{\bullet}, \dots, (r')^{\bullet}$ to the mutable vertices $1, \dots, r$.

We first deal with F -polynomials. We use [22, (5.3)], which details how F -polynomials change under one mutation. If the final mutation in \mathbf{p} is not at i , then we have $F_w^Q = F_{w'}^{Q'}$ by the inductive hypothesis. If it is at i , then using the inductive hypothesis, the formulas of [22, (5.3)] for F_w^Q and $F_{w'}^{Q'}$ are nearly the same. The formula for $F_{w'}^{Q'}$ can be obtained from that for F_w^Q by multiplying each term by products of $F_{x_q}^{Q'}$, where $q > r$ and x_q is an initial cluster variable. Since we never mutate at q in the mutation sequence \mathbf{p} , these F -polynomials are all 1, so $F_w^Q = F_{w'}^{Q'}$.

We now turn to g -vectors. We will use [39, pg. 3], which details how g -vectors change under one mutation. Again, if the final mutation in \mathbf{p} is not at i , then the g -vectors of w and w' are not affected by the final mutation and we have the desired equality by the inductive hypothesis. If the final mutation is at i , then [39, pg. 3] together with the inductive hypothesis show that, for $j \in [r]$, g_j and g'_j differ only by the j th coordinate of g -vectors $\mathbf{g}_{x_q}^{Q'}$, where $q > r$ and x_q is an initial cluster variable. In this case, $\mathbf{g}_{x_q}^{Q'} = \mathbf{e}_q$ as we never mutate at q in the mutation sequence \mathbf{p} , so the j th coordinate of this vector is 0. Thus we have $g_j = g'_j$ as desired. \square

6. DIMER FACE POLYNOMIALS AS F -POLYNOMIALS

In this section, we show that if G has property $(*)$, the dimer face polynomial D_G is an F -polynomial for a particular cluster algebra. We also give an explicit mutation sequence to reach this F -polynomial. The main result is stated in Theorem 6.8.

6.1. Reduction sequences for bipartite plane graphs. We now define the dual quiver of a bipartite plane graph.

Definition 6.1. Given a bipartite plane graph G , the dual quiver Q_G is constructed as follows:

- Place a mutable vertex in each non-infinite face f of G .
- For each edge e of G which separates two distinct non-infinite faces f, f' , draw an arrow across e so that the white vertex is on the right.
- Delete oriented 2-cycles, one by one, in any order.

See Figure 13 for an example of Q_G .

Remark 6.2. In the above definition of dual quivers for bipartite plane graphs, an oriented 2-cycle may arise for instance from a 2-valent vertex v or from two faces that border each other twice with an even number of edges between them. In the former case, deleting such a 2-cycle is equivalent to an edge contraction move removing v . In the latter case, this configuration cannot occur for a quadrilateral face in a graph with property $(*)$ (see the proof of Lemma 6.14). Consequently, deleting 2-cycles in Q_G will not affect the correspondence between square moves of bipartite plane graphs and quiver mutations.

Remark 6.3. Note that all vertices of the dual quiver Q_G defined above are mutable. This is slightly different than the convention taken when defining the dual quiver of a *plabic* graph (see e.g. [20, Definition 7.1.4]).

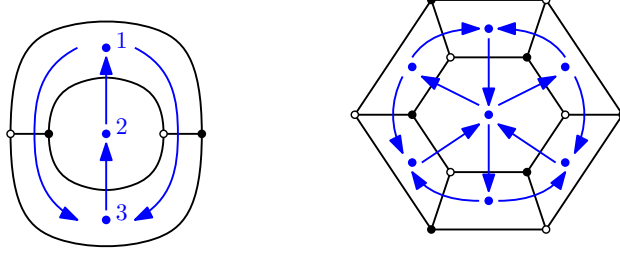
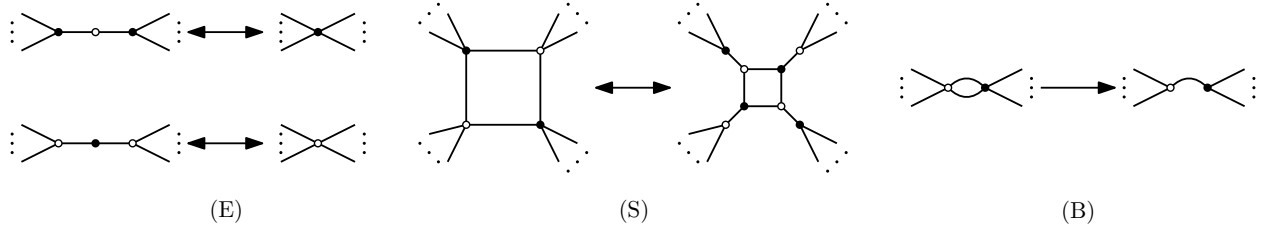


FIGURE 13. Two examples of Q_G , shown superimposed on G . Note that on the left, there are two arrows from 1 to 3.

We will show that the dimer face polynomial of G is an F -polynomial for $\mathcal{A}(Q_G)$. To specify which F -polynomial, we need some additional terminology.

Definition 6.4. We introduce the following operations on bipartite plane graphs: edge contraction/uncontraction, square move, and bigon removal, respectively.



On the left-hand side of (E), we assume that the two vertices of the same color are distinct and are degree at least 2. On the left-hand side of (S), we assume all vertices are degree at least 3. On the left side of (B), we assume both vertices are degree at least 2.

Definition 6.5. Let G be a graph with property (*). A *reduction sequence* for G is a sequence of the moves (E), (S), (B), which turn G into a graph with a single edge. Numbering the non-infinite faces of G , we represent a reduction sequence by the list $\mathbf{r} = (f_1, f_2, \dots, f_q)$ of faces at which (S) or (B) were performed. That is, f_1 is the first face at which (S) or (B) is performed, f_2 is the second, etc.

See Figure 14 for an example of a reduction sequence.

Proposition 6.6. Let G be a graph with property (*). Then, G has at least one reduction sequence.

The proof of Proposition 6.6, which appears in the next subsection, follows readily from existing work on *reduced plabic graphs* [47, 20].

We need one additional definition, based on [55, Section 2] and [15, Eq. (3.11)] which gave a weighting to matchings in the context of the Octahedron Recurrence (equivalently T -systems).

Definition 6.7. Let G be a plane graph and let M be a subset of the edges of G . We define the vector $\mathbf{h}^G(M) = (h_f)_{f \in \text{Face}(G)}$ by

$$(7) \quad h_f := |f|/2 - |M \cap f| - 1.$$

We will often, but not always, take M to be a matching of G ; sometimes M will instead be a matching of a subgraph of G .

We now state the main theorem of this section: the dimer face polynomial D_G is an F -polynomial for the cluster algebra with initial quiver Q_G . If $\mathbf{r} = (i_1, \dots, i_q)$, we write $\mu_{\mathbf{r}}(\Sigma)$ for the seed $\mu_{i_q} \circ \dots \circ \mu_{i_2} \circ \mu_{i_1}(\Sigma)$, so that the first entry of \mathbf{r} gives the first mutation performed, the second entry the second, etc.

Theorem 6.8. Let G be a graph with property (*) and let $\mathbf{r} = (f_1, \dots, f_q)$ be a reduction sequence for G . Consider a seed $\Sigma = (\mathbf{x}, Q_G)$. Let z be the cluster variable of $\mu_{\mathbf{r}}(\Sigma)$ labeling vertex f_q . We have

$$F_z^{Q_G}(y_1, \dots, y_n) = D_G(y_1, \dots, y_n).$$

Further, the g -vector $\mathbf{g}_z^{Q_G}$ of z is equal to \mathbf{h}_0^G , where $\hat{0}$ denote the bottom matching in our dimer lattice for graph G .

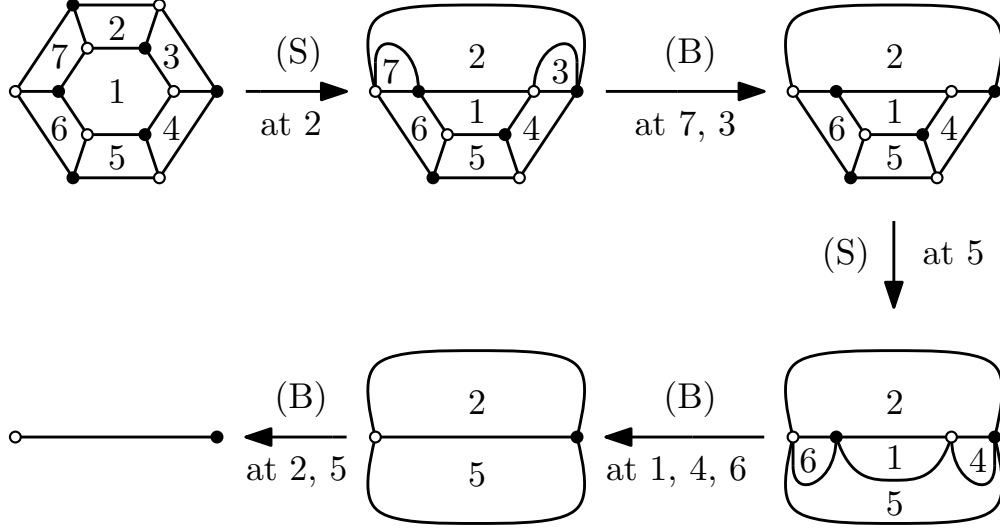


FIGURE 14. An illustration of the reduction sequence $\mathbf{r} = (2, 7, 3, 5, 1, 4, 6, 2, 5)$ for the graph G on the upper left. Arrows are labeled by the moves relating successive graphs; (E) moves are omitted.

See Figure 15 for an illustration of Theorem 6.8.

Remark 6.9. Theorem 6.8 implies that the dimer face polynomial of an arbitrary plane graph G is the F -polynomial of a cluster monomial in some cluster algebra. If G has no perfect matchings, then $D_G = 1$. If G has at least one perfect matching, we use Remark 2.6 to endow \mathcal{D}_G with a distributive lattice structure. Let $G' = G_1 \sqcup \cdots \sqcup G_r$ be the graph obtained by deleting all edges of G which are not in any perfect matching. We have $D_G = D_{G_1} \cdots D_{G_r}$, so D_G is a product of compatible F -polynomials for the cluster algebra with initial quiver $Q_{G'} = Q_{G_1} \sqcup \cdots \sqcup Q_{G_r}$. We note that $Q_{G'}$ may not be an induced subquiver of Q_G .

Using Theorem 6.8, we may readily give the cluster expansion of z , extending results in [55, 15, 57, 16] to cases of arbitrary graphs with property (*). We delay our proof of the cluster expansion until after the proof of Theorem 6.8. The formula here is reminiscent of formulas for twisted Plücker coordinates in [37, 40] and we discuss the relationship between our results and theirs in Section 8.

Corollary 6.10. *Let G , Σ , and z be as in Theorem 6.8. The Laurent polynomial expression for z in terms of the initial seed Σ is*

$$z = \sum_{M \in \mathcal{D}_G} \mathbf{x}^{\mathbf{h}_M^G} = \sum_{M \in \mathcal{D}_G} \prod_{f \in \text{Face}(G)} x_f^{|f|/2 - |M \cap f| - 1}$$

and the denominator vector of z (see Theorem 5.5) has all coordinates equal to 1.

We obtain a corollary on the Newton polytopes of the F -polynomials in Theorem 6.8 by applying Proposition 3.8 and Corollary 3.9.

Corollary 6.11. *Let G and z be as in Theorem 6.8. Then every integer point in the Newton polytope of $F_z^{Q_G} = D_G$ is a vertex, and the face lattice of the Newton polytope is isomorphic to the lattice of elementary subgraphs of G .*

There has been substantial interest in Newton polytopes of F -polynomials and Laurent polynomial expressions for cluster variables [29, 19, 38, 36]. By [36, Theorem 4.4], the Newton polytope $\text{Newton}(F)$ of any F -polynomial is *saturated*, meaning that all lattice points of $\text{Newton}(F)$ are exponent vectors of terms in F , and a lattice point is a vertex if and only if the corresponding term has coefficient 1. We remark that Corollary 6.11 recovers these results when $F = D_G$, as by Corollary 2.20 all coefficients of D_G are 1.

6.2. Results needed for the proof of Theorem 6.8. In this subsection, we build up to the proof of Theorem 6.8, proving some preparatory results and then comparing how the F -polynomial changes when a move is performed to G to how the dimer face polynomial changes. We deal separately with (E), (S), and

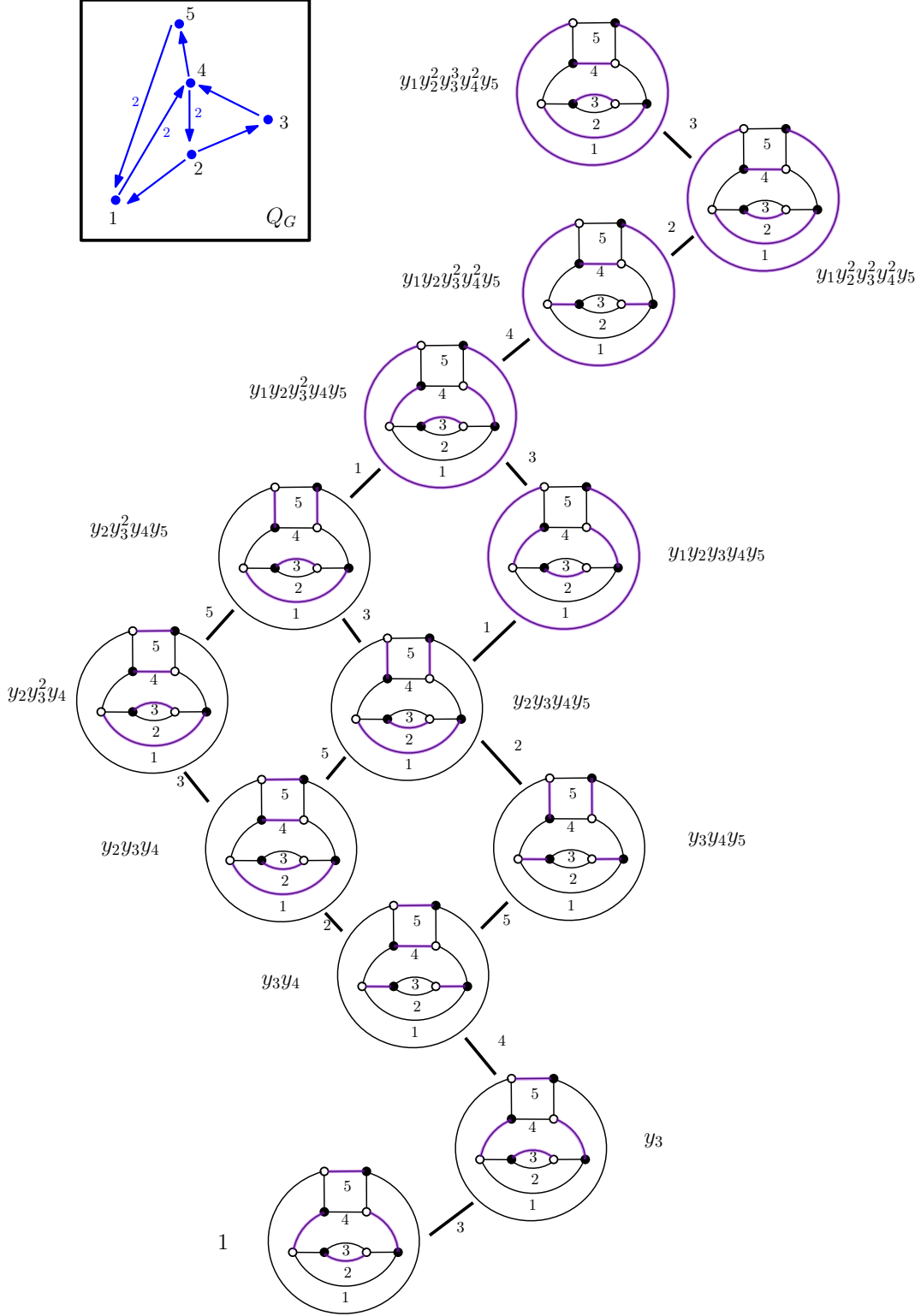


FIGURE 15. An example of \mathcal{D}_G and Q_G . Next to each matching M is its multivariate rank $\text{mrk}(M) = \mathbf{y}^{\text{ht}(M)}$. In Q_G , the numbers next to arrows are multiplicities. A reduction sequence for G is $(3, 2, 4, 5, 1)$. The cluster variable labeling vertex 1 in the seed $\mu_1 \circ \mu_5 \circ \mu_4 \circ \mu_2 \circ \mu_3(\mathbf{x}, Q_G)$ has F -polynomial D_G and g -vector $\mathbf{h}_0^G = (0, 0, -1, 0, 0)$.

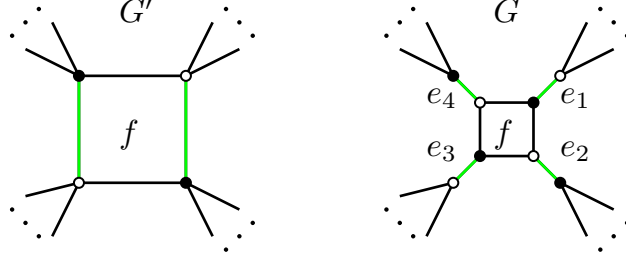


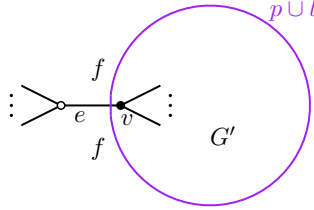
FIGURE 16. Graphs G' and G related by a square move at f , with the edges of G labeled as in the proof of Proposition 6.13. In green, a matching M of G and a matching of G' which agrees with M away from f .

(B) in Lemma 6.16, Theorem 6.18, and Theorem 6.20, respectively. In the next subsection, we use these results and induction to complete the proof of Theorem 6.8.

We start with a helpful lemma on the structure of graphs with property (*). See also [40, Lemma 3.7].

Lemma 6.12. *If G is a graph with property (*) and is not a single edge, then no edge of G has the same face on both sides.*

Proof. Suppose for the sake of contradiction that some edge e of G has a (finite or infinite) face f on both sides. Choose a short line segment l perpendicular to e , with endpoints q^+ and q^- in f . As f is path-connected, there is a path p from q^+ to q^- in f , which in particular does not intersect e . Now, the closed curve $p \cup l$ encloses some vertices of G . Let G' be the induced subgraph of G on these vertices. Note that G' includes exactly one vertex of e , say v , and is a connected component of $G \setminus e$.



By assumption, e is in some matching M of G . The matching M restricts to a perfect matching of $G' \setminus v$, so $G' \setminus v$ has an even number of vertices and G' has an odd number of vertices. Since G is not a single edge and is connected, e is adjacent to another edge e' . By assumption, there is a matching N of G which uses e' and thus does not use e (and this is true whether or not e' is incident to v or the other endpoint of e). Such a matching N would have to restrict to a perfect matching of G' . But G' has an odd number of vertices, a contradiction. \square

Now, we verify that the hypothesis of Theorem 6.8 is preserved under the three moves.

Proposition 6.13. *The set of graphs with property (*) is closed under moves (E), (S), (B).*

Proof. It is straightforward to verify that if G has property (*), then applying (E) or (B) results in another graph with property (*). Notice that on the left-hand side of (B) either both vertices have degree 2 or both have degree at least 3, or G would not have property (*).

For move (S), let G' be the graph on the left and G be the graph on the right, and f the face at which the square move is performed. We show that if G has property (*), then so does G' . The reverse argument is identical, as one can use (E) moves to assume all vertices of f are trivalent in G' . For every matching M of G , there is a matching of G' which agrees with M on all edges of G' that are not in f (see Figure 16). So, we only need to show that every edge of f is in some matching of G' . By assumption, for $i = 1, 2, 3, 4$, G has a matching M_i which uses e_i . If some M_i uses all of e_1, e_2, e_3, e_4 as shown on the right of Figure 16, then G' has a matching which admits an up-flip at f , shown on the left of Figure 16, and every edge of f is either in this matching or its up-flip.

We will, in fact, show that property (*) guarantees there is a matching of G' that contains all four edges e_1, e_2, e_3 , and e_4 . Assume otherwise. By assumption, for $i = 1, 2, 3, 4$, G has a matching M_i which uses e_i .

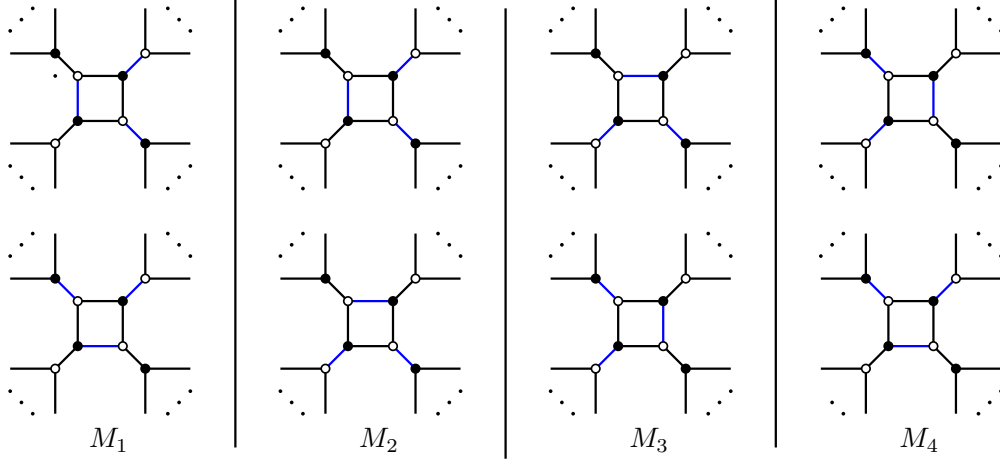


FIGURE 17. In the proof of Proposition 6.13, the options for the matching M_i around the face f .

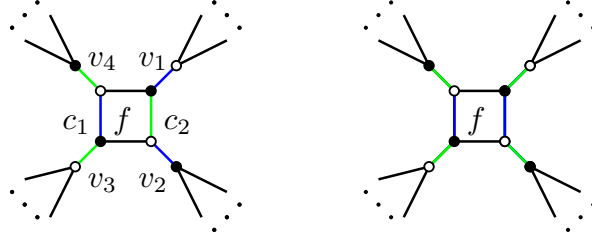


FIGURE 18. Left: the union $M_i \cup M_j$ in the proof of Proposition 6.13, with M_i in green. The edge of f in M_j is in the cycle C_1 , while the edge of f in M_i is in the cycle C_2 . Right: in green, the matching N in the proof of Proposition 6.13. This is obtained from M_i by removing all edges in $C_2 \cap M_i$ and adding all edges in $C_2 \cap M_j$.

If no M_i uses all of the e_i , there are two possibilities for M_i around f , shown in Figure 17. Note that M_i must also use either e_{i-1} or e_{i+1} , taking subscripts modulo 4.

Regardless of how you choose the M_i from the four columns of Figure 17, you will always obtain two matchings M_i, M_j containing opposite edges of f . In particular, if M_1 uses e_1 and e_2 without loss of generality, then either (i) M_2 or M_3 uses e_3 and e_4 or (ii) M_2 uses e_2 and e_3 while M_3 uses e_1 and e_4 . The union $M_i \cup M_j$ is a *double dimer* of G , and consists of a disjoint union of even cycles, with alternating edges in M_i and M_j , and paths, where every edge is in both M_i and M_j . In particular, each vertex of G has degree exactly 2 in $M_i \cup M_j$. Around f , the union $M_i \cup M_j$ looks like the left of Figure 18, with one edge of f in the cycle C_1 and the other edge in the cycle C_2 .

The cycles C_1 and C_2 are not the same. To see this, walk along C_2 starting at v_1 , then going to the edge in f , then to v_2 , and so on; call this the “counterclockwise walk” on C_2 . An edge e of C_2 is in M_i precisely if one encounters first the black vertex of e and then the white vertex in the counterclockwise walk. If $C_2 = C_1$, then the counterclockwise walk must leave v_2 , encounter v_4 , then the blue edge in f , then v_3 , then finally return to v_1 . Since $M_i \cup M_j$ is planar, this means some vertex of G has degree 4 in $M_i \cup M_j$, which is impossible.

As $C_1 \neq C_2$, the matching $N := (M_i \setminus C_2) \cup (M_j \cap C_2)$ is as pictured in Figure 18, and contains e_1, e_2, e_3, e_4 as desired. \square

We next show that reduction sequences always exist, which is Proposition 6.6.

Proof of Proposition 6.6. We induct on the number of non-infinite faces of G . The base case is when G is a single edge. The trivial sequence of no moves is a reduction sequence.

Now assume G has at least one non-infinite face. It suffices to show that one can apply (E) and (S) moves to G to obtain a graph G' with a bigon face f . Indeed, if G'' is the graph obtained from G' by applying (B) to f , then by induction, G'' has a reduction sequence \mathbf{r}'' . A reduction sequence of G is given by the sequence of moves to get from G to G' , then the move (B) at f , then \mathbf{r}'' .

We now show that there is a sequence of (E) and (S) moves which turns G into a graph with a bigon face. We use the theory of *reduced plabic graphs*, as presented in [20]. To make G into a plabic graph, choose any vertex v on the infinite face of G , embed G in a disk, and add an edge from v to a vertex on the disk, which we label 1. The resulting graph H is a plabic graph with one boundary vertex, which is not reduced as it has at least one face which does not touch the boundary of the disk.

By [20, Proposition 7.4.9], H can be transformed by the local moves (M1), (M2), (M3) of [20, Definition 7.1.3] into a bipartite plabic graph H' with a bigon face⁶, without ever creating internal leaves in the (M3) moves. By adding in extra (M2) moves to make the intermediate graphs bipartite, we may also obtain H' from H by a sequence of (E) and (S) moves. If no trivalent vertex in an (S) move is adjacent to the vertex 1, we still get a sequence of valid (E), (S) moves when we delete the vertex 1. We apply this sequence of moves to G gives a graph G' with a bigon face. If a trivalent vertex in an (S) move is adjacent to vertex 1, then we apply the sequence of moves up until that square move to G . The resulting graph has a square face with one degree 2 vertex w . Applying (E) to contract the edges adjacent to w gives a graph G' with a bigon face. \square

The next lemma establishes how the moves effect the dual quiver of G .

Lemma 6.14. *Suppose G has property (*). If G' is a graph obtained from G by move (E), move (S) at face f , or move (B) at face f then*

$$Q_{G'} = \begin{cases} Q_G \\ \mu_f(Q_G) \\ \mu_f(Q_G) \text{ with vertex } f \text{ deleted} \end{cases}$$

respectively.

Remark 6.15. For the cases of (E) and (S) moves, this has appeared previously in [53, Theorem 2] and [20, Prop. 7.1.5]. We note that the additional hypothesis (7.1.1) used in the latter is implied by the assumption that G has property (*) because of Lemma 6.12.

Proof of Lemma 6.14. (E): Performing move (E) either removes or introduces an oriented 2-cycle. Since oriented 2-cycles are deleted from Q_G , performing (E) does not change the dual quiver.

(S): We may assume using (E) moves that the vertices of face f are trivalent, as (E) does not change the dual quiver. Lemma 6.12 implies that among the four faces surrounding f , the consecutive ones are distinct; otherwise there would be an edge of G with the same face on both sides. Notice that none of the arrows dual to edges of f are in oriented 2-cycles, and so these four arrows are exactly the arrows incident to f in Q_G . It is now straightforward to check that $Q_{G'}$ is obtained from Q_G by adding an arrow $f' \rightarrow f''$ for each path $f' \rightarrow f \rightarrow f''$ in Q_G , reversing all arrows incident to f , and deleting oriented 2-cycles. This shows $Q_{G'} = \mu_f(Q_G)$.

(B): Property (*) implies that the vertices of the bigon face f are either both degree 2 or both degree at least 3. (If exactly one vertex were degree 2, an edge adjacent to the other vertex would never be used in a matching.) In the former case, G is just the bigon f , Q_G is a quiver with one vertex and no arrows, and $Q_{G'}$ is the empty quiver, and the claim holds.

So we may suppose both vertices of f are degree at least 3. Let f', f'' be the faces adjacent to f . These faces are distinct, as otherwise, one could use (E) to create an edge with the same face on both sides, contradicting Lemma 6.12. The arrows adjacent to f in Q_G are, say, $f' \rightarrow f \rightarrow f''$. The quiver $Q_{G'}$ is

⁶[20, Proposition 7.4.9] guarantees that one can turn H into a graph H' , not necessarily bipartite, with a “hollow digon” face. If the vertices of the digon are the same color, one can contract one of the edges to get a loop, then add a degree 2 vertex of the opposite color to create a bigon face with vertices of opposite colors. Then one can apply (M2) moves to make H' bipartite.

obtained from Q_G by replacing the path $f' \rightarrow f \rightarrow f''$ with the edge $f' \rightarrow f''$, deleting f and then possibly deleting a 2-cycle. This is exactly the same as $\mu_f(Q_G)$ with the vertex f deleted. \square

We now turn to how the F -polynomials in Theorem 6.8 and the dimer face polynomials D_G change under each of the moves.

We begin with (E) moves. The F -polynomials in Theorem 6.8 do not depend on the (E) moves in a reduction sequence for G . The next lemma, which is well known (see e.g. [27, Figure 23]), shows that the dimer face polynomials do not either.

Lemma 6.16. *Let G be a graph with property $(*)$ and suppose that G' is related to G by move (E). Then, identifying faces of G and G' , $D_G = D_{G'}$.*

Proof. There is a natural bijection ϵ between the dimer sets \mathcal{D}_G and $\mathcal{D}_{G'}$, given by



where the dimers agree on all edges that are not pictured (and the color of the vertices may be opposite). This map and its inverse are order-preserving: one can up-flip a face f in a dimer M of G if and only if one can up-flip the face f in the dimer $\epsilon(M)$ of G' . \square

For square and bigon moves, we will need the following result, relating F -polynomials computed with respect to adjacent initial seeds. This result is a combination of [14, Proposition 2.4] and [14, (9.1)]; in particular, [14, Proposition 2.4] involves two additional parameters h_b, h'_b , which are shown in [14, (9.1)] to equal $\min(0, g_b)$ and $\min(0, g'_b)$ respectively. We note that [14, Proposition 2.4] is essentially [22, (6.15), (6.28)], though in somewhat different notation.

Proposition 6.17. *Let $\Sigma = (\mathbf{x}, Q)$ be a seed and $\Sigma' := \mu_b(\Sigma)$. Choose z a mutable cluster variable in $\mathcal{A}(\Sigma)$, with g -vector $\mathbf{g}^\Sigma = (g_1, \dots, g_n)$ with respect to Σ and g -vector $\mathbf{g}^{\Sigma'} = (g'_1, \dots, g'_n)$ with respect to Σ' . Let $q_{ab} = \#\{a \rightarrow b \text{ in } Q\} - \#\{b \rightarrow a \text{ in } Q\}$. We set*

$$(8) \quad y'_a := \begin{cases} y_b^{-1} & \text{if } a = b \\ y_a(1 + y_b)^{q_{ab}} & \text{if } q_{ab} \geq 0 \\ y_a(1 + y_b^{-1})^{q_{ab}} & \text{if } q_{ab} \leq 0 \end{cases}$$

Then

$$(9) \quad (1 + y_b)^{\min(0, g_b)} F_z^\Sigma(y_1, \dots, y_n) = (1 + y'_b)^{\min(0, g'_b)} F_z^{\Sigma'}(y'_1, \dots, y'_n)$$

and

$$(10) \quad g'_a = \begin{cases} -g_b & \text{if } a = b \\ g_a + q_{ab}g_b - q_{ab} \min(0, g_b) & \text{if } q_{ab} \geq 0 \\ g_a - q_{ab} \min(0, g_b) & \text{if } q_{ab} \leq 0 \end{cases}$$

Since mutation is an involution, we may also reverse the roles of Σ, Σ' in Proposition 6.17, and the same result will hold.

Now we turn to square moves. Recall from Definition 6.7 the definition of the vector $\mathbf{h}^G(\hat{0})$. The next theorem shows that the conclusion of Theorem 6.8 is preserved under applying square moves to G .

Theorem 6.18. *Suppose G and G' are graphs with property $(*)$ related by a square move at face f . Let \mathbf{r} be a reduction sequence for G , and let z be as in Theorem 6.8. The sequence $\mathbf{r}' = (f, \mathbf{r})$ is a reduction sequence for G' ; define z' analogously to z , using G' instead. Let $\mathbf{g} := \mathbf{g}_z^{Q_G}$ and $\mathbf{g}' := \mathbf{g}_{z'}^{Q_{G'}}$ denote the g -vector of z and z' , respectively. Then*

- The resulting cluster variables z and z' are equal.
- We have $\mathbf{g} = \mathbf{h}^G(\hat{0})$ if and only if $\mathbf{g}' = \mathbf{h}^{G'}(\hat{0})$.
- Assuming $\mathbf{g} = \mathbf{h}^G(\hat{0})$ and $\mathbf{g}' = \mathbf{h}^{G'}(\hat{0})$, then $D_G = F_z^{Q_G}$ if and only if $D_{G'} = F_{z'}^{Q_{G'}}$.

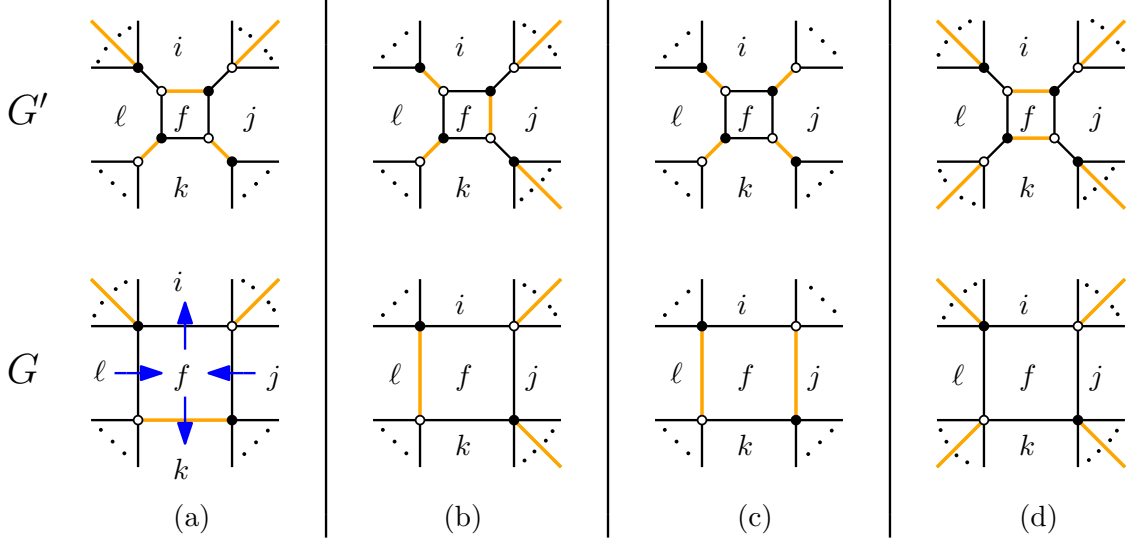


FIGURE 19. In orange, possible bottom matchings of G' (top) and G (bottom) in the proof of Theorem 6.18. We omit the 180 degree rotations of (a) and (b), since the arguments are identical for those cases. Matchings in the same column agree on all edges that are not shown. In Case (a), bottom, the arrows of Q_G involving f are in blue.

Proof. We first describe the relationship between the two F -polynomials and the two g -vectors. By Lemma 6.14, $Q_{G'} = \mu_f(Q_G)$. The F -polynomial depends only on the initial quiver, not the initial cluster variables, so we may choose to compute $F_z^{Q_G}$ by framing the seed $\Sigma = (\mathbf{x}, Q_G)$ and to compute $F_{z'}^{Q_{G'}}$ by framing the seed $\mu_f(\Sigma)$. With this choice, the mutation sequences to obtain z and z' differ by one entry and the two initial seeds are related by that same mutation, hence we obtain the equality $z = z'$. This shows our first claim and ensures that we are in exactly the situation of Proposition 6.17. So the g -vectors are related by (10) and we obtain $F_z^{Q_G} = F_z^\Sigma$ from $F_{z'}^{Q_{G'}} = F_z^{\mu_f(\Sigma)}$ by the substitution $y_i \mapsto y'_i$, where y'_i is defined in (8), and then multiplying by

$$\frac{(1 + y_f^{-1})^{\min(0, -g_f)}}{(1 + y_f)^{\min(0, g_f)}}.$$

For the second item of the theorem, recall that \mathbf{g}' is obtained from \mathbf{g} by (10) with $b = f$, and swapping the roles of Σ and Σ' (so swapping \mathbf{g} with \mathbf{g}' and Q with $\mu_b(Q)$) in (10), the equality still holds. Suppose $\mathbf{h}^G(\hat{0}) = \mathbf{g}$. If $\mathbf{h}^{G'}(\hat{0})$ is obtained from $\mathbf{h}^G(\hat{0})$ by (10), or if $\mathbf{h}^G(\hat{0})$ is obtained from $\mathbf{h}^{G'}(\hat{0})$ by (10) with $Q_{G'}$ in place of Q_G , then $\mathbf{h}^{G'}(\hat{0}) = \mathbf{g}'$. One may also reverse this argument by swapping G and G' everywhere. So it suffices to show that either $\mathbf{h}^{G'}(\hat{0})$ is obtained from $\mathbf{h}^G(\hat{0})$ by (10) with $b = f$, or that $\mathbf{h}^G(\hat{0})$ is obtained from $\mathbf{h}^{G'}(\hat{0})$ by (10) with $b = f$ and $Q_{G'}$ rather than Q_G .

There are 4 cases,

depending on the behavior of the bottom matching of G around f . See Figure 19 for an illustration.

Cases (a) and (b) differ since $\hat{0}$ includes a white-black edge of the face f in (a) but this is a black-white edge in case (b). Further, 90° rotations of cases (c) and (d) are impossible because such a rotation of case (c) would yield a matching of G that contains the black-white edges of f and thus admits a down-flip at f , so cannot be the bottom matching $\hat{0}$. Analogously, a 90° rotation of case (d) would yield a matching of G' containing the black-white edges of f which would not be the bottom matching.

Note that we may have $i = k$ or $j = \ell$ (but not both), and Lemma 6.12 implies no other faces can be the same. It is straightforward to verify that in each of the 4 cases, if no faces of G can be down-flipped in the matching using the edges in the bottom row of Figure 19, then no faces of G' can be down-flipped in the matching using the edges in the top row. That is, in each case, the top row of Figure 19 does in fact depict the bottom matching of G' .

In the arguments below, we use the notation $\mathbf{h}^G(\hat{0}) = (h_a)_{a \in \text{Face}(G)}$ and $\mathbf{h}^{G'}(\hat{0}) = (h'_a)_{a \in \text{Face}(G')}$. We follow the labeling of faces from Figure 19. In cases (a), (b),

$$h_f = 2 - 1 - 1 = 0 \quad \text{and} \quad h'_f = 2 - 1 - 1 = 0.$$

We also see that we add two edges to each of the faces i, j, k, ℓ when going from G to G' , and increase the number of edges per face in the bottom matching by one. No other faces are affected. Thus we have $\mathbf{h}^G(\hat{0}) = \mathbf{h}^{G'}(\hat{0})$. By inspection, in this case $\mathbf{h}^{G'}(\hat{0})$ is obtained from $\mathbf{h}^G(\hat{0})$ by (10) with $b = f$.

In case (c), we have $h_f = -1$ and $h'_f = 1$. One can compute that

$$h'_i = \begin{cases} h_i - 1 & \text{if } i \neq k \\ h_i - 2 & \text{if } i = k \end{cases}, \quad h'_j = h_j, \quad h'_k = \begin{cases} h_k - 1 & \text{if } i \neq k \\ h_k - 2 & \text{if } i = k \end{cases} \quad \text{and} \quad h'_\ell = h_\ell.$$

For example, the first equality is because we add two (or four) edges to i , and increase the number of edges in the bottom matching by two (or four). From the top left of Figure 19, we see q_{if} is either -1 or -2 , depending on if $i = k$. So we have

$$h'_i = h_i - q_{if} \min(0, h_f).$$

We also have $h'_j = h_j = h_j + q_{jf} h_f - q_{jf} \min(0, h_f)$, since $h_f < 0$. Analogous formulas hold for h'_k, h'_ℓ and all other entries of $\mathbf{h}^G(\hat{0})$ and $\mathbf{h}^{G'}(\hat{0})$ agree. So $\mathbf{h}^{G'}(\hat{0})$ is obtained from $\mathbf{h}^G(\hat{0})$ by (10) with $b = f$ for case (c) as well.

Case (d) is identical to case (c) if you swap G and G' and rotate face labels by 90° , i.e. rename i with j , j with k , etc. So the argument for case (c) shows $\mathbf{h}^{G'}(\hat{0})$ is obtained from $\mathbf{h}^G(\hat{0})$ by (10) using $Q_{G'}$ instead of Q_G and with $b = f$.

We now turn to the third item in the theorem, on F -polynomials. It suffices to verify that D_G can be obtained from $D_{G'}$ by the substitutions $y_f \mapsto y_f^{-1}$ and

$$y_i \mapsto y_i \left(\frac{y_f}{1 + y_f} \right)^{\#\{f \rightarrow i\}}, \quad y_j \mapsto y_j (1 + y_f)^{\#\{j \rightarrow f\}}, \quad y_k \mapsto y_k \left(\frac{y_f}{1 + y_f} \right)^{\#\{f \rightarrow k\}}, \quad y_\ell \mapsto y_\ell (1 + y_f)^{\#\{\ell \rightarrow f\}},$$

(where the exponents are based on the arrows of Q_G , and thus are all equal to 1 unless two faces coincide), followed by multiplication by

$$(11) \quad \frac{(1 + y_f^{-1})^{\min(0, -h_f)}}{(1 + y_f)^{\min(0, h_f)}} = \begin{cases} 1 & \text{in cases (a),(b) where } h_f = 0 \\ (1 + y_f) & \text{in case (c) where } h_f = -1 \\ (1 + y_f^{-1})^{-1} = y_f(1 + y_f)^{-1} & \text{in case (d) where } h_f = 1. \end{cases}$$

We will use this below after we first analyze the effect of the substitutions y_f, y_i, y_j, y_k , and y_ℓ .

We first consider terms of $D_{G'}$. Note that for each matching M of G' , there are either one or two matchings of G that agree with M away from f , which we will call N and N' . Similarly, for each matching N of G , there are either one or two matchings, called M and M' , which agree with N away from f . See Figure 20 for an illustration. Our method of proof is to show that for each of the possible bottom matchings in Figure 19, when we apply the specified substitutions and multiplication to $\mathbf{y}^{\text{ht}(M)}$ (or $\mathbf{y}^{\text{ht}(M)} + \mathbf{y}^{\text{ht}(M')}$, as appropriate), we obtain exactly $\mathbf{y}^{\text{ht}(N)}$ (or $\mathbf{y}^{\text{ht}(N)} + \mathbf{y}^{\text{ht}(N')}$, as appropriate). We determine the exponents of $y_f, y_i, y_j, y_k, y_\ell$ in $\text{ht}(M)$ (resp. $\text{ht}(M')$, $\text{ht}(N)$, and $\text{ht}(N')$) using Proposition 2.15. In this calculation, each term of $D_{G'}$ appears precisely once, and each term of D_G appears precisely once, so this verifies D_G is obtained from $D_{G'}$ by the substitutions and multiplication above.

There are 16 cases to consider since, up to rotation, the bottom matching $\hat{0}$ of G' can look locally around face f like one of the four matchings illustrated in Figure 19 (top row), and for each possible bottom matching, there are also four possible types of local configurations, up to rotation, for an arbitrary matching M , as illustrated in Figure 20 (top row). Applying the square move to $\hat{0}$ of G' yields the bottom matching $\hat{0}$ of G (as well as another matching in case (c)), and also replaces M (resp. M and M' in case (iv)) with N (resp. N and N' in case (iii)), a matching of G . The exponents of $y_f, y_i, y_j, y_k, y_\ell$ in $\text{ht}(N)$ are similarly computed using Proposition 2.15, and agree with the results of the aforementioned substitution and multiplication.

We begin by illustrating these arguments in the case when the bottom matching $\hat{0}$ of G' looks locally like the configuration of case (a).

Case (a), (i): Considering Figure 21, if M locally looks like case (i), then the local configuration around face f involves doubled edges and there are walks from faces i, j, k, ℓ to f which do not cross any edges of $\overrightarrow{M\Delta\hat{0}}$.

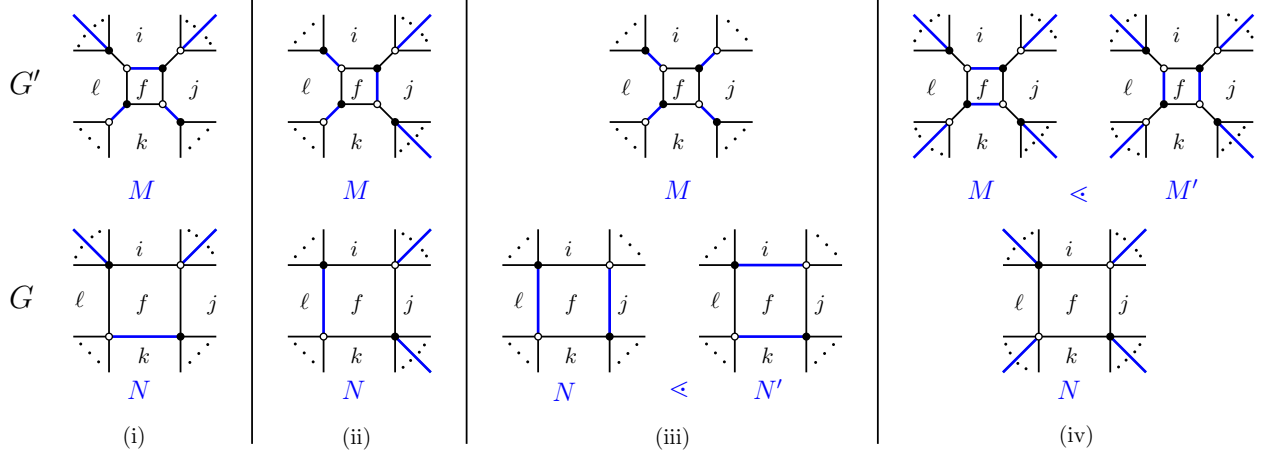


FIGURE 20. Correspondence between matchings of G' (top) and matchings of G (bottom) in the proof of Theorem 6.18. Matchings in the same column agree on the edges not pictured. For brevity, we do not picture the 180° rotations of the first two columns.

Thus, all 5 coordinates $\text{ht}(M)_i, \text{ht}(M)_j, \text{ht}(M)_k, \text{ht}(M)_\ell$, and $\text{ht}(M)_f$ are equal to each other. Furthermore, for this example, $\hat{0}_G$ is in case (a) so the quantity (11) equals 1, and under the specified substitution and multiplication, $\mathbf{y}^{\text{ht}(M)}$ is left invariant.

After applying the square move to get corresponding terms of D_G , we obtain $\overrightarrow{N\Delta\hat{0}}$ as in (i) of Figure 21. It is evident that $\text{ht}(N) = \text{ht}(M)$ in this case, so $\mathbf{y}^{\text{ht}(N)} = \mathbf{y}^{\text{ht}(M)}$, exactly as desired.

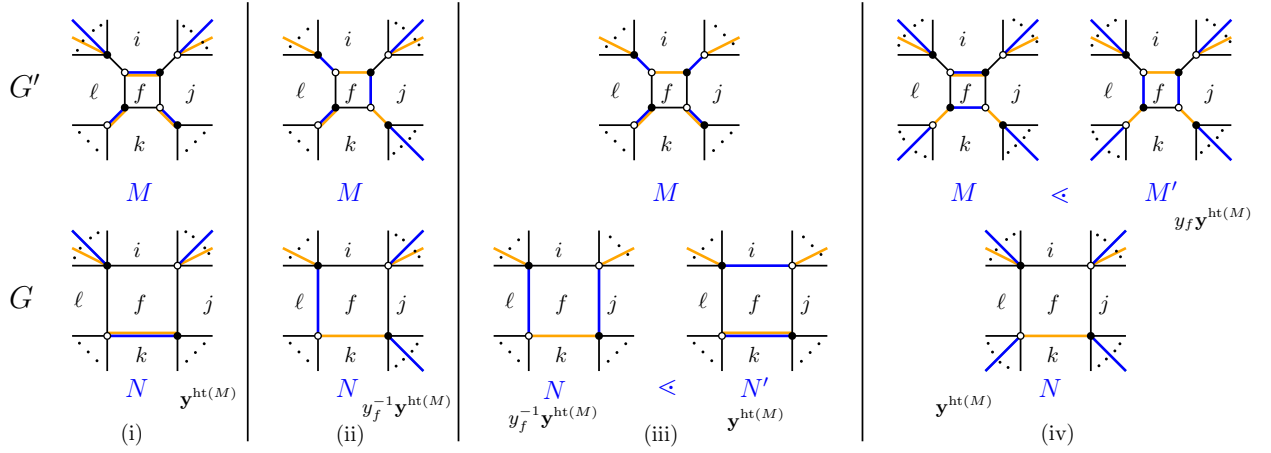


FIGURE 21. Orange edges give the bottom matching of G' (top) and G (bottom) in case (a) from Figure 19. In blue, matchings of G' (top) and the corresponding matchings of G (bottom). Next to each matching different from M is the corresponding term of the dimer polynomial, written in terms of $\mathbf{y}^{\text{ht}(M)}$.

Case (a), (ii): We repeat the above analysis, continuing to assume that the bottom matching $\hat{0}$ of G' is as in case (a), but letting M be as in case (ii). Then, a cycle in $\overrightarrow{M\Delta\hat{0}}$ separates faces i and j from the other three faces. Since the edge between i and f is in $\hat{0}$ and so oriented white-to-black in $\overrightarrow{M\Delta\hat{0}}$, $\text{ht}(M)_i = \text{ht}(M)_f - 1$ by Proposition 2.15. We also have $\text{ht}(M)_j = \text{ht}(M)_f - 1$ since there is a walk from i to j which passes through no edges of $\overrightarrow{M\Delta\hat{0}}$. The other two coordinates $\text{ht}(M)_k, \text{ht}(M)_\ell$ are equal to $\text{ht}(M)_f$ because there

are walks from faces k, ℓ to f which do not cross any edges of $\overrightarrow{M\Delta\hat{0}}$. Further, since $\hat{0}$ is in case (a), the quantity (11) equals 1 just as above.

Under the desired substitutions, one may check that the binomial factors arising from y'_i and y'_j cancel each other out, as do those from y'_k and y'_ℓ , so we obtain

$$\begin{aligned} y_f^r y_i^{r-1} y_j^{r-1} y_k^r y_\ell^r &\mapsto y_f^{-r} y_i^{r-1} \left(\frac{y_f}{1+y_f} \right)^{r-1} y_j^{r-1} (1+y_f)^{r-1} y_k^r \left(\frac{y_f}{1+y_f} \right)^r y_\ell^r (1+y_f)^r \\ &= y_f^{-1} (y_f^r y_i^{r-1} y_j^{r-1} y_k^r y_\ell^r). \end{aligned}$$

Under the specified substitution and multiplication, $\mathbf{y}^{\text{ht}(M)} \mapsto y_f^{-1} \mathbf{y}^{\text{ht}(M)}$.

Applying the square move to get the corresponding matching N of G , we see $\text{ht}(N) = \text{ht}(M) - \mathbf{e}_f$. In particular, the cycle in $\overrightarrow{M\Delta\hat{0}}$ separating faces i , and j from the rest of the local configuration now “bends” around face f in $N\Delta\hat{0}$ so that faces i, j and f are on the same side (see Figure 21 (ii)). So $\mathbf{y}^{\text{ht}(N)} = y_f^{-1} \mathbf{y}^{\text{ht}(M)}$, exactly as desired.

Case (a), (iii): If M is as in case (iii), then a cycle in $\overrightarrow{M\Delta\hat{0}}$ separates i from the other four faces. Since the edge between i and f is in $\hat{0}$ and so oriented white-to-black in $\overrightarrow{M\Delta\hat{0}}$, $\text{ht}(M)_i = \text{ht}(M)_f - 1$ by Proposition 2.15. The other three coordinates $\text{ht}(M)_j, \text{ht}(M)_k, \text{ht}(M)_\ell$ are equal to $\text{ht}(M)_f$ because there are walks from faces j, k, ℓ to f which do not cross any edges of $\overrightarrow{M\Delta\hat{0}}$. In this case, under the substitutions above, the binomial factors do not fully cancel out each other, and one may check that

$$\begin{aligned} y_f^r y_i^{r-1} y_j^r y_k^r y_\ell^r &\mapsto y_f^{-r} y_i^{r-1} \left(\frac{y_f}{1+y_f} \right)^{r-1} y_j^r (1+y_f)^r y_k^r \left(\frac{y_f}{1+y_f} \right)^r y_\ell^r (1+y_f)^r = y_f^r y_f^{-1} (1+y_f) y_i^{r-1} y_j^r y_k^r y_\ell^r \\ &= (1+y_f^{-1}) (y_f^r y_i^{r-1} y_j^r y_k^r y_\ell^r). \end{aligned}$$

Under the specified substitution and multiplication by (11) which equals 1, we get $\mathbf{y}^{\text{ht}(M)} \mapsto \mathbf{y}^{\text{ht}(M)} (1+y_f^{-1})$. We turn now to the corresponding terms of D_G . The corresponding matchings N and N' of G are as in column (iii) of Figure 21. Then $\text{ht}(N') = \text{ht}(M)$ and $\text{ht}(N) = \text{ht}(N') - \mathbf{e}_f = \text{ht}(M) - \mathbf{e}_f$ since N is obtained from N' by a down-flip at face f (cf. Proposition 2.18). So $\mathbf{y}^{\text{ht}(N')} + \mathbf{y}^{\text{ht}(N)} = (1+y_f^{-1}) \mathbf{y}^{\text{ht}(M)}$, exactly as desired.

Case (a), (iv): Finally, if M and M' are as in case (iv), then a cycle in $\overrightarrow{M\Delta\hat{0}}$ separates k from the other four faces. Since the edge between j and k is in $\hat{0}$ and so oriented white-to-black in $\overrightarrow{M\Delta\hat{0}}$ and $\overrightarrow{M'\Delta\hat{0}}$, we have $\text{ht}(M)_k = \text{ht}(M)_f + 1$ by Proposition 2.15. The other three coordinates $\text{ht}(M)_j, \text{ht}(M)_\ell$ are equal to $\text{ht}(M)_f$. Since M' is obtained from M by an up-flip at f , we have $\text{ht}(M') = \text{ht}(M) + \mathbf{e}_f$.

Again, under the substitutions above, the binomial factors do not fully cancel out each other, and one may check that $\mathbf{y}^{\text{ht}(M)}$ transforms as

$$\begin{aligned} y_f^r y_i^r y_j^r y_k^{r+1} y_\ell^r &\mapsto y_f^{-r} y_i^r \left(\frac{y_f}{1+y_f} \right)^r y_j^r (1+y_f)^r y_k^{r+1} \left(\frac{y_f}{1+y_f} \right)^{r+1} y_\ell^r (1+y_f)^r \\ &= y_f (1+y_f)^{-1} (y_f^r y_i^r y_j^r y_k^{r+1} y_\ell^r) \end{aligned}$$

while $\mathbf{y}^{\text{ht}(M')}$ transforms instead as

$$\begin{aligned} y_f^{r+1} y_i^r y_j^r y_k^{r+1} y_\ell^r &\mapsto y_f^{-r-1} y_i^r \left(\frac{y_f}{1+y_f} \right)^r y_j^r (1+y_f)^r y_k^{r+1} \left(\frac{y_f}{1+y_f} \right)^{r+1} y_\ell^r (1+y_f)^r \\ &= (1+y_f)^{-1} (y_f^r y_i^r y_j^r y_k^{r+1} y_\ell^r). \end{aligned}$$

Under the specified substitution and multiplication by (11) which equals 1, we get $\mathbf{y}^{\text{ht}(M)} + \mathbf{y}^{\text{ht}(M')} \mapsto \mathbf{y}^{\text{ht}(M)} y_f (1+y_f)^{-1} + \mathbf{y}^{\text{ht}(M)} (1+y_f)^{-1} = \mathbf{y}^{\text{ht}(M)}$. We turn now to the corresponding terms of D_G . The corresponding matching N of G is as in column (iv) of Figure 21. Then $\text{ht}(N) = \text{ht}(M)$, and so $\mathbf{y}^{\text{ht}(N)} = \mathbf{y}^{\text{ht}(M)}$, exactly as desired.

If the bottom matching $\hat{0}$ is not as in case (a), we utilize variants of the above arguments. For instance, if $\hat{0}$ is as in case (c), the analogous superpositions are illustrated in Figure 22. The algebraic substitutions and height calculations proceed analogously to above. The only substantive difference in argument is that the multiplicative factor (11) is instead $(1+y_f)$ in this case. This factor arises since the bottom matching $\hat{0}$ of G' corresponds via square move to two (not one) matchings of G . One of them is the corresponding bottom

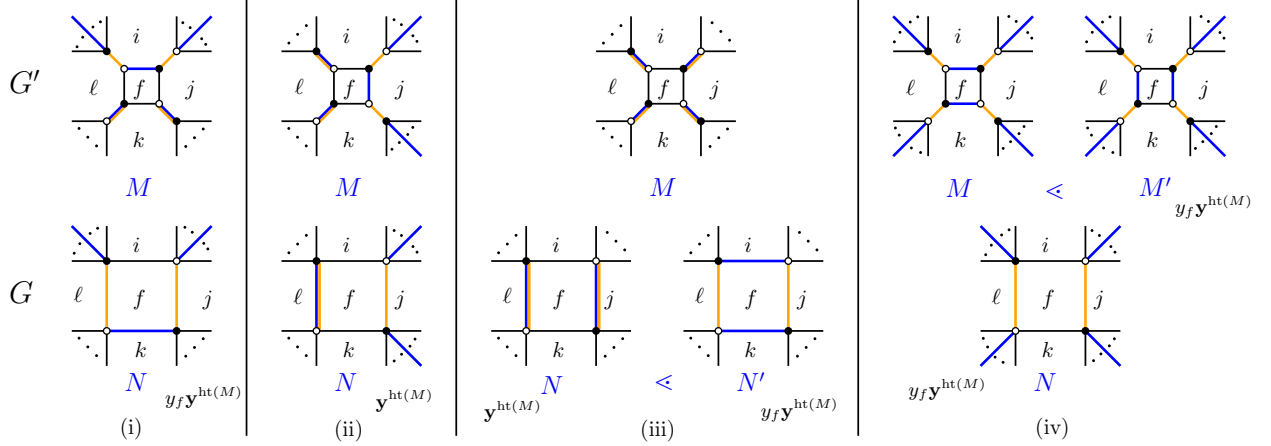


FIGURE 22. Orange edges give the bottom matching of G' (top) and G (bottom) in case (c) from Figure 19. In blue, matchings of G' (top) and the corresponding matchings of G (bottom). Next to each matching different from M is the corresponding term of the dimer polynomial, written in terms of $\mathbf{y}^{\text{ht}(M)}$.

matching of G , this is the one illustrated in column (c) of Figure 19, but a 90° rotation of this matching of G also arises, and that corresponds a height of y_f instead of 1, the second term of (11) in this case. The arguments for cases (b) and (d) are analogous to those for (a) and (c), although the multiplicative factor (11) is $y_f(1 + y_f)^{-1}$ in case (d) since two matchings of G' correspond to the bottom matching of G .

□

Remark 6.19. Theorem 6.18 asserts that under a square move, dimer face polynomial changes according to the substitutions in (8) followed by multiplication by (11). Similar results have been proved for partition functions in various contexts. In the case of plabic graphs (see Section 8), Postnikov shows in [47, Lemma 12.2] that, under a square move, the images of the boundary measurement map are related by applying a substitution $z_e \mapsto z'_e$, which becomes precisely the substitution in (8) under the change of variables between $\{z_e\}$ and $\{y_f\}$ in Remark 3.5. Translating his results into the language of matchings (cf. the discussion of urban renewal in [40, Section 3.4]), for plabic graphs, under a square move, the partition functions for *almost perfect matchings with a fixed boundary* are related by the substitution $z_e \mapsto z'_e$ in [40, Figure 7], followed by simultaneous rescaling. There is an alternative indirect proof of Theorem 6.18 using Postnikov's result and the transformations between partition functions and the dimer face polynomials in Remark 3.5. See also [37, 7.6] where Marsh and Scott use shear weights and Plücker relations for the special case of reduced plabic graphs for Grassmannians.

A related argument appears in Speyer's work [55, Sec 4.2] for the special case of graphs from the Octahedron recurrence and using a different definition of face weights. Goncharov and Kenyon [27, Theorem 4.7] approach a larger class of graphs associated to cluster integrable systems and use the Cluster-Poisson structure to demonstrate that under a square move, the partition function changes according to the substitutions $y_i \mapsto y'_i$.

We now examine the effect of bigon removal.

Theorem 6.20. Suppose G is a graph with property $(*)$ and G' is obtained from G by a bigon removal at face f . Let \mathbf{r}' be a reduction sequence for G' , and let z' be as in Theorem 6.8. The sequence $\mathbf{r} = (f, \mathbf{r}')$ is a reduction sequence for G ; define z analogously to z' , using G instead. Let $\mathbf{g} := \mathbf{g}_z^{Q_G}$ and $\mathbf{g}' := \mathbf{g}_{z'}^{Q_{G'}}$ denote the g -vector of z and z' , respectively. If $F_z^{Q_{G'}} = D_{G'}$ and $\mathbf{g}' = \mathbf{h}^{G'}(\hat{0})$, then $F_z^{Q_G} = D_G$ and $\mathbf{g} = \mathbf{h}^G(\hat{0})$.

Proof. Let $\Sigma = (\mathbf{x}, Q_G)$ and set $\Sigma'' := \mu_f(\Sigma)$. Note that z is the cluster variable of $\mu_{\mathbf{r}}(\Sigma'')$ indexed by the final mutation in the reduction sequence. We have that F_z^Σ and $F_z^{\Sigma''}$ are related as in Proposition 6.17.

By Lemma 6.14, the quiver $Q_{G'}$ differs from $Q'' = \mu_f(Q_G)$ by deleting vertex f . In other words, $Q_{G'}$ is the induced subquiver of Q'' on all vertices besides f . Applying Proposition 5.11 with $w = z'$ and $w' = z$,

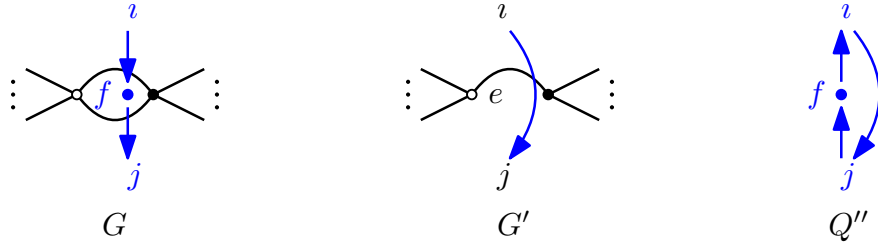


FIGURE 23. Left: The graph G near the face f and the arrows of Q_G adjacent to f in the proof of Theorem 6.20. Center: The graph G' and the arrow contributed by the faces i and j . Right: The arrows of $\mu_f(Q_G) = Q''$ that differ from those of Q_G .

we have that $F_z^{\Sigma''}$ is equal to $F_z^{Q_{G'}}$, and the g -vectors $\mathbf{g}' = \mathbf{g}_z^{Q_{G'}}$ and $\mathbf{g}'' := \mathbf{g}_z^{\Sigma''}$ agree in all coordinates except the coordinate g_f'' of the latter vector.

We first use the equalities $F_z^{\Sigma''} = F_z^{Q_{G'}} = D_{G'}$ together with some properties of F -polynomials to deduce the value of g_f'' . Suppose the faces adjacent to f in G are i, j , and let e be the edge of f which is not deleted in the bigon removal, so e is an edge shared by i, j in G' . Say e is white-black in j and black-white in i . See Figure 23. We claim

$$(12) \quad g_f'' = \begin{cases} 0 & \text{if } e \notin \hat{0}_{G'} \\ 1 & \text{if } e \in \hat{0}_{G'}. \end{cases}$$

By Theorem 5.10, a Laurent polynomial formula for z in terms of the cluster \mathbf{u} of Σ'' is

$$F_z^{\Sigma''}(\hat{y}_1, \dots, \hat{y}_n) \cdot \mathbf{u}^{\mathbf{g}''}.$$

If you put this expression over a common denominator and write it in lowest terms, you obtain the expression from Theorem 5.5 (1). In particular, by Theorem 5.5 (2), the resulting expression does not have u_f as a factor of the denominator, as z is compatible with u_f . It also does not have u_f as a factor of the numerator. Because of the arrow configuration in Q'' (see Figure 23, right) the variable u_f is in the numerator of \hat{y}_i and in the denominator of \hat{y}_j . We next determine how y_i and y_j appear in terms of $F_z^{\Sigma''}$.

Suppose that $e \notin \hat{0}_{G'}$. Then for any term $\mathbf{y}^{\text{ht}(M)}$ of $D_{G'} = F_z^{\Sigma''}$, either $\text{ht}(M)_i = \text{ht}(M)_j$ or $\text{ht}(M)_i = \text{ht}(M)_j + 1$. Indeed, as i, j are adjacent faces, there is at most one cycle C in $\overrightarrow{M\Delta 0}$ which encircles one of i, j but not the other. If there is such a cycle, then C must contain e . This implies $e \in M$, so e is oriented black-to-white. This means that e is left-to-right with respect to the dual edge of the dual graph G^* oriented from i to j . Using Proposition 2.15, this implies $\text{ht}(M)_i = \text{ht}(M)_j + 1$. A similar argument shows that if $e \in \hat{0}_{G'}$, then in any term $\mathbf{y}^{\text{ht}(M)}$ of $D_{G'}$, either $\text{ht}(M)_i = \text{ht}(M)_j$ or $\text{ht}(M)_i = \text{ht}(M)_j - 1$. Using this, we will determine how u_f appears in terms of $F_z^{\Sigma''}(\hat{y}_1, \dots, \hat{y}_n)$.

If $e \notin \hat{0}_{G'}$, the above paragraph implies u_f only appears in numerators of terms in $F_z^{\Sigma''}(\hat{y}_1, \dots, \hat{y}_n)$. When we write $F_z^{\Sigma''}(\hat{y}_1, \dots, \hat{y}_n)$ over a (least) common denominator, u_f still appears only in the numerator, and does not appear in all terms since F -polynomials have constant term 1. Thus, $g_f'' = 0$; otherwise, u_f would be a factor of either the numerator or denominator of z .

If $e \in \hat{0}_{G'}$, then u_f appears with exponent 0 or -1 in terms of $F_z^{\Sigma''}(\hat{y}_1, \dots, \hat{y}_n)$. There is at least one term in which u_f appears with exponent -1 : there is some matching M of G' which uses an edge adjacent to e . Thus, e is in a cycle of $\overrightarrow{M\Delta 0}$, and is oriented white-to-black in this cycle. Using Proposition 2.15, we have $\text{ht}(M)_i = \text{ht}(M)_j - 1$, so u_f appears with exponent -1 in this term. Thus, when $F_z^{\Sigma''}(\hat{y}_1, \dots, \hat{y}_n)$ is written over a least common denominator, u_f is a factor of the denominator, u_f^2 is not, and u_f is not a factor of the numerator. This implies that $g_f'' = 1$; otherwise, u_f would be a factor of the denominator or the numerator of z . This shows (12).

Now, we show that $\mathbf{g} = \mathbf{h}^G(\hat{0})$. All coordinates of \mathbf{g}'' which are not indexed by f agree with the coordinates of $\mathbf{g}' = \mathbf{h}^{G'}(\hat{0})$. Also, \mathbf{g}, \mathbf{g}'' are related by (10). The two possible bottom matchings of G' and G are given in Figure 24, left. It is easy to see that if $e \notin \hat{0}_{G'}$, then $h_f^G = 0$ and all other coordinates of $\mathbf{h}^G(\hat{0})$ are the same as those of $\mathbf{h}^{G'}(\hat{0})$. This agrees with \mathbf{g} , computed using (10) with \mathbf{g} taking the role of \mathbf{g}' , \mathbf{g}'' taking the

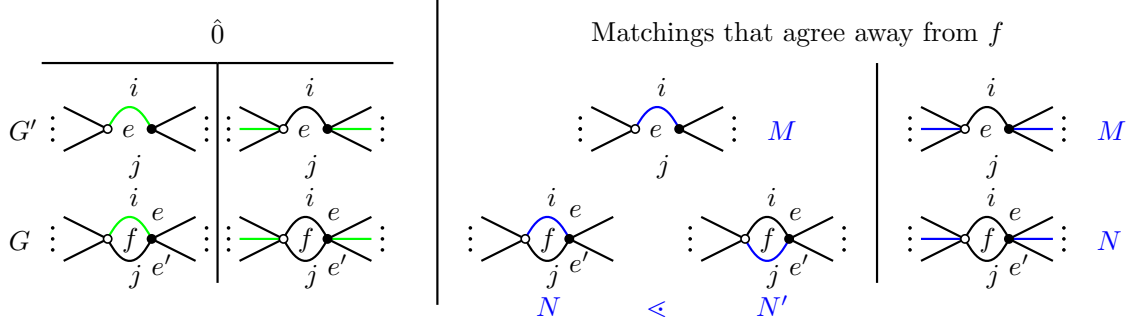


FIGURE 24. Left: The two possibilities for bottom matchings of G' and G . Right: Correspondence between matchings of G' (top) and G (bottom). Matchings in the same column agree on the edges not pictured.

role of \mathbf{g} , and q_{ab} computed using Q'' . If $e \in \hat{0}_{G'}$, then $h_f^G = -1$, which is equal to g_f . We also have that $h_j^G = h_j^{G'} + 1$, since in G , one fewer edge of j is in the bottom matching. All other coordinates of $\mathbf{h}^G(\hat{0})$ and $\mathbf{h}^{G'}(\hat{0})$ agree. This again agrees with \mathbf{g} , computed using (10).

Finally, we show that $F_z^{Q_G} = D_G$, using Proposition 6.17 together with the assumption that $F_z^{\Sigma''} = F_z^{Q_{G'}} = D_{G'}$. By Proposition 6.17, F_z^{Σ} is obtained from $F_z^{\Sigma''}$ by the substitutions

$$(13) \quad y_f \mapsto y_f^{-1}, \quad y_i \mapsto y_i(1 + y_f), \quad y_j \mapsto y_j(1 + y_f^{-1})^{-1} = y_j \frac{y_f}{1 + y_f}$$

followed by multiplication by

$$\begin{cases} 1 & \text{if } g_f = 0 \\ 1 + y_f & \text{if } g_f = -1. \end{cases}$$

So it suffices to show that D_G can be obtained from $D_{G'}$ by the same substitutions and multiplication.

As in the proof of Theorem 6.18, for each matching M of G' there are one or two matchings N, N' of G which agree with M away from f . Distinct matchings of G' correspond to distinct matchings of G , and every matching of G corresponds to some matching of G' . See Figure 24, right. We will compare the term $\mathbf{y}^{\text{ht}(M)}$ in $D_{G'}$ to $\mathbf{y}^{\text{ht}(N)}$ or $\mathbf{y}^{\text{ht}(N)} + \mathbf{y}^{\text{ht}(N')}$ in D_G to verify they are related by (13) and the appropriate multiplication.

We consider the case then the bottom matching of G' uses e (Figure 24, far left) and $g_f = -1$, as the other case is similar.

Suppose a matching M of G' does not use e , so $\overrightarrow{M\Delta\hat{0}}$ has a cycle using e . As argued previously, this implies that $r := \text{ht}(M)_j = \text{ht}(M)_i + 1$. When the edge e' is added, every cycle of $\overrightarrow{M\Delta\hat{0}}$ which encircles j becomes a cycle of $\overrightarrow{N\Delta\hat{0}}$ which encircles f and j . So $\mathbf{y}^{\text{ht}(N)} = y_f^{r+1} \mathbf{y}^{\text{ht}(M)}$. On the other hand, under (13), $y_i^r y_j^{r+1} \mapsto (y_i^r y_j^{r+1}) y_f^{r+1} (1 + y_f)^{-1}$, so under (13) and multiplication by $1 + y_f$, $\mathbf{y}^{\text{ht}(M)} \mapsto \mathbf{y}^{\text{ht}(N)}$.

If M does use e , then $\text{ht}(M)_i = \text{ht}(M)_j =: r$. We have

$$\mathbf{y}^{\text{ht}(N')} + \mathbf{y}^{\text{ht}(N)} = y_f^r \mathbf{y}^{\text{ht}(M)} + y_f^{r+1} \mathbf{y}^{\text{ht}(M)} = (1 + y_f) y_f^r \mathbf{y}^{\text{ht}(M)}.$$

On the other hand, under (13), $y_i^r y_j^r \mapsto (y_i^r y_j^r) y_f^r$, so after multiplication by $1 + y_f$, we have $\mathbf{y}^{\text{ht}(M)} \mapsto \mathbf{y}^{\text{ht}(N')} + \mathbf{y}^{\text{ht}(N)}$. \square

6.3. Proofs of Theorem 6.8 and Corollary 6.10.

Proof of Theorem 6.8. We now prove Theorem 6.8. By Lemma 6.16, (E) moves do not change D_G ; by Lemma 6.14 (E) moves do not change Q_G and thus do not change any F -polynomials. So we may assume, by replacing G with another graph related by (E) moves, that one may apply a move at f_1 in G .

We proceed by induction on the length of the reduction sequence \mathbf{r} . If $\mathbf{r} = (f_1)$ consists of a single face, then G is a bigon, and Q_G is a single vertex. One can verify that $D_G = 1 + y_f = F_z^{Q_G}$, and that $\mathbf{h}^G(\hat{0}) = (-1) = \mathbf{g}$.

Now, suppose $\mathbf{r} = (f_1, \mathbf{r}')$ is length at least 2. Let G' be the graph obtained from G by performing the appropriate move at f_1 ; it has reduction sequence \mathbf{r}' , of shorter length. If f_1 is a square face, then the inductive hypothesis together with Theorem 6.18 (with the roles of G and G' swapped) imply that $\mathbf{g} = \mathbf{h}^G(\hat{0})$ and $D_G = F_z^{Q_G}$. If f_1 is a bigon, then the inductive hypothesis together with Theorem 6.20 imply that $\mathbf{g} = \mathbf{h}^G(\hat{0})$ and $D_G = F_z^{Q_G}$. This completes the proof. \square

Proof of Corollary 6.10. Let \mathbf{g} and F respectively denote the g -vector and F -polynomial of z with respect to Σ . Recall from Definition 5.9 that for each face $a \in \text{Face}(G)$, or equivalently every vertex a of the quiver, we define the exchange ratio

$$\hat{y}_a := \frac{\prod_{f \rightarrow a} x_f}{\prod_{a \rightarrow f} x_f}.$$

By Theorem 6.8, we know that $\mathbf{x}^{\mathbf{g}} = \mathbf{x}^{\mathbf{h}^G(\hat{0})}$.

So, appealing to Theorem 5.10, to show the desired cluster expansion, it suffices to show that

$$D_G(\hat{y}_f) = \sum_{M \in \mathcal{D}_G} \mathbf{x}^{\mathbf{h}^G(M) - \mathbf{h}^G(\hat{0})}.$$

We argue equality term by term, traveling up the dimer lattice. The term indexed by $\hat{0}$ on the right and left sides is 1. Assume we have equality for the term indexed by N and suppose $N \triangleleft M$ are related by an up-flip at face a . On the left-hand side, we multiply the term indexed by N by \hat{y}_a . On the right-hand side, we multiply by

$$\mathbf{x}^{\mathbf{h}^G(N) - \mathbf{h}^G(M)} = \prod_{f \in \text{Face}(G)} x_f^{|M \cap f| - |N \cap f|}.$$

Every white-black edge of a which is in f contributes 1 to the power of x_f , while every black-white edge of a which is in f contributes -1 to the power of x_f . Since each white-black edge of a which is in f also contributes an arrow $f \rightarrow a$, and each black-white edge contributes an arrow $a \rightarrow f$, we see that

$$\prod_{f \in \text{Face}(G)} x_f^{|M \cap f| - |N \cap f|} = \hat{y}_a.$$

This shows the terms indexed by M on both sides are equal.

For the denominator vector statement, notice that $|f|/2 - |M \cap f| - 1 \geq -1$, and equality occurs precisely when f can be flipped in M . So x_f appears in the term $\mathbf{x}^{\mathbf{h}^G(M)}$ with negative exponent if and only if f can be flipped in matching M , in which case the exponent of x_f is -1 . By Corollary 2.21, every face can be flipped in some matching, so every x_f appears in some term with exponent -1 . So

$$z = \frac{P(\mathbf{x})}{\prod_{f \in \text{Face}(G)} x_f}$$

where $P(\mathbf{x})$ is not divisible by any x_f . This gives the desired statement about the denominator vector. \square

7. FURTHER CLUSTER ALGEBRA APPLICATIONS TO LINKS

In this section, we focus on a link diagram L and the corresponding graphs $G_{L,i}$. We first show that all of the dimer face polynomials $\{D_{G_{L,i}}\}_i$ are F -polynomials in a single cluster algebra. We then discuss the relationship between certain moves, which appeared recently in [2] to prove a stronger statement, and the graph moves in Definition 6.4. Finally, we focus on 2-bridge links, whose Alexander polynomials were previously connected to type A F -polynomials and were computed using matchings of *snake graphs* [1, Section 8] based on earlier work on snake graphs and continued fractions [4] on the one hand, and on cluster algebras and Jones polynomials [35, Sections 5 and 6] on the other. In this case, we show that $G_{L,i}$ is not a snake graph, but does have the same dimer lattice.

7.1. All multivariate Alexander polynomials in one cluster algebra. In Section 4, we showed that the Alexander polynomial of a link with diagram L can be obtained by choosing any segment i of L and specializing the polynomial $D_{G_{L,i}}$. The graphs $G_{L,i}$ satisfy property $(*)$, so Theorem 6.8 shows that $D_{G_{L,i}}$ is an F -polynomial for the cluster algebra $\mathcal{A}(\mathbf{x}, Q_{G_{L,i}})$. In this section, we show that all of the polynomials $\{D_{G_{L,i}}\}_i$ are F -polynomials of a single larger cluster algebra. This was conjectured in [1]. It was also proved, using categorical techniques, in [2],

while we were in the final stages of preparing this manuscript.

We first need a slightly extended notion of dual quiver Q_G .

Definition 7.1. Let G be a bipartite plane graph. The *extended dual quiver* Q_G^{ext} is defined according to the same procedure as in Definition 6.1, except there is also a mutable vertex in the infinite face, and arrows are drawn across every edge separating two distinct faces.

Theorem 7.2. Let L be a connected prime-like link diagram with no nugatory crossings and G_L the face-crossing incidence graph. For a segment i , let $\hat{0}_{L,i}$ denote the bottom matching of the graph $G_{L,i}$ and let f_i denote the face containing i . Then for every segment i , there is a cluster variable z_i in the cluster algebra $\mathcal{A}(\Sigma_0) = \mathcal{A}(\mathbf{x}, Q_{G_L}^{\text{ext}})$ such that

$$F_{z_i}^{\Sigma_0}(\mathbf{y}) = D_{G_{L,i}}(\mathbf{y}).$$

Further,

- (1) the g -vector of z_i is equal to $\mathbf{h}^G(\hat{0}_{L,i}) - \mathbf{e}_{f_i}$ and so has entries

$$g_f = \begin{cases} 0 & \text{if } f = f_i \\ |f \cap \hat{0}_{L,i}| + 1 & \text{else;} \end{cases}$$

- (2) the formula for z_i in terms of the initial cluster is

$$z_i = \sum_{M \in \mathcal{D}_{G_{L,i}}} \mathbf{x}^{\mathbf{h}^G(M) - \mathbf{e}_{f_i}}$$

- (3) the denominator vector of z_i has entries

$$d_f = \begin{cases} 0 & \text{if } f \text{ shares a white vertex with } f_i \\ 1 & \text{else.} \end{cases}$$

We note that the existence of the cluster variables z_i and the formula for their denominator vectors were also obtained in [2]. For an illustration of Theorem 7.2, see Figure 25.

Proof. Choose a segment i of L .

For the existence of the cluster variable z_i , note that G_L and $Q_{G_L}^{\text{ext}}$ may both be drawn on the sphere. Stereographically project both G_L and $Q_{G_L}^{\text{ext}}$ to the plane so that the face f_i is the infinite face. Deleting the white vertices of f_i in G_L yields the graph $G_{L,i}$. Deleting the vertices of $Q_{G_L}^{\text{ext}}$ labeled by faces sharing a white vertex with f_i yields the quiver $Q_{G_{L,i}}$. That is, the quiver $Q_{G_{L,i}}$ is an induced subquiver of Q_{G_L} . By Theorem 6.8, $D_{G_{L,i}}$ is an F -polynomial in the cluster algebra $\mathcal{A}(Q_{G_{L,i}})$, obtained from the initial seed by mutation sequence \mathbf{r} . By Proposition 5.11, there is a cluster variable z_i of $\mathcal{A}(\mathbf{x}, \mathbf{y}, Q_{G_L}^{\text{ext}})$, again obtained by the mutation sequence \mathbf{r} , whose F -polynomial is $D_{G_{L,i}}$.

Since $Q_{G_{L,i}}$ omits face f_i and its neighbors, mutation sequence \mathbf{r} cannot include these, hence z_i is compatible with the initial cluster variables

$$\{x_f : f = f_i \text{ or } f \text{ adjacent to } f_i\}.$$

This, together with Corollary 6.10, also implies that the denominator vector of z_i is as claimed in (3).

We prove (1) and (2) together. First, for all faces f of G_L which are also faces of $G_{L,i}$, Theorem 6.8 and Proposition 5.11 implies that

$$g_f = |f|/2 - |f \cap \hat{0}_{L,i}| - 1.$$

This is equal to the coordinate h_f of $\mathbf{h}^G(\hat{0}_{L,i})$ by definition. So we only need to compute g_f for f containing a white vertex of f_i . Second, an identical proof as the proof of Corollary 6.10 shows that

$$D_{G_{L,i}}(\hat{y}_f) = \sum_{M \in \mathcal{D}_{G_{L,i}}} \mathbf{x}^{\mathbf{h}^G(M) - \mathbf{h}^G(\hat{0}_{L,i})}.$$

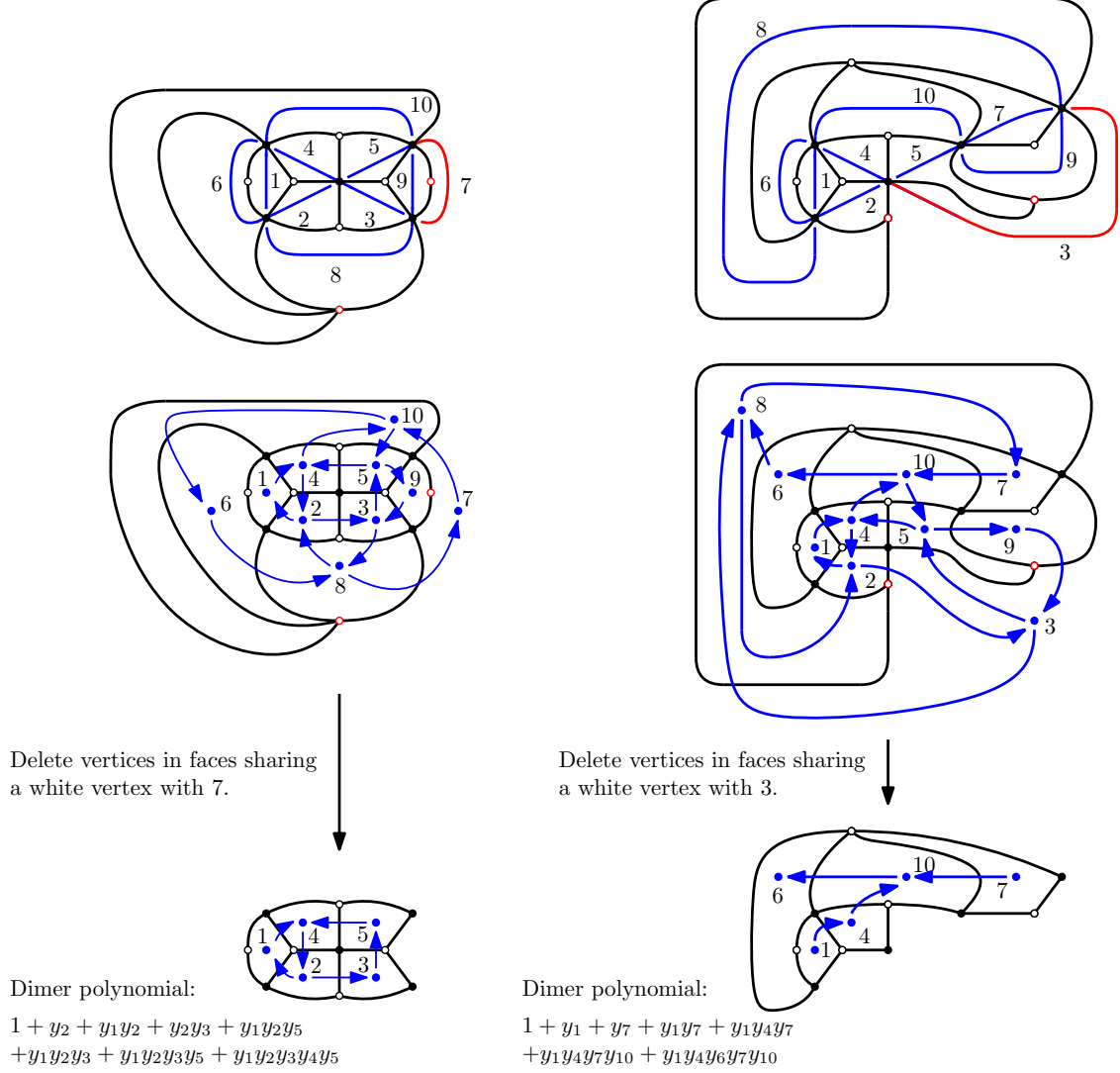


FIGURE 25. Top: two different stereographic projections of the link diagram L and graph G_L from Figure 7. On the left, the infinite face of G_L is f_7 . On the right, it is f_3 . Center: the corresponding stereographic projections of the quiver $Q_{G_L}^{\text{ext}}$. Bottom: The graphs $G_{L,i}$ for $i = 7$ (left) and $i = 3$ (right), their dual quivers, and their dimer polynomials, which are F -polynomials of $\mathcal{A}(Q_{G_L}^{\text{ext}})$ by Theorem 7.2. By Theorem 4.10, both polynomials specialize to the Alexander polynomial of L .

We will utilize Theorems 5.5 and 5.10 to determine the remaining entries of the g -vector. In particular, we use that

$$(14) \quad \mathbf{x}^g D_{G_{L,i}}(\hat{y}_f) = \frac{P_{z_i}^{\Sigma_0}(\mathbf{x})}{\prod_{f \in \text{Face}(G_L)} x_f^{d_f}}$$

where $P_{z_i}^{\Sigma_0}(\mathbf{x})$ is as in Theorem 5.5, and in particular is a polynomial which has no x_f as a factor.

Suppose f is a face containing a white vertex of f_i . When we write $D_{G_{L,i}}(\hat{y}_f)$ as a rational expression in lowest possible terms, it is possible that it will have a factor of x_f . The exponent of x_f is

$$\min_{M \in \mathcal{D}_{G_{L,i}}} |\hat{0}_{L,i} \cap f| - |M \cap f| = |\hat{0}_{L,i} \cap f| - \max_{M \in \mathcal{D}_{G_{L,i}}} |M \cap f|.$$

Because $d_f = 0$, (14) implies that multiplying by $x^{\mathbf{g}}$ must exactly cancel this factor of x_f . That is,

$$(15) \quad g_f = -|\hat{0}_{L,i} \cap f| + \max_{M \in \mathcal{D}_{G_{L,i}}} |M \cap f|.$$

If $f = f_i$, then no edges of f are in $G_{L,i}$, so (15) implies that $g_f = 0$. In this case, the corresponding coordinate h_f of $\mathbf{h}^G(\hat{0}_{L,i})$ is $h_f = |f|/2 - 0 - 1 = 1$. So $h_{f_i} - 1 = g_{f_i}$, as desired.

If f contains a white vertex of f_i but is not equal to f_i , then the other white vertex of f , say v , is not in f_i . Otherwise, one can show that L is not prime-like. So exactly two edges of f , the ones adjacent to v , are in $G_{L,i}$. Since every edge of $G_{L,i}$ is in some matching, there is some matching that contains one of these edges; since these edges are adjacent, no matching contains both. Thus

$$\max_{M \in \mathcal{D}_{G_{L,i}}} |M \cap f| = 1 \quad \text{and} \quad g_f = 1 - |\hat{0}_{L,i} \cap f| = |f|/2 - |\hat{0}_{L,i} \cap f| - 1 = h_f.$$

This completes the proof of (1). Item (2) now follows by multiplying $D_{G_{L,i}}(\hat{y}_f)$ by $\mathbf{x}^{\mathbf{g}}$. \square

Combining Theorem 4.10 and Theorem 7.2, we obtain the following corollary.

Corollary 7.3. *Let L be a connected prime-like link diagram with no nugatory crossings and with segments numbered $1, \dots, s$. Let G_L be the face-crossing incidence graph, set $Q_L := Q_{G_L}^{\text{ext}}$ and for any segment i of L , let z_i be as in Theorem 7.2. Then the Alexander polynomial Δ_L of L can be obtained from any one of the F -polynomials $F_{z_1}^{Q_L}(\mathbf{y}), \dots, F_{z_s}^{Q_L}(\mathbf{y})$ in $\mathcal{A}(Q_L)$ using the specialization of Theorem 4.10.*

7.2. Comparison of moves. In [2], Bazier-Matte and Schiffler show that all cluster variables z_i from Theorem 7.2 are in fact compatible, using an explicit mutation sequence from the initial quiver⁷ $Q_{G_L}^{\text{ext}}$. Their mutation sequence involves two moves on the link diagram: a “diagram Reidemeister III” move and a “diagram bigon reduction” move, not to be confused with the graph bigon removal moves from Definition 6.4! In this section, we summarize how to reinterpret these moves as compositions of bigon removals and square moves in the face-incidence graph G_L .

See the top rows of Figures 26 and 27 for a depiction of diagram bigon reduction and diagram Reidemeister III moves. We emphasize that these are operations on a link diagram without crossing data, as they ignore the crossing information. In [2], diagram bigon reduction corresponds to the mutation sequence a, b , where segments a, b are as in Figure 26. Diagram RIII corresponds to mutation sequence a, b, c, a , where segments a, b, c are as in Figure 27.

The bottom rows of Figures 26 and 27 show the effect of the diagram moves on the face-crossing incidence graph G_L . Each diagram move corresponds to a sequence of (B) or (S) moves. The sequence of moves gives exactly the mutation sequence that [2] assign to each diagram move. In summary, Figures 26 and 27 shows that the mutation sequence of [2] can be interpreted in terms of G_L , the face-incidence graph of the link diagram.

7.3. Example: 2-bridge links, snake graphs, and type A F -polynomials. In this section, we focus on the special case of 2-bridge links. A number of papers obtained the Alexander polynomials of 2-bridge links by specializing type A F -polynomials [1, 46, 35]. By [43, 44], type A F -polynomials are dimer face polynomials for *snake graphs*. (Since snake graphs have property $(*)$ and exhibit type A Dynkin quivers as their dual quivers, see Lemma 7.10, this identification of their dimer face polynomials as type A F -polynomials can also be deduced from Theorem 6.8. See also [52], which provides F -polynomials for such snake graphs in the context of their connection to continued fractions.) This also implies that the Alexander polynomials of 2-bridge links are specializations of snake graph dimer face polynomials. Here, we give an alternate proof of these specializations, and to do so we first consider a different but related family of graphs, which arise as face-crossing incidence graphs of 2-bridge links. In particular, when L is (the standard regular diagram of) a 2-bridge link, and i is a distinguished segment we call the *lower segment* of L , we give a concrete description of $G_{L,i}$ and show that $Q_{G_{L,i}}$ is a type A quiver. The graphs $G_{L,i}$ have previously appeared in work of Propp [50, Section 4]. We recall Propp’s proof that $G_{L,i}$ has the same dimer lattice, and thus dimer face polynomial, as a snake graph.

We define 2-bridge links using their Conway notation, following [41].

⁷Technically their initial quiver is $Q_{G_L}^{\text{ext}}$ with the arrows reversed. They also show that the mutation sequence to the seed with cluster $\{z_i\}$ returns to the opposite of the initial quiver.

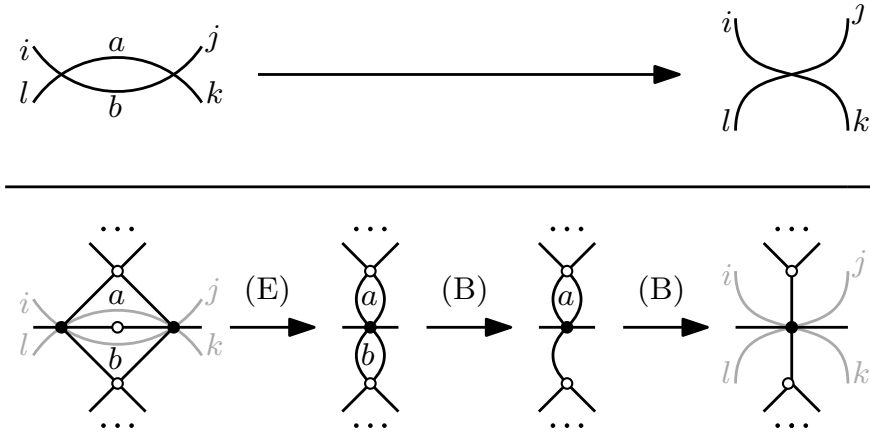


FIGURE 26. Top: diagram bigon reduction on a link diagram L . Bottom: the effect of diagram bigon reduction on the graph G_L , which is a sequence of bigon removals.

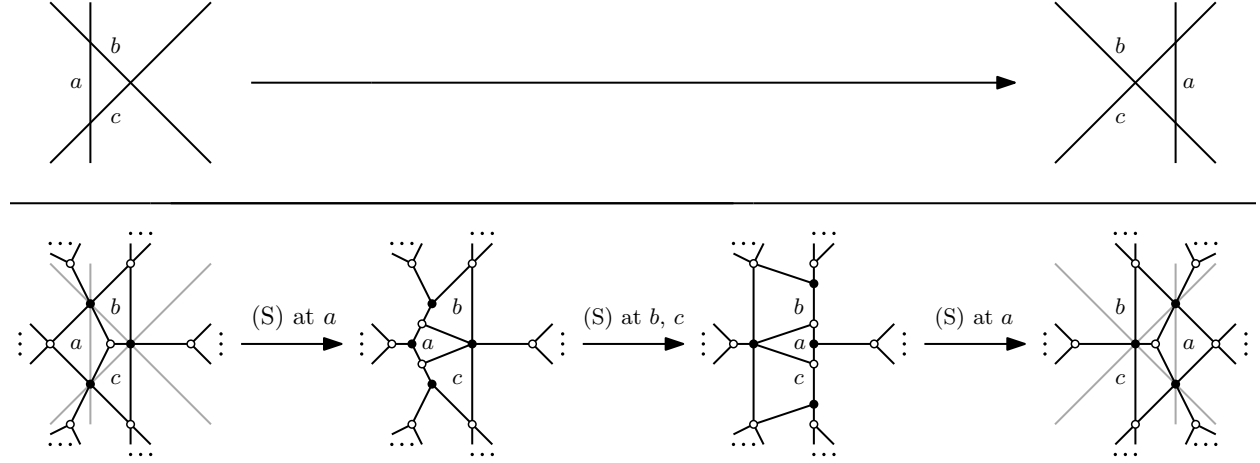


FIGURE 27. Top: diagram Reidemeister III on a link diagram L . Bottom: the effect of diagram Reidemeister III on the graph G_L . Assuming that there are no nugatory crossings either before or after the move, all faces of G_L depicted here are square, and the move can be written as a sequence of four square moves. This sequence of four square moves is the “Y- Δ ” move of Goncharov and Kenyon [27, Figure 30].

Definition 7.4 ([41]). Let $\alpha_1, \dots, \alpha_m$ be positive integers. The diagram $C(\alpha_1, \dots, \alpha_m)$ is the alternating diagram of the form shown in Figure 28. The red highlighted segment in Figure 28 is the **lower segment** of the standard regular diagram. A link is a **2-bridge link** if it has a diagram of the form $C(\alpha_1, \dots, \alpha_m)$.

For $L = C(\alpha_1, \dots, \alpha_m)$ and i the lower segment, the graph $G_{L,i}$ is easy to describe. It is obtained by gluing together subgraphs of the following type.

Definition 7.5. Let k be a positive integer. The **downward k -birdwing** is the bipartite plane graph shown in Figure 29. The **upward k -birdwing** is the downward k -birdwing reflected across the horizontal axis. The downward 0-birdwing is a single vertical edge, with white vertex on top.

Lemma 7.6. For $L = C(\alpha_1, \dots, \alpha_m)$ a 2-bridge link and i the lower segment, $G_{L,i}$ can be obtained as follows. In a line from right to left, place a downward $(\alpha_1 - 1)$ -birdwing, then a disjoint upward $(\alpha_2 - 1)$ -birdwing, a disjoint $(\alpha_3 - 1)$ -birdwing, etc. For $j = 1, \dots, m - 1$, draw a **connecting edge** from the rightmost white (resp. black) vertex of the j^{th} birdwing to the leftmost black (resp. white) vertex of the $(j + 1)^{\text{th}}$ birdwing.

We call graphs constructed as in Lemma 7.6 **flock graphs**. See Figure 30 for an example of Lemma 7.6.

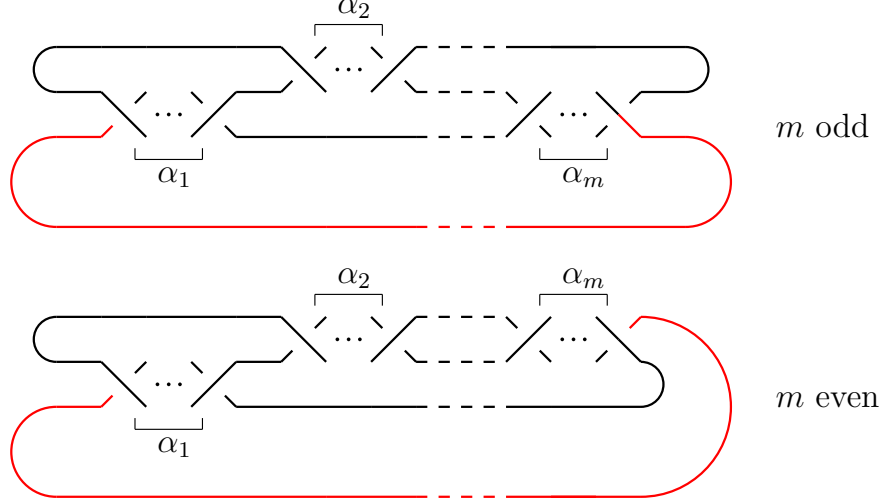


FIGURE 28. The diagram $C(\alpha_1, \dots, \alpha_m)$ of a 2-bridge link. The lower segment is in red. Note that the crossing information depends on the parity of each α_i .

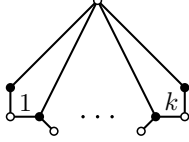


FIGURE 29. A downward k -birdwing.

Proof. This is clear from the definition of $C(\alpha_1, \dots, \alpha_m)$ and of the graph $G_{L,i}$. Indeed, by inspection, the downward $(\alpha_1 - 1)$ -birdwing is precisely the subgraph of $G_{L,i}$ generated by the white vertices corresponding to the regions enclosed by the first α_1 crossings and the region above them, as well as the black vertices corresponding to those crossings. The $(\alpha_j - 1)$ -birdwing is similarly the subgraph of $G_{L,i}$ generated by the white vertices of regions enclosed by the α_j crossings and the region above or below them, and the black vertices of those crossings. The connecting edges surround the segment of $C(\alpha_1, \dots, \alpha_m)$ which goes from the α_j crossings to the α_{j+1} crossings. \square

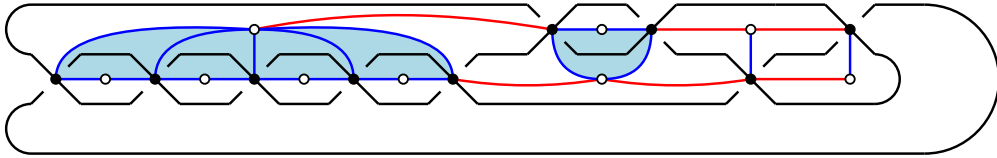


FIGURE 30. The diagram $L = C(5, 2, 1, 1)$ and the graph $G_{L,i}$, where i is the lower segment. The birdwings are shown in blue, while the connecting edges are in red.

Lemma 7.7. *For $L = C(\alpha_1, \dots, \alpha_m)$ a 2-bridge link and i the lower segment, the quiver $Q_{G_{L,i}}$ is a type A quiver (i.e. it is an orientation of a path).*

Proof. The leftmost and rightmost non-infinite faces of $G_{L,i}$ are adjacent to a unique non-infinite face of $G_{L,i}$. All other non-infinite faces are adjacent to two others. Thus, $Q_{G_{L,i}}$ is an orientation of a path. \square

In [50, Section 4], Propp shows that flock graphs have the same dimer lattices as *snake graphs*. A snake graph is a connected bipartite plane graph obtained by gluing together squares along one edge so that they “snake” up and to the right in the plane. See Figure 31, right, for an example. A more precise definition following [4, Sec. 2] appears below.

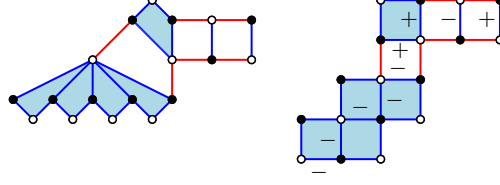


FIGURE 31. Left: The graph $G_{C(5,2,1,1),i}$. Right, the snake graph $\mathcal{G}(5,2,1,1)$. The sign sequence for the snake graph is $(-, -, -, -, -, +, +, -, +)$.

Definition 7.8. Let $(\alpha_1, \dots, \alpha_m)$ be a sequence of positive integers whose sum is $d + 1$. The associated **sign sequence** $(s_1, \dots, s_{d+1}) \in \{+, -\}^{d+1}$ consists of α_1 minuses, then α_2 pluses, then α_3 minuses, and so on. The **snake graph** $\mathcal{G}[\alpha_1, \dots, \alpha_m]$ consists of d boxes B_1, \dots, B_d glued together as follows.

- Place B_1 in the plane so that its edges are parallel to the axes. Label the bottom edge with $s_1 = -$.
- Suppose B_1, \dots, B_j are already placed, and either the bottom or left edge of B_j is labeled with s_j . If $s_{j+1} \neq s_j$, glue B_{j+1} to B_j along the edge of B_{j+1} parallel to the labeled edge. If $s_{j+1} = s_j$, glue B_{j+1} to B_j along the unique edge of B_j which shares a vertex with the labeled edge of B_j and is either the top or the right edge. In both cases, label the shared edge of B_{j+1} and B_j with s_{j+1} .
- Although there is no B_{d+1} to glue to B_d , we label an edge of B_d with s_{d+1} according to the rules above.

We properly color the vertices of $\mathcal{G}[\alpha_1, \dots, \alpha_m]$ so that the bottom left vertex is white. If two parallel edges of B_j are labeled with s_j and s_{j+1} , we call the other two edges **connecting edges** and draw them in red.

Remark 7.9. If the connecting edges of $\mathcal{G}[\alpha_1, \dots, \alpha_m]$ are removed, we are left with a disjoint union of m *zig-zags*, consisting of $\alpha_j - 1$ boxes for $j = 1, \dots, m$. Said differently, $\mathcal{G}[\alpha_1, \dots, \alpha_m]$ consists of m zig-zags attached using connecting edges. See Figure 31, right for an example; the edges of the zig-zags are in blue.

As a companion to Lemma 7.7, we also note the following result describing the dual quivers for snake graphs, using the same proof.

Lemma 7.10. For a snake graph $G = \mathcal{G}[\alpha_1, \dots, \alpha_m]$ defined as in Definition 7.8, the quiver Q_G is a type A quiver (i.e. it is an orientation of a path).

The following proposition was shown in [50, Section 4]; we include the proof here for the convenience of the reader.

Proposition 7.11. Let $L = C(\alpha_1, \dots, \alpha_m)$ be a 2-bridge link and let i be the lower segment. The dimer lattices of $G_{L,i}$ and the snake graph $\mathcal{G}[\alpha_1, \dots, \alpha_m]$ are isomorphic.

Proof. Let G be the graph constructed as follows: place two rows of m vertices v_1, \dots, v_m and u_1, \dots, u_m in the plane, and color v_1 white, u_1 black, and have the colors alternate along the rows. Add α_j edges between v_j and u_j . Then add connecting edges from v_j to v_{j+1} and from u_j to u_{j+1} .

We will show that using (E) moves, both $G_{L,i}$ and $\mathcal{G} := \mathcal{G}[\alpha_1, \dots, \alpha_m]$ can be transformed into G . The result will then follow by Lemma 6.16.

For the graph $G_{L,i}$, each k -birdwing may be contracted to two vertices with $k + 1$ edges between them (see Figure 32 for an example). So by Lemma 7.6, it is clear that $G_{L,i}$ can be transformed to G using (E) moves.

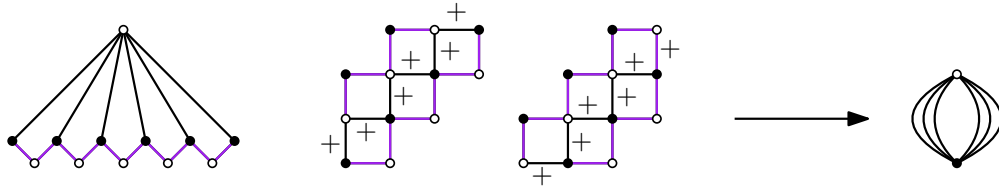


FIGURE 32. Using (E) moves to turn a birdwing or a zig-zag into two vertices connected by multiple edges.

We now turn to the snake graph \mathcal{G} . Note that any edge of \mathcal{G} which is in a zig-zag but is not labeled by a sign can be contracted away using (E) moves, since one of the vertices in such an edge is degree 2. Performing these moves collapses a zig-zag with $k - 1$ boxes into a pair of vertices connected by k edges (see Figure 32 for an example). So, using Remark 7.9, \mathcal{G} can be transformed into a properly colored graph G' consisting of edges of multiplicity $\alpha_1, \dots, \alpha_m$ connected via connecting edges in a line. Rotating 45 degrees to the right, we see that the first of these edges has the white vertex on top, since the bottom left vertex of \mathcal{G} is white. Thus, $G' = G$. \square

We summarize the content of this section in the following proposition.

Proposition 7.12. *Let $L = C(\alpha_1, \dots, \alpha_m)$ be a 2-bridge link and i its lower segment. Let $\mathcal{G} := \mathcal{G}(\alpha_1, \dots, \alpha_m)$ be the corresponding snake graph. The multivariate Alexander polynomial $D_{G_{L,i}}$ is equal to dimer face polynomial $D_{\mathcal{G}}$ of the snake graph. Moreover, it is a type A F -polynomial $F_z^{Q_{G_{L,i}}}$. In particular, the Alexander polynomial Δ_L may be obtained from any of these polynomials by the specialization of Theorem 4.10.*

Proof. That $D_{G_{L,i}}$ is a type A F -polynomial is a consequence of Theorem 6.8 and Lemma 7.7. The equality of $D_{G_{L,i}}$ and $D_{\mathcal{G}}$ follows from Proposition 7.11. The last sentence is implied by Theorem 4.10. \square

8. APPLICATIONS TO CLUSTER STRUCTURES ON POSITROID VARIETIES

In this section, we relate our results to another common occurrence of bipartite plane graphs in cluster algebras: reduced plabic graphs and the cluster structure on open positroid varieties. In particular, we use our results to show for an open positroid variety, every Plücker coordinate and every twisted Plücker coordinate is a cluster monomial.

8.1. Background on plabic graphs and open positroid varieties. In this section, we denote by $\text{Gr}_{k,n}$ the Grassmannian of k -planes in \mathbb{C}^n , and denote by P_I the Plücker coordinate on $\text{Gr}_{k,n}$ indexed by the k -element subset $I \subset [n]$. We assume familiarity with [40, 25], and point the reader to those sources for the geometric and combinatorial details omitted here.

Plabic graphs were originally defined by Postnikov [47], and in that formulation were not required to be bipartite. Here we largely follow the conventions of [40, Section 3.1], adding Postnikov's *leafless* assumption [47, Definition 12.5] for simplicity.

Definition 8.1. A **plabic graph** of type (k, n) is a planar bicolored graph G embedded in a disk with n black boundary vertices $1, \dots, n$ on the boundary of the disk such that

- each internal (i.e. non-boundary) vertex is adjacent only to vertices of the opposite color;
- each boundary vertex is adjacent to exactly zero or one internal vertex;
- any vertex of degree 1 is adjacent to a boundary vertex;
- G has $n - k$ more black vertices than white vertices.

A plabic graph G is **reduced** if no sequence of (E) or (S) moves applied to G produces a bigon face. The **dual quiver with frozen** Q_G^{fr} of G is the quiver obtained from Q_G by freezing vertices corresponding to faces adjacent to the infinite face.

Plabic graphs were introduced by Postnikov [47] to parametrize positroid cells, which stratify the totally nonnegative Grassmannian. Inspired by his work, Knutson–Lam–Speyer introduced *open positroid varieties*, which stratify $\text{Gr}_{k,n}$ [33]. Each reduced plabic graph G of type (k, n) corresponds to an open positroid variety $\Pi_G^\circ \subset \text{Gr}_{k,n}$. Reduced plabic graphs related by (E) and (S) moves correspond to the same open positroid variety. Each open positroid variety Π_G° is cut out by the vanishing of certain Plücker coordinates and the non-vanishing of others (see Lemma 8.4).

For any reduced plabic graph G , there is a combinatorial procedure to label its faces with Plücker coordinates $\{P_{I_f}\}_{f \in \text{Face}(G)}$, called the *source*⁸ Plücker coordinates of G . These are non-vanishing on Π_G° . The **source seed** Σ_G associated to G is the seed whose quiver is Q_G^{fr} and whose cluster is $\{P_{I_f}\}_{f \in \text{Face}(G)}$.

⁸One may also label the faces of G with its *target* Plücker coordinates. This will produce the target seed rather than the source seed. The target and source seeds are related by two applications of the twist map, followed by rescaling by Laurent monomials in frozen variables.

The following theorem is due to Scott [53] in the case of the top-dimensional positroid variety, Serhiyenko–Sherman-Bennett–Williams [54] in the case of open Schubert varieties, and Galashin–Lam [25] for arbitrary open positroid varieties.

Theorem 8.2. *Let G be a reduced plabic graph and Σ_G the corresponding source seed. Then*

$$\mathbb{C}[\Pi_G^\circ] = \mathcal{A}(\Sigma_G).$$

Further, if G, G' are related by a square move, then Σ_G and $\Sigma_{G'}$ are related by mutation.

In [40], Muller–Speyer introduced an automorphism τ on Π_G° called the *twist*⁹. (Their definition was motivated by previous work of Marsh–Scott [37] who defined a twist map in the case of Grassmannians, i.e. the top-dimensional positroid variety. The Marsh–Scott twist differs from the Muller–Speyer twist for the top-dimensional positroid variety by rescaling.) While we do not need its precise definition here, Muller–Speyer provided a formula for “twisted Plücker coordinates” $P_J \circ \tau$ in terms of the source Plückers of G . This formula involves almost perfect matchings of G .

Definition 8.3. Let G be a plabic graph of type (k, n) . An **almost-perfect matching** M of G is a subset of edges which covers each internal vertex exactly once and does not include any edges between boundary vertices. The **boundary** of M is

$$\partial M := \{i \in [n] : i \text{ is covered by an edge of } M\}.$$

As G is type (k, n) , ∂M has size k .

We have the following lemma, which will be useful later and follows from [47, Lemma 11.10] and [33, Corollary 5.12].

Lemma 8.4. *Let G be a reduced plabic graph of type (k, n) . The Plücker coordinate P_J is not identically zero on the positroid variety Π_G° if and only if G has an almost perfect matching with boundary J .*

We may flip a face in an almost-perfect matching, just as in Definition 2.3. We define a binary relation \leq on the almost perfect matchings of G with a fixed boundary using flips, exactly as in Theorem 2.5.

Theorem 8.5 ([40, Theorem B.1]). *Let G be a reduced plabic graph. Then the set of almost perfect matchings of G with boundary I , endowed with the binary relation \leq , is a distributive lattice.*

In what follows, if G is a plabic graph, let $\hat{0}_J$ denote the minimal matching with boundary J . We let x_f denote the source Plücker coordinate P_{I_f} . For $f \in \text{Face}(G)$, let w_f denote the number of white vertices in f and let

$$\text{bd}_f(J) := |\{j \in J : j \text{ is not adjacent to degree 1 vertex and the boundary edge } (j-1, j) \text{ is in } f\}|.$$

We use the notation

$$\mathbf{x}^{\text{bd}(J)} := \prod_{f \in \text{Face}(G)} x_f^{\text{bd}_f(J)}.$$

If G is a plabic graph and M a subset of edges which are not in the boundary of the disk, we define the vector $\mathbf{h}^G(M) = (h_f)_{f \in \text{Face}(G)}$ by

$$h_f := w_f - |M \cap f| - 1.$$

Note that if f is not adjacent to the boundary of the disk, then $w_f = |f|/2$.

Proposition 8.6 ([40, Proposition 7.10]). *Let G be a reduced plabic graph. Then for any Plücker coordinate P_J ,*

$$P_J \circ \tau = \mathbf{x}^{\text{bd}(J)} \sum_{M: \partial M = J} \mathbf{x}^{\mathbf{h}^G(M)}.$$

We note that the equalities in Proposition 8.6 are consistent with Lemma 8.4, since if there are no almost perfect matchings with boundary J , the sum in Proposition 8.6 is zero.

Remark 8.7. For the special case they consider, Marsh–Scott prove a formula [37, Theorem 1.1] which, suitably rescaled, is algebraically equivalent to that of Proposition 8.6, see [18, Remark 3.7, Proposition 3.8] for the derivation.

⁹They define the left and right twists, which are inverses of each other. We use the left twist here.

Finally, we need a result relating the twist map to the cluster structure on $\mathbb{C}[\Pi_G^\circ]$, which was proved independently by [49, 6]. Recall that a cluster monomial is a monomial of compatible cluster variables times a Laurent monomial in frozen variables.

Theorem 8.8. *Let G be a reduced plabic graph. Then*

$$\begin{aligned}\tau^* : \mathbb{C}[\Pi_G^\circ] &\rightarrow \mathbb{C}[\Pi_G^\circ] \\ P_J &\mapsto P_J \circ \tau\end{aligned}$$

is a quasi-cluster homomorphism. In particular, τ^ and its inverse take cluster monomials to cluster monomials.*

8.2. All Plückers are cluster monomials. In this section, we will utilise Theorem 6.8 to show the following theorem.

Theorem 8.9. *Let Π_G° be an open positroid variety, and let P_J be a Plücker coordinate which is not identically zero on Π_G° . Then P_J and its twist $P_J \circ \tau$ are both cluster monomials in $\mathbb{C}[\Pi_G^\circ] = \mathcal{A}(\Sigma_G)$.*

Remark 8.10. The statement of Theorem 8.9 also holds for the target cluster structure on $\mathbb{C}[\Pi_G^\circ]$, since by [49, 6] the source and target cluster structure have the same cluster monomials.

Remark 8.11. In the special case when P_J is a source (or target) Plücker coordinate for some reduced plabic graph G' for Π_G° , then P_J is a cluster variable in $\mathbb{C}[\Pi_G^\circ]$ by [25] (see Theorem 8.2) and its twist is a cluster monomial by [49, 6] (see Theorem 8.8). Similarly, if P_J is a unit in $\mathbb{C}[\Pi_G^\circ]$, then by [26, Theorem 1.3 (1)] it is a Laurent monomial in frozen variables and in particular is a cluster monomial. So in these special cases, Theorem 8.9 was already known. In particular, when Π_G° is the unique top-dimensional positroid variety, Theorem 8.9 was known for all Plücker coordinates, since all Plücker coordinates are source Plücker coordinates for some plabic graph (in this case, by [37, Proposition 8.10], twists of Plücker coordinates are cluster variables times a Laurent monomial in frozen variables).

However, for most positroids, only a small fraction of the nonzero Plücker coordinates are source (or target) Plückers. For example, some positroid varieties Π_G° have only one reduced plabic graph and only $|\text{Face}(G)|$ source Plücker coordinates, but have many more nonzero, non-unit Plücker coordinates.

To prove Theorem 8.9, we would like to connect Proposition 8.6 to Theorem 6.8. The latter theorem involves *perfect matchings* of graphs with property $(*)$, while the twist formula uses *almost perfect matchings* of plabic graphs. We first need some technical results to relate these two scenarios.

For G a plane graph, let \leq_G be the binary relation on \mathcal{D}_G where $M \leq_G M'$ if M is obtained from M' by a sequence of down-flips on simply connected faces. Recall from Remark 2.6 that there is a refinement \leq of \leq_G which endows \mathcal{D}_G with the structure of a distributive lattice. The following lemma gives a sufficient condition for this refinement \leq to be equal to \leq_G .

Proposition 8.12. *Let G be a plane graph such that every non-infinite face is simply connected. Let $H = H_1 \sqcup \cdots \sqcup H_r$ be the graph obtained from G by deleting all edges which are not in any perfect matching. If (\mathcal{D}_G, \leq_G) is a poset with a unique minimum or maximum, then every non-infinite face of H is a face of G . Further, (\mathcal{D}_G, \leq_G) is the Cartesian product of the distributive lattices $(\mathcal{D}_{H_i}, \leq_{H_i})$, and is also equal to (\mathcal{D}_H, \leq_H) .*

Proof. Note that $\mathcal{D}_G, \mathcal{D}_H$ and the product $\prod_i \mathcal{D}_{H_i}$ are all in natural bijection. So we identify the matchings in all three sets. We also identify a face with the edges in its boundary. We let \leq denote the partial order on the product $\prod_i \mathcal{D}_{H_i}$.

If $M <_G M'$ are related by a flip at face f of G , then all edges of f are in a perfect matching of G . Thus, f is also a face of some H_i , which implies $M < M'$. This means that if $M \leq_G M'$, then $M \leq M'$. In particular, \leq_G is a coarsening of \leq . This implies that if (\mathcal{D}_G, \leq_G) has a unique minimum (resp. maximum), it agrees with the minimum (resp. maximum) of (\mathcal{D}_G, \leq) .

Now, suppose for the sake of contradiction that some non-infinite face of H is not a face of G . This face may not be simply connected. One connected component of the boundary of this face is the boundary of a non-infinite face f of some H_i . The face f is not a face of G . Since H_i has property $(*)$ by construction, Corollary 2.21 implies f can be flipped in some matching of G_i . That is, there exist a matching of G containing all white-black edges of f , and there exists a matching of G containing all black-white edges of f . However, since f is not a face of G , we cannot perform a flip at f .

The set

$$WB = \{M \in \mathcal{D}_G : M \text{ contains the white-black edges of } f\}$$

is an order filter in (\mathcal{D}_G, \leq_G) . Indeed, if $M \in WB$, then for any face F' adjacent to f , either M contains a black-white edge of f' or M does not contain some white-black edge of f' . So if M' is obtained from M by an up-flip at some face f' , f' is not adjacent to f and M' is also in WB . By the definition of \leq_G , this implies that if $M \in WB$, then so are all M' with $M' \geq_G M$.

Similarly, the set

$$BW = \{M \in \mathcal{D}_G : M \text{ contains the black-white edges of } f\}$$

is an order ideal in (\mathcal{D}_G, \leq_G) .

In the case that (\mathcal{D}_G, \leq_G) has a unique minimal element $\hat{0}$, this implies $\hat{0}$ is in BW . As we already argued, $\hat{0}$ is also the minimum element of (\mathcal{D}_G, \leq) . But this is impossible; since f is a face of G_i and $\hat{0}$ contains the black-white edges of f , we can perform a down-flip at f in H_i . So $\hat{0}$ cannot be minimal in (\mathcal{D}_G, \leq) , a contradiction. An identical argument leads to a contradiction in the case that (\mathcal{D}_G, \leq_G) has a unique maximal element, exchanging BW for WB .

This completes the argument that every non-infinite face of H is a face of G . In particular, every non-infinite face of H is simply connected. This, in turn, implies that every non-infinite face of each H_i is a face of H and thus of G . So, if a face of G_i can be flipped in some matching in $\prod_i \mathcal{D}_{H_i}$, it is also a face of G and of H and can be flipped in those graphs as well. This shows that every cover relation in (\mathcal{D}_G, \leq) is also a cover relation in (\mathcal{D}_G, \leq_G) and (\mathcal{D}_H, \leq_H) and so the posets coincide. \square

Lemma 8.13. *Let G be a reduced plabic graph, and let J be the boundary of some almost perfect matching of G . Let $H = H_1 \sqcup \cdots \sqcup H_r$ be the plane graph obtained from G by deleting*

- (1) *all boundary vertices;*
- (2) *all internal vertices adjacent to boundary vertices $\{j \in J\}$;*
- (3) *all edges which are not in any almost perfect matching of G with boundary J*

so that every connected component H_i of H has property (). Then under the natural identification of edges of H with edges of G , the lattice of almost-perfect matchings of G with boundary J (see Theorem 8.5) is isomorphic to (\mathcal{D}_H, \leq_H) and the product of lattices $\prod_i (\mathcal{D}_{H_i}, \leq_{H_i})$.*

Further, every non-infinite face of H is a face of G , and the dual quiver Q_H is an induced subquiver of Q_G^{fr} consisting only of mutable vertices.

Proof. Reducedness implies that G is connected and so its faces are simply connected. Once we perform the deletions in steps (1) and (2), we have a plane graph G' whose non-infinite faces are simply connected. Note that G' has at least one perfect matching, since any almost-perfect matching of G with boundary J restricts to a perfect matching of G' . Also, every non-infinite face of G' is a face of G , and the lattice of almost-perfect matchings of G with boundary J is clearly isomorphic to $(\mathcal{D}_{G'}, \leq_{G'})$. By Theorem 8.5, this implies that $(\mathcal{D}_{G'}, \leq_{G'})$ has a unique minimal element. Applying Proposition 8.12 to G' , we get an isomorphism between $(\mathcal{D}_{G'}, \leq_{G'})$, (\mathcal{D}_H, \leq_H) and the product $\prod_i (\mathcal{D}_{H_i}, \leq_{H_i})$. By the same proposition, we also have that every non-infinite face of H is a face of G .

The statement about the dual quiver follows from the fact that every non-infinite face of H is a face of G , and the definition of the dual quiver. \square

Remark 8.14. Consider the graph G' from the proof of Lemma 8.13. As mentioned therein, the dimers of G' are in natural bijection with the almost perfect matchings of G with boundary J . In [40, Appendix B], they explicitly avoid using G' to prove Theorem 8.5. We point out that we make crucial use of Theorem 8.5 to deduce properties of the dimers of G' , rather than the other way around. In particular, we use Theorem 8.5 when we invoke Proposition 8.12, to ensure that deleting the edges of G' that are not in any dimer does not create any new faces or any new flips.

Lemma 8.15. *Let G be a reduced plabic graph, and let J and $H = H_1 \sqcup \cdots \sqcup H_r$ be as in Lemma 8.13. Then*

$$D_H(\mathbf{y}) = \prod_i D_{H_i}(\mathbf{y})$$

is a product of compatible F -polynomials for the cluster algebra $\mathcal{A}(\mathbf{x}, Q_G)$.

Proof. If H_i is a single edge, then $D_{H_i} = 1$, so we may ignore those components.

For each i where H_i is not a single edge, the quiver Q_{H_i} is a connected component of the quiver Q_H . By Lemma 8.13 the quiver Q_H is an induced subquiver of Q_G , implying that Q_{H_i} is also an induced subquiver of Q_G . Since H_i has property $(*)$ by construction, $D_{H_i}(\mathbf{y})$ is the F -polynomial of a cluster variable z'_i in $\mathcal{A}(\mathbf{x}, Q_{H_i})$ by Theorem 2.5. By Proposition 5.11, $D_{H_i}(\mathbf{y})$ is also the F -polynomial of a cluster variable z_i in $\mathcal{A}(\mathbf{x}, Q_G)$, and in particular can be obtained from the initial seed just by mutating at the subquiver Q_{H_i} . Since the quivers Q_{H_i} and Q_{H_j} are disjoint for $i \neq j$, z_i and z_j are compatible. \square

Proof of Theorem 8.9. Fix a reduced plabic graph G . Fix P_J which is not identically zero on Π_G° or equivalently, J such that G has an almost-perfect matching with boundary J .

We will show that $P_J \circ \tau$ is a cluster monomial. By Theorem 8.8, this implies that P_J is a cluster monomial as well.

Recall from Proposition 8.6 that the formula for $P_J \circ \tau$ in terms of the seed $\Sigma_G = (\{x_f\}, Q_G^{\text{fr}})$ is

$$P_J \circ \tau = \mathbf{x}^{\text{bd}(J)} \sum_{N: \partial N = J} \mathbf{x}^{\mathbf{h}^G(N)}.$$

If G has a unique matching with boundary J , then this matching is $\hat{0}_J$ and the sum above is trivial. So in this case,

$$P_J \circ \tau = \mathbf{x}^{\text{bd}(J)} \mathbf{x}^{\mathbf{h}^G(\hat{0}_J)}.$$

Notice that since no faces can be flipped, any face of G not adjacent to the boundary of the disk satisfies $w_f - 1 \geq |\hat{0}_J \cap f|$, so the entry h_f of $\mathbf{h}^G(\hat{0}_J)$ is nonnegative. We also have $\text{bd}_f(J) = 0$ for such faces. Thus, for any mutable vertex f of Q_G^{fr} , x_f appears in $P_J \circ \tau$ with a nonnegative power. So $P_J \circ \tau$ is a cluster monomial.

If G has more than one almost-perfect matching with boundary J , let $H = H_1 \sqcup \dots \sqcup H_r$ be as in Lemma 8.13. Say H_1, \dots, H_p have at least one non-infinite face, and H_{p+1}, \dots, H_r are single edges. By Lemma 8.15, the dimer face polynomial $D_H(\mathbf{y}) = \prod_i D_{H_i}$ is a product of compatible F -polynomials in $\mathcal{A}(\Sigma_G)$. For $i \in [p]$, let z_i denote the cluster variable in $\mathcal{A}(\Sigma_G)$ whose F -polynomial is $D_{H_i}(\mathbf{y})$.

By an argument similar to the proof of Corollary 6.10,

$$z_i = \mathbf{x}^{\mathbf{g}_i} \sum_{M \in \mathcal{D}_{H_i}} \mathbf{x}^{\mathbf{h}^G(M) - \mathbf{h}^G(\hat{0}_{H_i})}.$$

By Theorem 6.8 and Proposition 5.11, for $f \in \text{Face}(H_i)$, the g -vector entry is $g_f = w_f - |\hat{0}_{H_i} \cap f| - 1$. For other faces of G corresponding to mutable vertices of Q_G^{fr} , the g -vector entry is

$$g_f = \max_{M \in \mathcal{D}_{H_i}} |M \cap f| - |\hat{0}_{H_i} \cap f|.$$

This follows by a very similar argument to the proof of Theorem 7.2. In particular, g_f is zero unless f is a face of H_i or is adjacent to a face of H_i .

Now, we consider the formula for the cluster monomial $z_1 z_2 \dots z_p$ in terms of the initial cluster. Using that the dimer lattice on H is the product of dimer lattices on H_1, \dots, H_r and that the components H_{p+1}, \dots, H_r do not contribute to the exponents for terms of the sum, we obtain

$$z_1 \dots z_p = \left(\prod_{i=1}^p \mathbf{x}^{\mathbf{g}_i} \right) \sum_{M \in \mathcal{D}_H} \mathbf{x}^{\mathbf{h}^G(M) - \mathbf{h}^G(\hat{0}_H)}.$$

If $f \in \text{Face}(H)$, then at most one z_i has g -vector with nonzero g_f . So the exponent of x_f in $\prod_{i=1}^p \mathbf{x}^{\mathbf{g}_i}$ is again

$$w_f - |\hat{0}_{H_i} \cap f| - 1 = w_f - |\hat{0}_H \cap f| - 1.$$

Otherwise, if $f \notin \text{Face}(H)$ and corresponds to a mutable vertex in Q_G^{fr} , the exponent of x_f in $\prod_{i=1}^p \mathbf{x}^{\mathbf{g}_i}$ is

$$(16) \quad \sum_{i=1}^p \max_{M \in \mathcal{D}_{H_i}} |M \cap f| - |\hat{0}_{H_i} \cap f| = \sum_{i=1}^r \max_{M \in \mathcal{D}_{H_i}} |M \cap f| - |\hat{0}_{H_i} \cap f| = \max_{M \in \mathcal{D}_H} |M \cap f| - |\hat{0}_H \cap f|.$$

The first equality holds because for $i = p+1, \dots, r$, the term corresponding to H_i is zero, and the second holds because $H = H_1 \sqcup \dots \sqcup H_r$. Note that the rightmost expression in (16) is at most $w_f - 1 - |\hat{0}_H \cap f|$,

because if it were $w_f - |\hat{0}_H \cap f|$, then the face f could be flipped in some matching and thus would be a face of H , contradicting our assumption.

In summary, by multiplying $z_1 \cdots z_p$ by some monomial Z in $\{x_f : f \notin \text{Face}(H)\}$, we can obtain

$$(17) \quad Z \cdot z_1 \cdots z_p = \mathbf{x}^{\mathbf{h}^G(\hat{0}_H)} \sum_{M \in \mathcal{D}_H} \mathbf{x}^{\mathbf{h}^G(M) - \mathbf{h}^G(\hat{0}_H)} = \sum_{M \in \mathcal{D}_H} \mathbf{x}^{\mathbf{h}^G(M)}.$$

As all cluster variables $\{x_f : f \notin \text{Face}(H)\}$ are compatible with z_1, \dots, z_p , the left hand side of (17) is a cluster monomial.

Finally, a matching M of H differs from a matching N of G with boundary J only at the edges adjacent to a boundary vertex $j \in J$. So $|M \cap f|$ differs from $|N \cap f|$ only if x_f is a frozen variable in Σ_G , and in this case,

$$|M \cap f| = |N \cap f| - |\{j \in J : \text{vertex } j \in f\}|.$$

So we may rewrite (17) using almost perfect matchings of G with boundary J as

$$Z \cdot z_1 \cdots z_p = \left(\prod_{f \in \text{Face}(G)} x_f^{|\{j \in J : j \in f\}|} \right) \sum_{N : \partial N = J} \mathbf{x}^{\mathbf{h}^G(N)}.$$

By Proposition 8.6,

$$\left(\frac{\mathbf{x}^{\text{bd}(J)}}{\prod_{f \in \text{Face}(G)} x_f^{|\{j \in J : \text{vertex } j \in f\}|}} \right) Z \cdot z_1 \cdots z_p = P_J \circ \tau.$$

The left hand side is also a cluster monomial. By definition, $\text{bd}_f(J) = 0$ if f is not adjacent to the boundary of the disk, so $\mathbf{x}^{\text{bd}(J)}$ is a monomial in frozen variables. Also, the denominator above is a product of frozen variables. So the left hand side is a cluster monomial times a Laurent monomial in frozens, and thus is a cluster monomial. This shows that $P_J \circ \tau$ is a cluster monomial, as desired. \square

ACKNOWLEDGEMENTS

The authors are grateful to Mario Sanchez and Jim Propp for inspiring conversations. KM is supported by the National Science Foundation under Award No. DMS-1847284 and Award No. DMS-2348676. GM is supported by the National Science Foundation under Award No. DMS-1854162. MSB is supported by the National Science Foundation under Award No. DMS-2103282. Any opinions, findings, and conclusions or recommendations expressed in this material are those of the author(s) and do not necessarily reflect the views of the National Science Foundation.

REFERENCES

1. Véronique Bazier-Matte and Ralf Schiffler, *Knot theory and cluster algebras*, Adv. Math. **408** (2022), 108609.
2. ———, *Knot theory and cluster algebras II: The knot cluster*, arXiv:2405.16592 (2024).
3. Gerhard Burde and Heiner Zieschang, *Knots*, De Gruyter, 2002.
4. İlke Çanakçı and Ralf Schiffler, *Snake graphs and continued fractions*, European Journal of Combinatorics **86** (2020), 103081.
5. Peigen Cao and Fang Li, *The enough g -pairs property and denominator vectors of cluster algebras*, Math. Ann. **377** (2020), no. 3-4, 1547–1572.
6. Roger Casals, Ian Le, Melissa Sherman-Bennett, and Daping Weng, *Demazure weaves for reduced plabic graphs (with a proof that Muller–Speyer twist is Donaldson–Thomas)*, arXiv:2308.06184 (2023), Preprint.
7. Giovanni Cerulli Irelli, Bernhard Keller, Daniel Labardini-Fragoso, and Pierre-Guy Plamondon, *Linear independence of cluster monomials for skew-symmetric cluster algebras*, Compos. Math. **149** (2013), no. 10, 1753–1764.
8. Moshe Cohen, *Dimer Models for Knot Polynomials*, ProQuest LLC, Ann Arbor, MI, 2010, Thesis (Ph.D.)—Louisiana State University and Agricultural & Mechanical College. MR 4463794
9. Moshe Cohen, Oliver T. Dasbach, and Heather M. Russell, *A twisted dimer model for knots*, Fund. Math. **225** (2014), no. 1, 57–74. MR 3205565
10. Moshe Cohen and Mina Teicher, *Kauffman’s clock lattice as a graph of perfect matchings: a formula for its height*, Electron. J. Combin. **21** (2014), no. 4, Paper 4.31, 39. MR 3292268
11. Henry Cohn, Noam Elkies, and James Propp, *Local statistics for random domino tilings of the aztec diamond*, Duke Mathematical Journal **85** (1996), no. 1, 117.
12. John H Conway and Jeffrey C Lagarias, *Tiling with polyominoes and combinatorial group theory*, Journal of combinatorial theory, Series A **53** (1990), no. 2, 183–208.
13. Richard H Crowell, *Genus of alternating link types*, Annals of Mathematics **69** (1959), no. 2, 258–275.

14. Harm Derksen, Jerzy Weyman, and Andrei Zelevinsky, *Quivers with potentials and their representations II: applications to cluster algebras*, Journal of the American Mathematical Society **23** (2010), no. 3, 749–790.
15. Philippe Di Francesco, *T-systems, networks and dimers*, Communications in Mathematical Physics **331** (2014), 1237–1270.
16. Richard Eager and Sebastián Franco, *Colored bps pyramid partition functions, quivers and cluster transformations*, Journal of High Energy Physics **2012** (2012), no. 9, 1–44.
17. Noam Elkies, Greg Kuperberg, Michael Larsen, and James Propp, *Alternating-sign matrices and domino tilings (Part I)*, Journal of Algebraic Combinatorics **1** (1992), 111–132.
18. Moriah Elkin, Gregg Musiker, and Kayla Wright, *Twists of $Gr(3, n)$ cluster variables as double and triple dimer partition functions*, arXiv preprint arXiv:2305.15531 (2023).
19. Jiarui Fei, *Combinatorics of F -polynomials*, Int. Math. Res. Not. IMRN (2023), no. 9, 7578–7615.
20. Sergey Fomin, Lauren Williams, and Andrei Zelevinsky, *Introduction to cluster algebras. Chapter 7*, arXiv:2106.02160 (2021).
21. Sergey Fomin and Andrei Zelevinsky, *Cluster algebras I: foundations*, Journal of the American mathematical society **15** (2002), no. 2, 497–529.
22. ———, *Cluster algebras IV: coefficients*, Compositio Mathematica **143** (2007), no. 1, 112–164.
23. Sebastián Franco, Amihay Hanany, David Vegh, Brian Wecht, and Kristian D Kennaway, *Brane dimers and quiver gauge theories*, Journal of High Energy Physics **2006** (2006), no. 01, 096.
24. Chris Fraser, *Quasi-homomorphisms of cluster algebras*, Advances in Applied Mathematics **81** (2016), 40–77.
25. Pavel Galashin and Thomas Lam, *Positroid varieties and cluster algebras*, Ann. Sci. Éc. Norm. Supér. (4) **56**, no. 3, 859–884.
26. Christof Geiss, Bernard Leclerc, and Jan Schröer, *Factorial cluster algebras*, Doc. Math. **18** (2013), 249–274.
27. Alexander B Goncharov and Richard Kenyon, *Dimers and cluster integrable systems*, Annales scientifiques de l’École Normale Supérieure, vol. 46, 2013, pp. 747–813.
28. In-Jee Jeong, Gregg Musiker, and Sicong Zhang, *Gale-Robinson sequences and brane tilings*, Discrete Mathematics & Theoretical Computer Science (2013), no. Proceedings.
29. Adam Kalman, *Newton polytopes of cluster variables of type A_n* , arXiv:1310.0555 (2013).
30. Louis H. Kauffman, *Formal knot theory*, Dover books on mathematics, Dover Publications, 2006.
31. Richard Kenyon, *Lectures on dimers*, arXiv preprint arXiv:0910.3129 (2009).
32. ———, *The dimer model*, Exact methods in low-dimensional statistical physics and quantum computing (2010), 341–361.
33. Allen Knutson, Thomas Lam, and David E. Speyer, *Positroid varieties: juggling and geometry*, Compos. Math. **149** (2013), 1710–1752.
34. Kyungyong Lee and Ralf Schiffler, *Positivity for cluster algebras*, Annals of Mathematics (2015), 73–125.
35. ———, *Cluster algebras and Jones polynomials*, Selecta Math. (N.S.) **25** (2019), no. 4, Paper No. 58, 41.
36. Fang Li and Jie Pan, *Recurrence formula, positivity and polytope basis in cluster algebras via Newton polytopes*, arXiv:2201.01440 (2022), Preprint.
37. Bethany R Marsh and Jeanne S Scott, *Twists of Plücker coordinates as dimer partition functions*, Communications in Mathematical Physics **341** (2016), no. 3, 821–884.
38. Amal Mattoo and Melissa Sherman-Bennett, *Saturation of Newton polytopes of type A and D cluster variables*, Comb. Theory **2** (2022), no. 2, Paper No. 6, 37. MR 4449814
39. Greg Muller, *The existence of a maximal green sequence is not invariant under quiver mutation*, Electron. J. Combin. **23** (2016), no. 2, Paper 2.47, 23.
40. Greg Muller and David E. Speyer, *The twist for positroid varieties*, Proc. Lond. Math. Soc. (3) **115** (2017), no. 5, 1014–1071. MR 3733558
41. Kunio Murasugi and Bohdan Kurpita, *Knot theory and its applications*, Springer, 1996.
42. Kunio Murasugi and Alexander Stoimenow, *The Alexander polynomial of planar even valence graphs*, Advances in Applied Mathematics **31** (2003), no. 2, 440–462.
43. Gregg Musiker and Ralf Schiffler, *Cluster expansion formulas and perfect matchings*, Journal of Algebraic Combinatorics **32** (2010), 187–209.
44. Gregg Musiker, Ralf Schiffler, and Lauren Williams, *Positivity for cluster algebras from surfaces*, Adv. Math. **227** (2011), no. 6, 2241–2308.
45. ———, *Bases for cluster algebras from surfaces*, Compositio Mathematica **149** (2013), no. 2, 217–263.
46. Wataru Nagai and Yuji Terashima, *Cluster variables, ancestral triangles and Alexander polynomials*, Adv. Math. **363** (2020), 106965, 37. MR 4051847
47. Alexander Postnikov, *Total positivity, Grassmannians, and networks*, arXiv:math/0609764 (2006).
48. Alexander Postnikov, David Speyer, and Lauren Williams, *Matching polytopes, toric geometry, and the totally non-negative Grassmannian*, J. Algebraic Combin. **30** (2009), no. 2, 173–191.
49. Matthew Pressland, *Quasi-coincidence of cluster structures on positroid varieties*, arXiv:2307.13369 (2023), Preprint.
50. James Propp, *The combinatorics of frieze patterns and Markoff numbers*, arXiv preprint math/0511633 (2005).
51. ———, *Lattice structure for orientations of graphs*, arXiv preprint math/0209005v4 (2024, original version from 2002).
52. Michelle Rabideau, *F -polynomial formula from continued fractions*, Journal of Algebra **509** (2018), 467–475.
53. J. S. Scott, *Grassmannians and cluster algebras*, Proc. London Math. Soc. **92** (2006), 345–380.
54. Khrystna Serhiyenko, Melissa Sherman-Bennett, and Lauren Williams, *Cluster structures in Schubert varieties in the Grassmannian*, Proc. London Math. Soc. **119** (2019), 1694–1744.
55. David E Speyer, *Perfect matchings and the octahedron recurrence*, Journal of Algebraic Combinatorics **25** (2007), 309–348.

- 56. William P Thurston, *Conway's tiling groups*, The American Mathematical Monthly **97** (1990), no. 8, 757–773.
- 57. Panupong Vichitkunakorn, *Solutions to the T -systems with principal coefficients*, The Electronic Journal of Combinatorics **23** (2016), no. 2, P2–44.